CHAPTER 1

INTRODUCTION

Water pollution is one of the largest environmental problems facing society today. Each year, millions of tons of toxic pollutants are discharged into rivers, lakes, and oceans by industry. The major source for this discharge is the wastewater or process waters that are emitted in mass quantities as a result of industrial processes. After entering the environment, these pollutants adversely affect the quality of life, not only for flora and fauna that live next to these bodies of water but for human as well. Because of this, the treatment of wastewater is of utmost importance.

Wastewater containing heavy metal ions is generated in large quantities from the mining, ore processing, microelectonics, metal finishing and photographic industries. These water contain toxic Ag, Au, Cd, Co, Cr, Cu, Ni, Pb, and Zn ions in the range of 50 to 1000 parts per million (ppm). They must be adequately treated before discharged into waste steams or be recycled within a processing plant. The specific discharge concentration limits vary according to the size of the industrial operations and the type of the pollutants. They range from 0.1-0.3 ppm for Ag, Pb and Cd ions to 0.8-1.1 ppm for As and Au ions (U.S. Environmental Protection Agency 1992).

Treatment methods for metal removal from wastewater include precipitation, ion exchange, reverse osmosis, and electrodialysis. Precipitation is the simplest process to remove heavy metal ions. The method consists of adjusting the pH of the wastewater to

greater than 9 by adding NaOH or $Ca(OH)_2$. The metal ions react with the hydroxyl ions to form metal hydroxide precipitates, which are then allowed to settle by gravity in a settling pound and removed by filtrations. The method, however, generates hazardous solid sledges, that must be further disposed in accordance with the regulation of hazardous solid wastes.

Ion exchange uses a bed of cation exchange resins to remove metal ions, and a bed of anion exchange resins to remove SO_4^{2-}, NO_3^- and other anions from wastewater. This process produces purified water suitable for recycle within a process plant. Ion exchange is a batch operation and the resin must be periodically regenerated using a brine solution. The resin regeneration produces concentrated metal ion solutions that need to be further treated.

Reverse osmosis is a membrane technology in which a micro-porous polymeric membrane, permeable to water and impermeable to metal salts, is used to separate the metal pollutants from a wastewater under a pressure. High separation rate, continuous operation, ease of installation and low cost make reverse osmosis an attractive method for water-desalination. However, most industrial wastewaters are acidic and the reverse osmosis has not been widely used because of the deterioration of cellulose acetate and polyamide membranes in the acidic environments. The process also produces a metal ion concentrate that must be further treated.

Electrodialysis uses cation-exchange and anion-exchange membranes to remove metal salts from wastewater. The cation-exchange membrane is permeable only to metal ions, whereas the anion-exchange membrane is permeable only to anions. Wastewater containing heavy metal ions is placed between a pair of cation and anion-exchange membranes. The cathode placed behind the cation-exchange membrane and the anode placed behind the anion-exchange membrane are used to produce a desired electric field. Metal ions, which are attracted by negative potential, migrate toward the cathode compartment through the cation-exchange membrane, and anions, which are attracted by positive potential, migrate through the anion-exchange membrane toward the anode compartment. In the middle compartment between the two ion-exchange membranes, water eventually becomes free of metal salt. Modern ion exchange membranes are chemically stable and highly conductive, and electrodialysis has become a promising method for treating industrial wastewater. The method, however, has the same drawback as the reverse osmosis and ion exchange, i.e., it produces metal ion concentrates that must be disposed of with another technology.

Electrolysis is a “clean” process for treating wastewater containing heavy metal ions. The method is capable of freeing toxic metal ion by electrodepositing them in metallic form at the cathode of an electrolytic cell. The deposited metals can be recycled in a metal or alloy processing plants. The wastewater free of the pollutants may be then discharged to waste stream. One inherent problem associated with the electrolytic method is that the cathode current efficiency for the metal recovery decreases with metal ion concentrations in wastewater. A recent study by (Chin 2000) reveals that the current efficiency is nearly

100% when the metal ion concentrations are greater than 50-100 ppm. However, the current efficiency decreases to less than 1% when the metal ion concentration becomes less than 1 ppm, leading to a high-energy consumption for treating wastewater containing dilute metal ions.

From the brief description for the different techniques for metal removal given above, It seems that the drawback of the electrolytic method can be addressed by the electrodialysis process, which is capable of removing heavy metal ions from wastewater to their discharge limits (1ppm or less) with simple and low cost operation. The electrolytic method is more efficient to recover metals from the highly concentrated metal streams generated by the electrodialysis operation. A study will be undertaken to examine the feasibility of integrating the two processes into a single operation. An integrated electrolytic-electrodialysis cell will be designed and constructed. Wastewater containing heavy metal ions will be fed to the electrodialytic part of the cell to produce non-toxic clean water suitable for discharge or reuse in a process plant. The highly concentrated streams of metal ions generated by electrodialysis in the side compartments as a result for the diffusion of the metal ions through the cation exchange membranes are treated in the electrolytic part of the cell.

CHAPTER 2

LITERATURE REVIEW

This chapter presents the literature review for electrolytic method and electrodialytic method. Each section starts with the description of the process, presents the major concepts, the researchers' achievements and concludes with the major advantages and disadvantages of the technique.

2.1 Electrolytic Method:

Many heavy metal ions can be recovered from wastewater by electrodepositing them in metallic form. However, the current efficiency is low due to simultaneous hydrogen ion reduction reaction in the aqueous environment. The extent of hydrogen ion reduction reaction depends on the metal ion concentration, pH, the hydrogen overpotential and the metal deposition potential in a given aqueous environment. Figure 2.1 shows a plot of hydrogen overpotential at 1 mA/cm^2 (Pourbaix 1963) versus the standard metal deposition potential for several metals in 1 N HCl at 25^o C.

The diagonal line in the Figure 2.1 divides the figure into two regimes. In the regime above the diagonal line (designated by "II"), the hydrogen overpotential is more positive than the metal deposition potential, and one would expect little or no metal deposition reaction because of excessive hydrogen ion reduction reaction. On the other hand, the metal ions in the regime below the diagonal line (designated by "I", where the hydrogen

overpotential is more negative than the metal deposition potential) can be easily recovered at the cathode. These ions include: Ag, Au, Cd, Cu, Hg, Ni, Pb, Pt, Zn, etc. An example of this was the use of a silver tower electrolyzer (Hickman et al. 1993; Cedrone, 1956) to recover silver from spent photographic fixing solutions. Zhou and Chin (1993,1994) described an electrolytic process for simultaneously recovering heavy metal ions from wastewater at the cathode and destruction of cyanide ions at the anode. Khristoskova and Lazavou (1984) studied an electrolytic process to remove hexa-valent chromium from wastewater. Shifrin et al. (1979) discussed the advantage of adding RuO_2 to a TiO_2 anode to treat wastewater. Saito (1979) described a process for the recovery of bromide from a solution containing carboxylic or phenolic compounds. The environmental and economic factors of the electrolytic metal recovery process were discussed by O'Keefe and Ettel (1987).

To treat large volume of wastewater and to reduce metal concentration to a low level, many different cell designs have been reported in the literature. Hertwig et al. (1992) and Tison (1981) used a rotary drum electrode to recover copper. Fleishmann et al. (1971a) used a fluidized bed as the cathode to plate copper onto metal particles. Bennion and Newman (1972) used a flow-through porous-electrode to remove copper ions from dilute solutions. Robertson and Dossenbach (1981) developed a gas-sparging cell to improve mass transfer in an electrolytic cell for wastewater treatment.

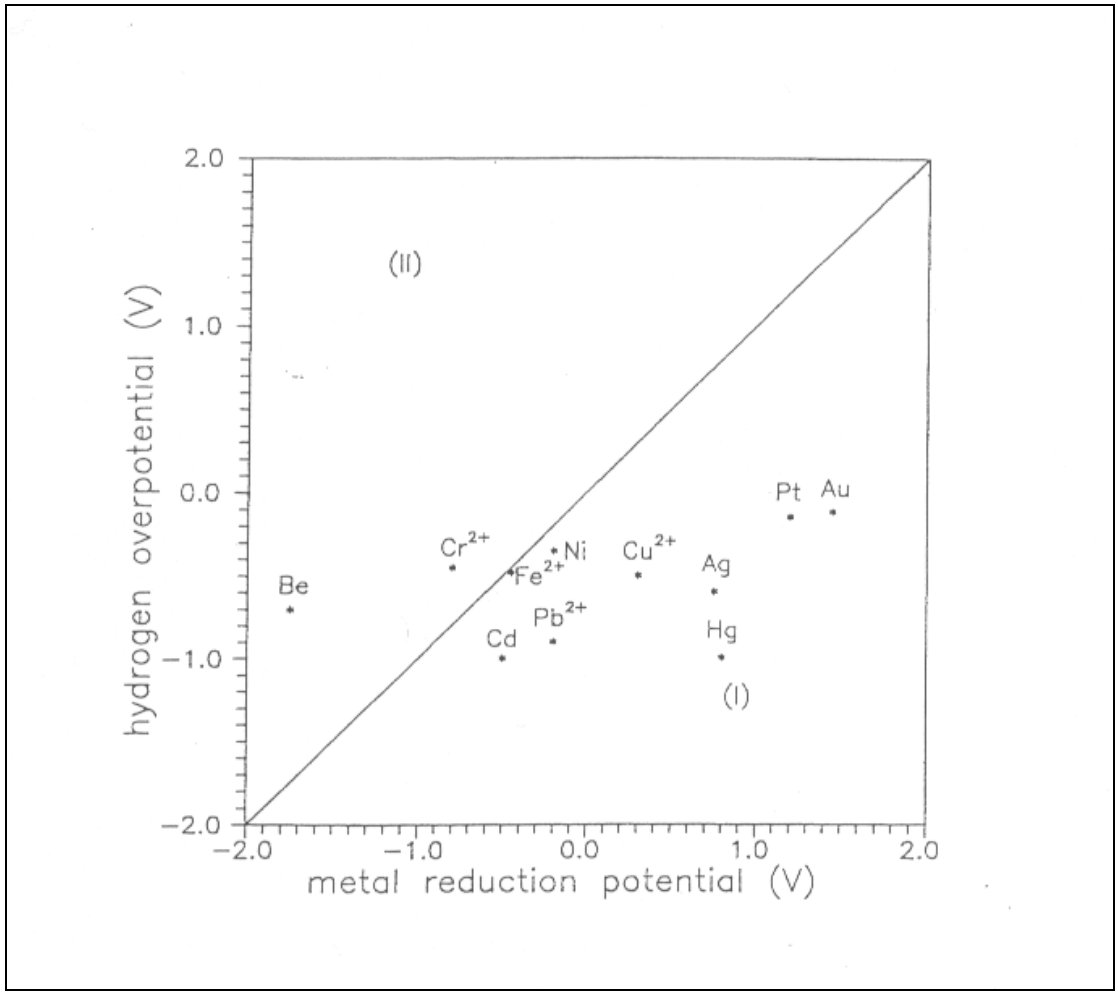

Figure 2.1: Hydrogen overpotential versus the standard metal ion reduction potential for various metal ions in 1 N HCl at 25^{o}.

Holland (1978) described an ECO-cell developed by Ecological Engineering Ltd, in the United Kingdom. The cell consisted of an inner rotating cylinder cathode with a diaphragm and an outer stationary cylinder as the anole. To obtain a high conversion for metal recovery, the cathode compartment was divided into 6 to 12 sections by internal baffles. Electrolyte flowed through a small annular gap between the baffles and the rotating cylinder to effectively provide a high mass transfer rate. Robertson et al. (1983) developed a Swiss-roll cell. Two foil and two thin separators were placed on one another and were rolled around an axis and pressed into a cylinder container. The electrolyte was pumped through the gap provided by the cell separator. The cell was suited for wastewater treatment due to its large surface area. This concept was also used by Du Pont de Nemours and Company to develop an extended surface electrolytic cell ("ESE" cell, 1975). A Chemelec cell was developed (Lopez-Cacicedo, 1975) by the Electricity Council Research Center in the U.K. This cell consisted of a vertical container in which two horizontal parallel metal meshes were used as the electrodes and glass beads were employed to generate fluidization between the electrodes to obtain a high mass transfer rate. A bipolar trickle tower cell was developed by the University of Southampton and University of Newcastle (Fleishmann et al. 1971b). In this cell, the anode and cathode were located on the top and bottom of the cell, and layers of electrical conductive material separated by insulating meshes were sandwich between the anode and cathode. When a terminal voltage was applied to the tower, bipolarity was induced in each conductive layer. The trickle tower possessed a large electrode surface area. An electrochemical flow cell developed by the University of Southampton (Fleishmann et

al., 1976) used a rotating disk as an electrode. In this cell, the gap between the rotating disk electrode and the counter electrode was small, yielding a low IR drop in the solution. A general review of the electrochemical removal of metals from dilute solutions was given by Kuhn (1979). A thorough review of electrochemical cell design for metal recovery was given by Robertson (1983). The basic electrochemistry and engineering principles were discussed by Weininger (1987).

2.1 Electrodialytic Method:

Membrane process proved their reliability in a large number of applications (Cartwright 1991). Electrodialysis, for example, has been practically applied for purification by means of desalination in medical, food, chemical and metallurgical industries (Sata and Kawamura 2000; Resbeut et al. 1992). The electrodialysis technique was developed mainly for desalination and concentration of seawater (Seto et al. 1978; Amor et al. 1998), but later it was applied for the recovery of metals from the metal finishing wastewater and in the metallurgical industries (Resbeult et al. 1998; Chaudhary 2000; Grib et al. 2000). Recently, electrodialysis has been applied for the removal and treatment of industrial effluents from wastewater (Davis 1994; Chin and Ong 1995; Bal and Vaidya 1998). In this process, ion migration through an ion exchange membrane take place when a potential gradient is applied across the membrane; electrostatic interaction within the membrane plays a key role in the transfer of ions (Ogutveren et al. 1997). Electrodialysis has the advantage of linking energy expenditure to the quantity of electrolytes to be extracted and not to the volume of water to be treated. This process enables low ion concentrations to be brought up to higher levels with low energy requirement.

The electrodialysis cell consists of a series of pairs of cation and anion-exchange membranes and a pair of electrodes installed at both ends as shown in the Figure 2.2. By applying direct electric potential to the electrodes, the cations in the solution move towards the cathodes and anions towards anode. The cations permeate through cation-exchange membrane but anions do not. On the other hand, anions permeate through anion-exchange membrane but cations do not. Thus two effluent streams are produced, one stream contains concentrated metal salts and the other stream is pure water. Electrodialysis can be operated in batch mode as well as in continuous operation. The range of operation can be substantially increased by polarity reversal. In this case the direction of the current and hence the ion flux is reversed periodically. Scaling of membranes can be avoided by this technique. Electrodialysis has been successfully applied to industrial effluents which have a relatively low salt concentration such as water-streams from electroplating plants, the semiconductor and the pharmaceutical industries (Ogutveren et al. 1997; Tokuyama corp. Brochure).

Different types of ion exchange membranes have been used in the electrodialysis cell. The most common are the Neosepta ion exchange membranes supplied by the Tokuyama corp., Japan, Nafion, membranes from Du Pont Co., CDS and ADP cation and anion-exchange membranes (Morgane Solvay) and Selemion CMV and selemion AMV membranes, etc. the electrodes are typically made from the stainless steel, graphite, platinum-coated titanium, copper, titanium mesh coated with mixed metal oxide and stainless steel mesh cathodes.

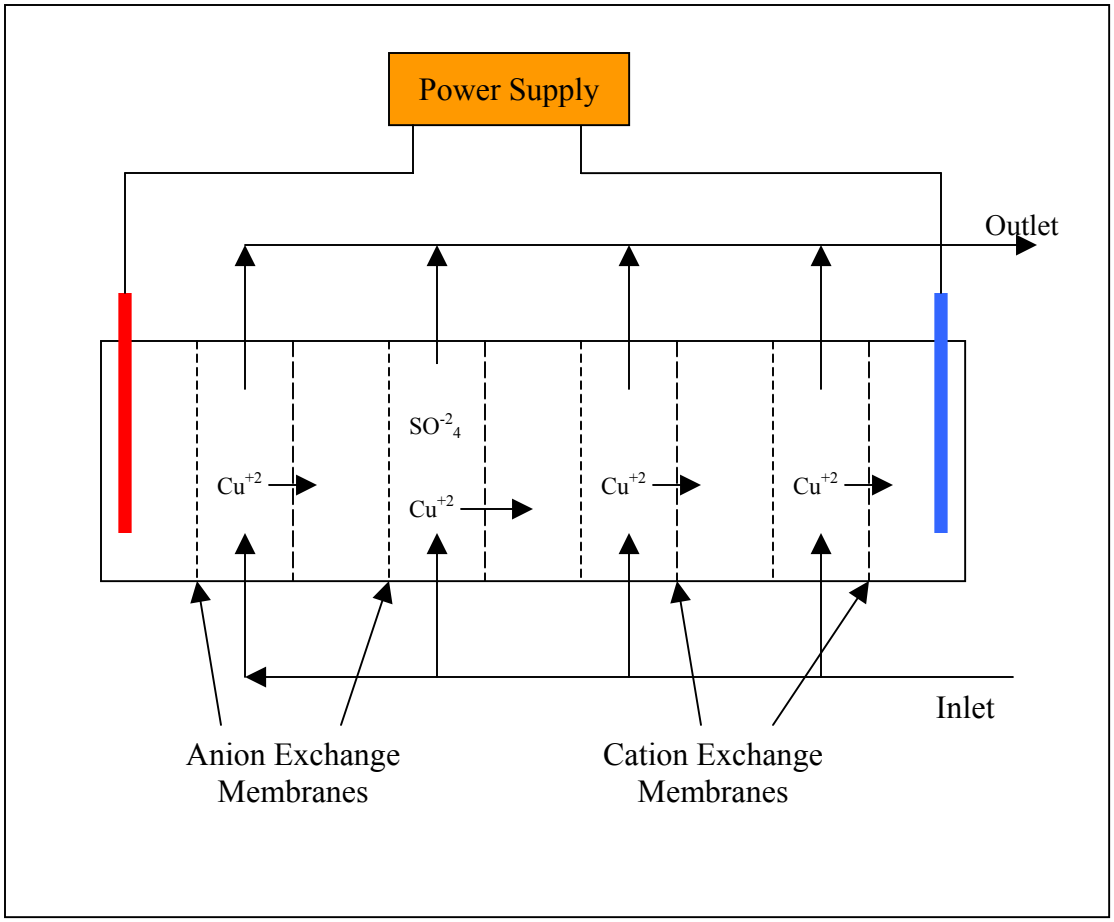

Figure 2.2: Removal of Metal Ions by Electrodialysis

Electrodialysis offers several advantages for the treatment of industrial wastewater (Komgold 1978; Itoi et al. 1980; Ogutveren et al. 1997):

- Complete recycling of water and wastewater constituents leads to considerable saving on water costs.
- Investment costs are relatively low, even for small sized treatment plants.
- Continuous operation at relatively low energy costs.
- Electrolyte solution is concentrated to more than 30% depending on feed condition.
- It is suitable for low concentrated feeds for metals removal and in this electrolyte solution is desalted to less than 10 ppm.
- Electrolyte is separated from organic chemicals in aqueous solutions.
- In neutral, acidic, or slightly basic conditions, ion-exchange membrane is durable for a long period of time without any change of electrochemical properties.

Electrodialysis has been successfully applied in laboratory and pilot plant tests to a wide range of industrial waste streams in order to study its technical and economic feasibility. Some of the examples include regeneration of chemical copper plating baths, recycling of rinsing waters from chemical plating processes, recycling of electroplating rinsing water, recycling of rinsing water from a phosphate plating and recovery of sulfuric acid from pickling solutions etc. (Korngold 1978).

The following gives a brief account of the recent technological developments of lectrodialysis techniques applied to the treatment of industrial wastewater:

A continuous flow electrodialysis cell has been used by Xue et al. (1992) for the purification of industrial wastewater consisting of an acidic process water stream and a spent alkaline process stream. Saracco et al. (1993) described an electrodialytic process for the separation of NaCl and Na_2CO_3 salts in an industrial wastewater of a leaching operation using ion-permselective membranes. Wastewater containing ammonium nitrate from the nuclear fuel manufacturing works was denitrified by three stages of electrodialysis cell to recover nitric acid and ammonia by Sawa et al (1995).

Cherif et al. (1997) described an electrodialysis method for the recovery of nitric acid and sodium hydroxide from an industrial wastewater containing $NaNO_3$, using a three compartments electrodialysis cell. In another study electrodialysis has been successfully applied for the removal of copper from wastewater. The pH of the treated water was 6.5-7.5 whereas pH of the wastewater was 9.0. This eliminates the need of adjusting pH of the wastewater before discharging into the waste streams. In addition, the operation cost of this method was reduced because of the recovery of copper in the cathode compartment. Rodrigues et al. (1999) studied the electrodialysis of an industrial wastewater (or rinse water from chromating bath) containing 4600 ppm of Cr (VI) besides other metallic contaminants using ion exchange membranes (Selemiom AMT and CMT). The results showed that 99.9% of Cr (VI) was recovered resuting in a treated water with a chromium concentration of 4 mg/l. These results show that electrodialysis can be used to treat these effluents, and this water could be reused as rinse water. The solution in the anodic compartment reached 7200 mg/l of Cr (VI), which could be reused on the chromating bath itself. Shim et al. (1999) discussed the removal of vanadium (III)

and Iron (II) ions from a simulated decontamination waste solution by electrodialysis technique through the Nafion 117 cation exchange membrane. The treatment of industrial wastewater from an alumina plant to produce deionized water was carried out by membranes technology by the combination of the electrodialysis and reverse osmosis techniques. The research showed that the method is effective and on the basis of experimental results a process for the wastewater treatment with a capacity of 120 tons was designed (Zhou et al 1999).

Ribeiro et al. (2000) studied the removal of Cu, Cr and As from chromated copper arsenate timber waste using electrodialysis cell. The highest recovery rates obtained were 93% of Cu, 95%of Cr, and 99% of As. Lixin et al. (2000) carried out electrodialysis to recover acetic acid from dilute wastewater containing 0.2 wt. % acetic acid. The results showed that up to 70 wt% acetic acid solution could be recovered. In a similar study, Wisniewski et al. (2000) investigated water and acid recovery from the effluent after metal etching rinsing using electrodialysis systems. The results showed that water of good quality, with no acid and metal salts, was obtained. The hydrochloric acid from the electrodialysis concentrate was recovered by monoselective electrodialysis and the acid solution was concentrated by 74 times compared to raw wastewater. In a related study, Yu and Admassu (2000) developed a theoretical model of an electrodialysis process for the removal of metal ions in process stream of the pulp and paper industry. The model predicts the concentration profiles of cations as electrolytes in electrodialysis channels.

CHAPTER 3

PROBLEM DESCRIPTION AND RESEARCH OBJECTIVES

This chapter discusses the major advantages and disadvantages of the two major techniques that are available to recover the metal ions electrochemically from the wastewater streams as they were deduced from the literature reviews. The idea of the integration of the two techniques, namely electrolytic and electrodialytic is also discussed. It concludes with the objective of the research.

3.1 Description of the Problem:

There are essentially two major electrochemical approaches to recover heavy metal ions from the wastewater streams; namely, electrolytic deposition of metal ions on cathode and the electrodialysis. The electrolytic approach, presented in Figure 3.1 is attractive as it recovers metal ions in valuable metallic form. However, the ohmic losses and mass transfer resistances increase sharply when the concentration of the ions decreases in the cell. A number of reactor configurations have been proposed to improve the mass transfer for example, Tumbling barrel, packed bed etc. Despite the improved mass transfer in these configurations, at lower concentration, the technique becomes ineffective and expensive because of reduced conductivity. One way to solve this problem is to add a salt to increase the conductivity of the electrolyte. However, this may result in increasing the total dissolved solids (TDS) in the wastewater.

The electrodialysis is effective in removing metal ions from a relatively diluted wastewater. The ohmic resistances are made small by decreasing the distance between membranes. Concentration polarization and mass transfer resistance are some associated problems but these can be handled by better designs. However, the major drawback of this process is that it generates a concentrated wastewater stream, which needs further treatment.

The above two techniques can be integrated using the conventional integration as in Figure 3.2. In the conventional integration, both cells are placed next to each other. The main wastewater stream coming to the system is spilt into two streams before it is being injected into the electrodialytic cell. The resulting two streams are fed to the electrodialytic cell in a countercurrent fashion. When a potential difference is applied, concentrated solutions of metal ions are formed in alternative compartments of the cell due to the metal ion migration through the cation exchange membranes. Water can be then withdrawn as an outlet from the system. The concentrated streams of metal ions in the electrodialytic cell are directed to the electrolytic cell. The metal ions are recovered in the metallic form on the cathode of the cell as a result of the applied potential. The electrolytic cell fails to bring the concentration of metal ion to few ppms because of the reduction in the conductivity of the system as the metal ion concentration drops down. Consequently, the outlet stream of the electrolytic cell can be merged with the main wastewater stream and pumped again to the electrodialytic cell. However, this system is unattractive because the system is complicated, the wastewater has to be pumped back

and forth which would contribute to the overall system power. In addition, the power consumption is relatively high in the electrodialytic cell.

Because of these drawbacks, it was found that it would be worth if the two processes were integrated in the fashions presented in Figure 3.3 (a) for the batch system and Figure 3.3 (b) for the flow system where the disadvantages of the conventional integration can be eliminated or at least minimized. The new integrated method is made up of a number of single units connected in series. Each single unit has a cation exchange membrane, anion exchange membrane and two electrodes (cathode and anode) placed directly behind the pair of membranes. Wastewater is paced in the space between the membranes in Figure 3.3 (a) while it flows in the space between the membranes as in Figure 3.3 (b). Catholyte compartments and anolyte compartments, which are located between any two-wastewater compartments, are separated from each other with partitions that are permeable of ions only. When the potential across the membrane is applied, the metal ions will start to diffuse to the catholyte compartments. In the catholyte compartments, the metal ions will be reduced and recovered in the metallic form on the cathode surface. To test the functionality of the integrated method, a single unit as in the Figure 3.3 (c) is design. A pair of cation and anion exchange membranes is used and two electrodes are placed behind them. As a result, the system is divided into three compartments: anolyte compartment, wastewater compartment and catholyte compartment.

3.2 Objectives of the Research:

The objectives of the research are:

a. To integrate the electrolytic and electrodialytic methods synergically.

b. To investigate the effect of some parameters that influence the performance of the integrated process such as the applied potential, the concentration of the sulfuric acid in the side compartments and membrane spacing.

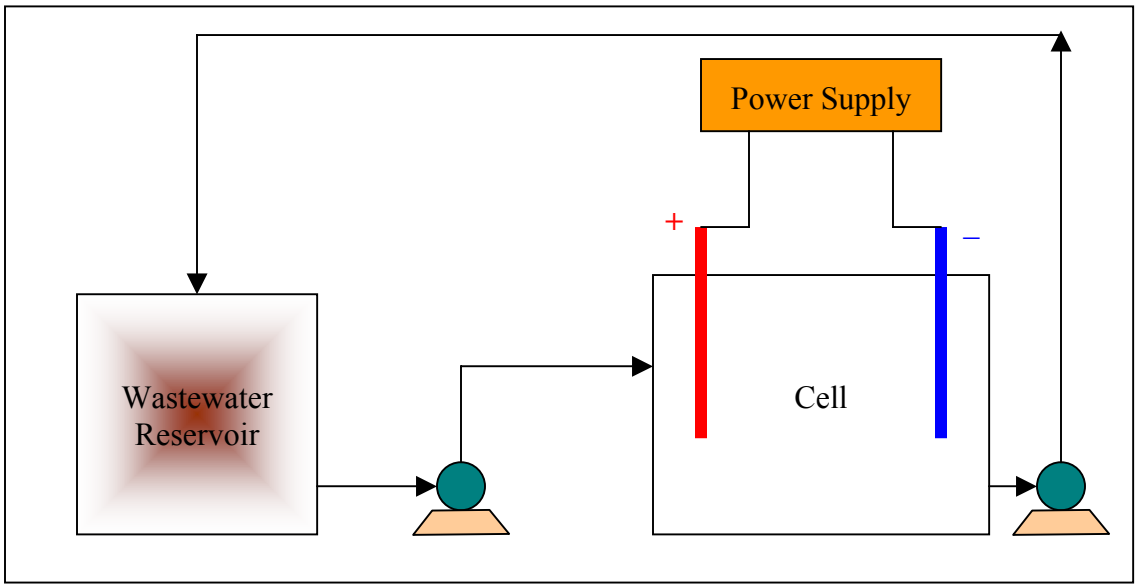

Figure 3.1: Electrochemical Removal of Metal Ions

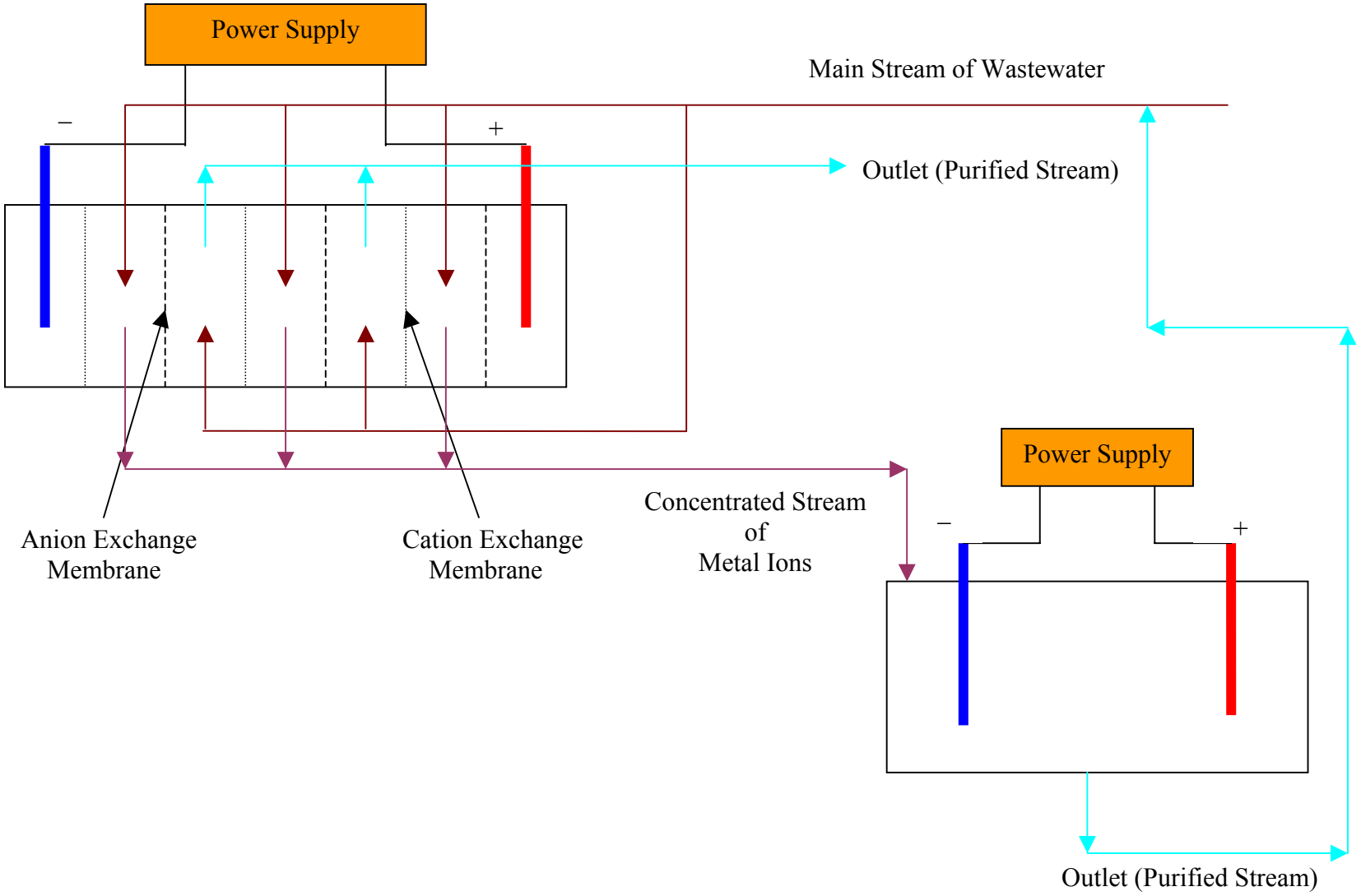

Figure 3.2: Conventional Integration of the electrolysis and electrodialysis

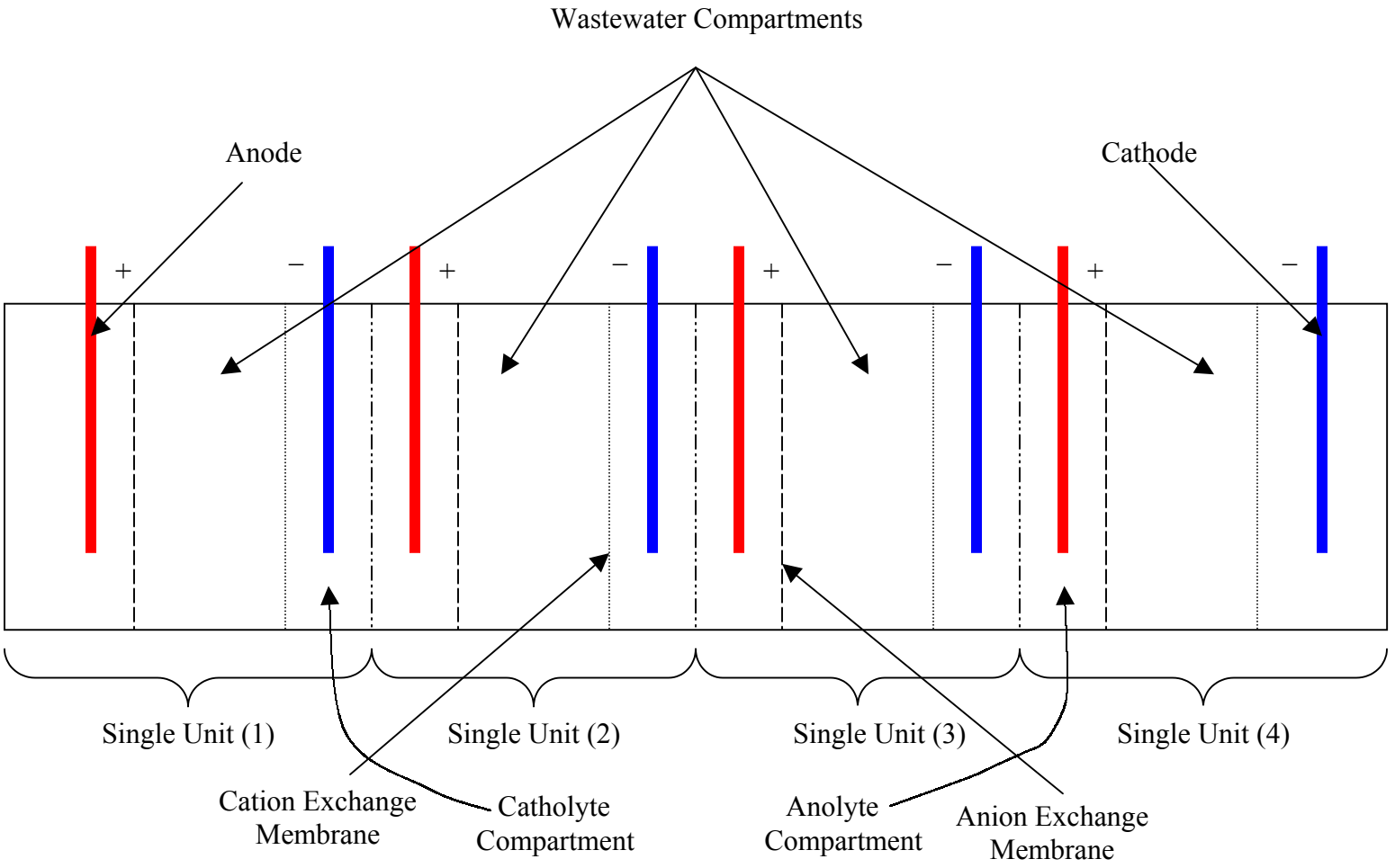

Figure 3.3 (a): Removal of Heavy Metal Ions Using the Integrated Method (Batch System)

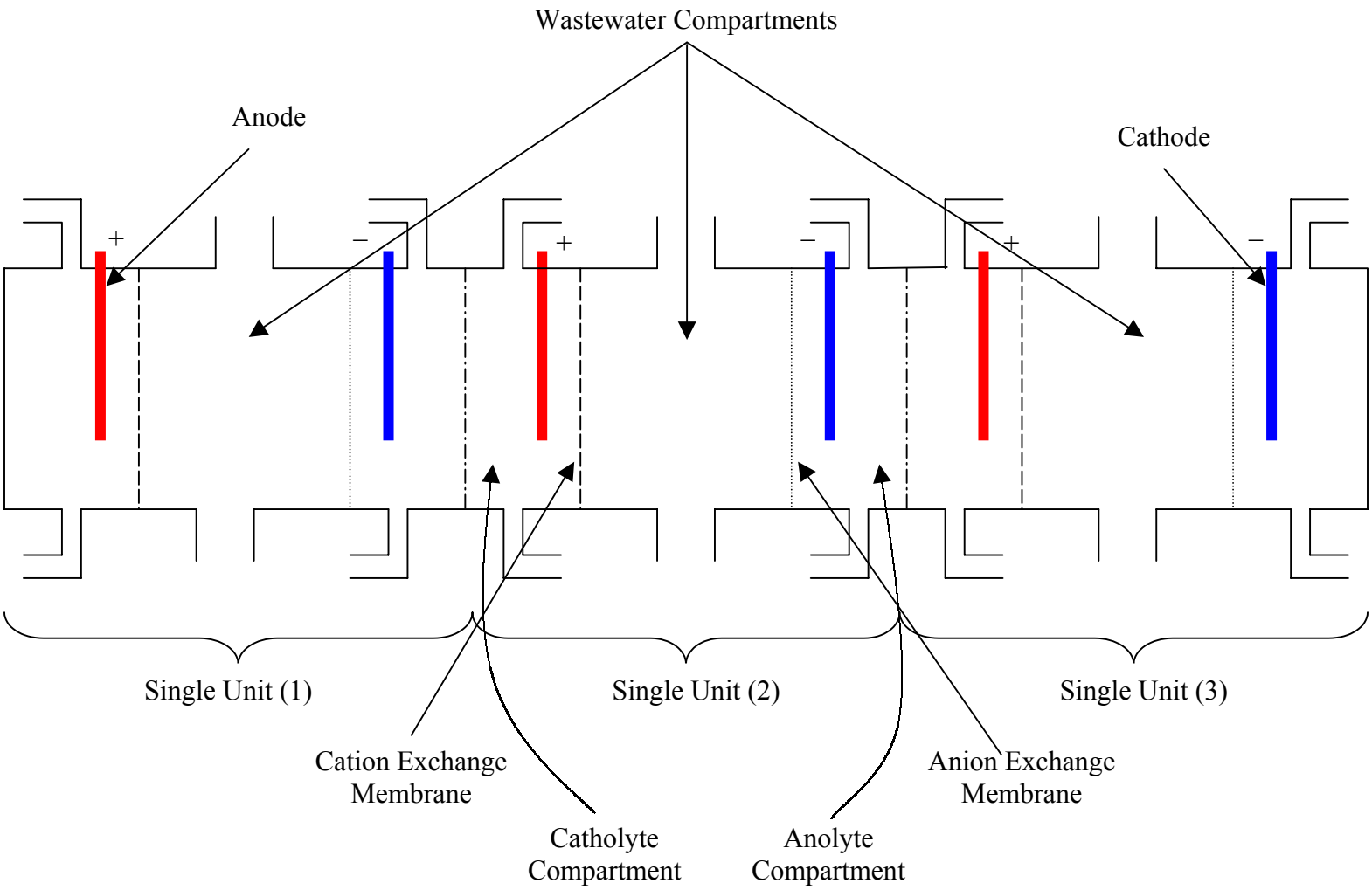

Figure 3.3(b): Removal of Heavy Metal Ions Using the Integrated Method (Flow System)

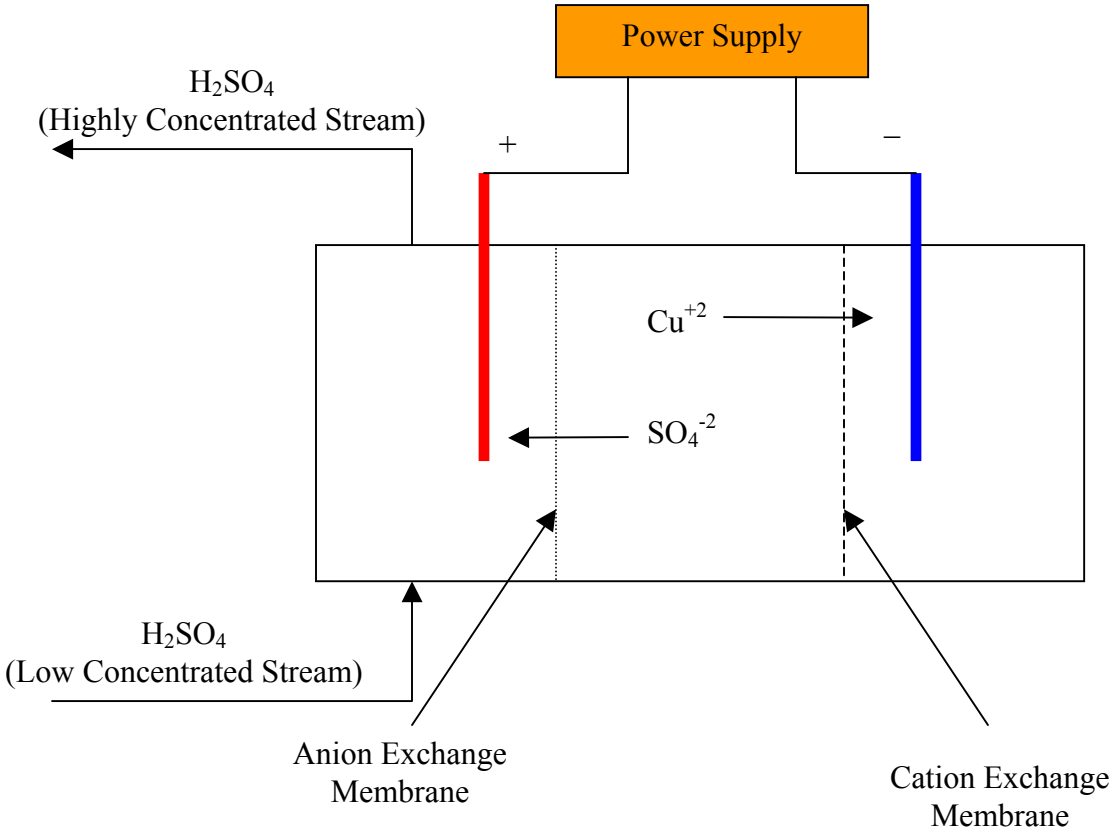

Reaction in the catholyte compartment: $2H_2O + 2e^- \rightarrow H_2(g)\uparrow + 2OH^-$

Reaction in the anolyte compartment: $2H_2O \rightarrow O_2(g) + 4H^+ + 4e^-$

Figure 3.3 (c): Removal of heavy metal ions using the integrated process (Single Unit)

CHAPTER 4

EXPERIMENTAL PROCEDURE AND SET-UP

This chapter describes the experiment setup and the construction of the main equipment, which is the integrated cell. In addition, this chapter describes the experimental procedure that was followed to achieve the desired objectives and the range of control variables changed while experiments were done.

4.1 Experimental Set-up:

An integrated electrodialytic and electrolytic cell was fabricated in a rectangular perplex tank as shown in Figure 4.1 and Figure 4.2. The cell as a single unit is 25 cm long, 10.5 cm high and 12.5 cm deep when the distance between the membranes is 7.1 cm while it is 22.9 cm long, 10.5 cm high and 12.5 cm deep when the distance between the membranes is 5.0. The dimensions of the anolyte compartment as well as the catholyte compartment were constant in all the cases. The catholyte compartment is 11.4 cm long, 10.5 cm high and 12.5 cm deep. The anolyte compartment is 6.5 cm long, 10.5 cm high and 12.5 cm deep.

The anion and cation membranes were procured from commercial supplier (Tokuyama). The pairs of the membranes used are identified as CM-1 and CM-2. They were cut in a square shape with a dimension of 15.0 cm long and 13.0 cm wide. They were stuck in their positions by using anti-acidic silicon glue. The system electrodes, which were

acquired from a commercial car battery, were cut in a rectangular shape with the following dimension: 12.5 cm long and 10.0 cm wide. Their grooves were made 0.5 cm far from the membranes in the catholyte compartment and anolyte compartment.

A Germany-made D.C. power supply was utilized. The input voltage is 220 V and it gives a range of 0.0 V to 20.0 V as an output voltage. Two multimeters, which are identified by DM 7333, were used. They were made in korea by Goldstar Corporation.

Wastewater samples collected during the experiments were analyzed using atomic absorption spectrophotometer technique. The equipment shown in Figure 4.3 was made in USA by PERKIN ELMER and its model number is 3100.

4.2 Experimental Procedure:

The integrated cell, D.C. power supply, voltammeter and the ammeter were connected as in Figure 4.1 and tested in a batch mode. The synthetic wastewater containing copper ions was used for the experiments. This wastewater was prepared by dissolving 4.00 g of copper sulfate penta hydrate ($CuSO_4.5H_2O$) and 7.1749 g of sodium sulfate in one litter of deionized water to get a copper concentration of almost 1000 ppm. Side Compartments were filled with sulfuric acid (H_2SO_4). A predefined potential difference between the two pairs of the electrodes was maintained. For a set of potential differences, current drawn by the circuit was recorded at various time intervals. As far as concentration data are concerned, 0.2 ml samples were drawn at different time interval and diluted five hundred

times by pouring them in 100 ml volumetric flask and adding 10 ml of 0.5 M nitric acid (HNO_3) and deionized water till the 100 ml mark was reached. Samples were taken till a complete depletion in terms of color occurred and stored in glass bottles. Atomic Absorption equipment was utilized to analyze the samples collected as shown in Figure 4.3.

4.3 Range of Control Variables:

The main variables and parameters changed in the experiments were:

- Cell Potential –anode to cathode voltage (V).
- Distance between membranes.
- Concentration of the sulfuric acid in the side compartments.

The range of these controlled variables used in the present work are shown in Table 4.1. All experiments were carried out at the room temperature of 25±2^{o}C.

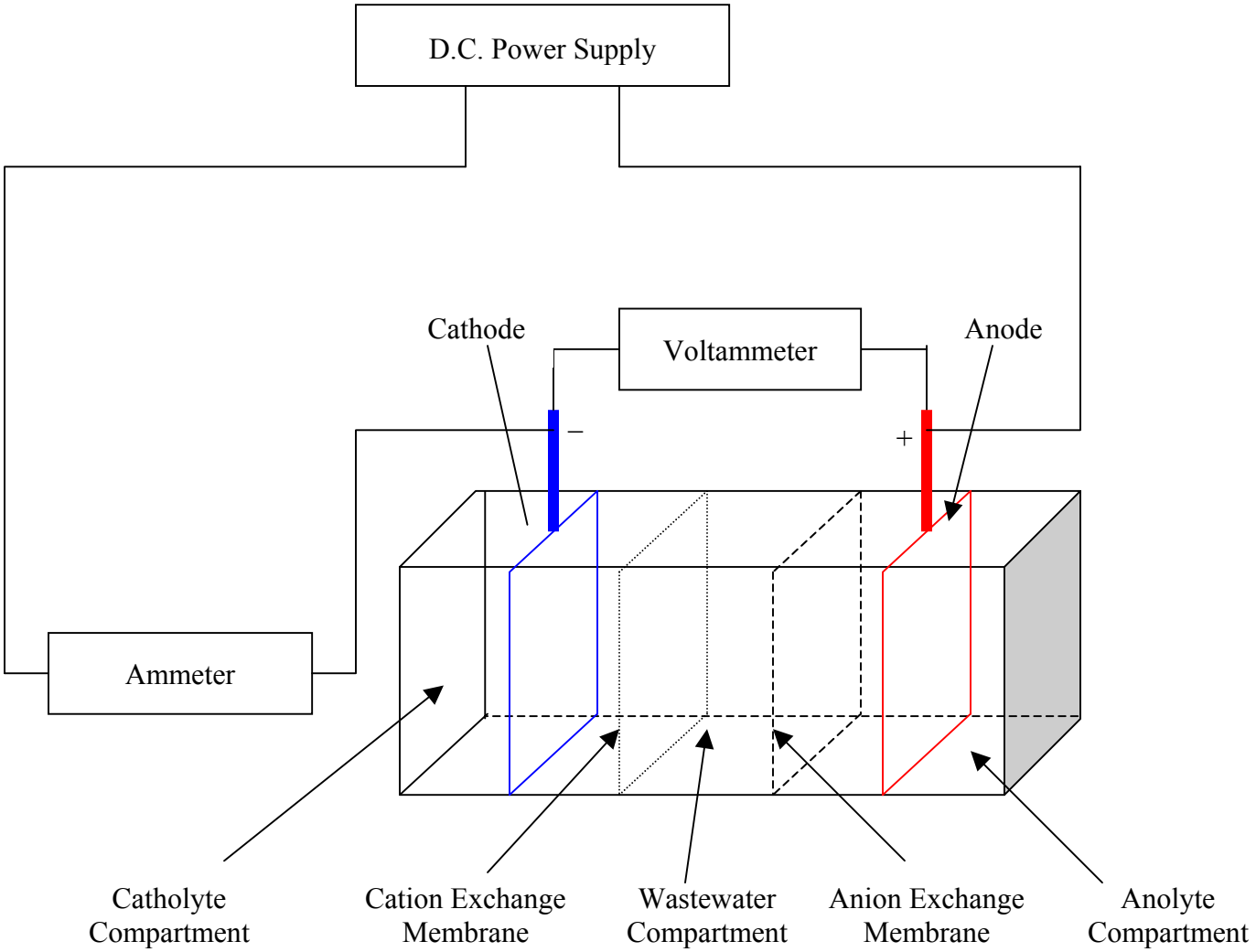

Figure 4.1: schematic diagram of the experimental set-up

Figure 4.2: Photograph of the experimental Setup

28

Figure 4.3: PERKIN ELEMER Atomic Absorption Spectrometer

29

Table 4.1: Ranges of variable parameters in the experiments

Distance Between Electrodes (cm)	H_2SO_4 concentration in the side compartments (M)	Potential (V)						
7.1	0.5	5.0	8.0	10.0	12.0	15.0	19.0	21.0
	0.25	5.0	8.0	10.0	12.0	15.0	19.0	21.0
5.0	0.5	5.0	8.0	10.0	12.0	15.0	19.0	21.0
	0.25	5.0	8.0	10.0	12.0	15.0	19.0	21.0

30

CHAPTER 5

RESULTS AND DISCUSSION

This chapter discusses the result of the copper removal from wastewater using an integrated electrolytic-electrodialytic cell. First, it presents the general performance of the process followed by discussion of various parameters that affect the performance of the integrated cell. Subsequently, the effect of the selected parameters namely; cell potentials, distance between membranes and the concentration of the side compartments on the apparent reaction rate constant is discussed. This follows, similar discussion on the power consumption and the current efficiency.

5.1 Integration of Electrolytic and Electrodialytic Process:

The objective of this work is to integrate these two processes and to take advantage of each technique. Initially, it was proposed to use Electrodialysis to decrease the concentration of the wastewater and integrate electrolytic cell to recover metal ions in the metallic form. After a set of initial experimentation, it was proposed to integrate these processes as shown in Figure 3.2 (c).

The integrated approach presented in Figure 3.2 (c) operated in a batch mode consists of a pair of membranes and electrodes. The pair of membranes, which are cation exchange membrane and anion exchange membrane, divides the system into three compartments: Anode compartment, wastewater compartment and catholyte compartment. In addition,

one electrode is placed behind each piece of membrane to supply the desirable potential difference. The electrode placed behind the cation exchange membrane is referred to as cathode and connected to the negative polarity of the power supply while the electrode placed behind the anion exchange membrane is referred to as anode and connected to the positive polarity of the power supply. Untreated wastewater which is the copper sulfate solution is placed in the middle compartment while side compartments are filled with sulfuric acid solution. When a certain potential is applied, the copper ions will diffuse though the cation exchange membrane toward the catholyte compartment. On the surface of the cathode, the reduction reaction of the copper ions will take place:

$$Cu^{+2}(aq) + 2e^{-} \rightarrow Cu(s) \quad , at\ cathode \qquad (5.1)$$

On the other hand, the side reaction that involves the reduction of water molecules and evolution of hydrogen gas would also happen on the cathode surface if high potentials were applied.

$$2H_2O + 2e^{-} \rightarrow H_2(g)\uparrow + 2OH^{-} \quad , \ at\ cathode \qquad (5.2)$$

However, the same potential that creates the diffusing of the copper will create similarly the diffusing of sulfate ions through the anion exchange membrane toward the anode compartment. On the surface of the anode, the oxidation reaction of water molecules will take place:

$$2H_2O \rightarrow 2H^{+}(aq) + 2e^{-} + O_2(g)\uparrow \ , \ at\ anode \qquad (5.3)$$

The protons being produced from the above reaction will increase the PH in the anode compartment and will combine with sulfate ions to form the sulfuric acid as a by-product. Treated water can be finally obtained from the middle compartment. This approach will offer the following advantages over the separate electrolytic and electrodialytic process:

1. Wastewater is purified to a very low concentration of metal ions in the electrodialytic part of the cell.
2. The heavy metal ions in the concentrated byproduct of electrodialytic cell are recovered as solid metal, which could be recycled.
3. As the metal deposition takes place in the concentrated solution in the cathode compartment of the electrolytic cell, the current efficiency will be high. This will reduce the power consumption rendering the proposed novel process more economical. Consequently, diluted solutions of contaminated wastewater can be treated.
4. Sulfuric acid will form as a by-product in the anode compartment.
5. No further treatment will be needed for the cathode compartment as in the electrodialytic cell.

5.2 Performance of the Proposed Method:

As mentioned earlier, the integrated cell is made up of three compartments: catholyte compartment, wastewater compartment and anolyte compartment. They are separated from each other by cation exchange membrane located between the catholyte

compartment and wastewater compartment and anion exchange membrane located between wastewater compartment and anolyte compartment. In all the experiments, the side compartments were filled with sulfuric acid of either 0.5 M or 0.25 M concentration. On the other hand, the middle compartment was filled with synthetic wastewater containing copper ions of almost 1000 ppm. In one of the experiments, the side compartments were filled with 0.5 M sulfuric acid while the middle one was filled with wastewater containing 955 ppm copper ions. When a potential of 12.0 V was applied, the copper ions started to diffuse through the cation exchange membrane and consequently their concentration dropped as time passed. The diffused copper ions through the cation exchange membrane to the catholyte compartment were reduced on the surface of the electrode to give the copper in the metallic form.

$$Cu^{+2}(aq) + 2e^{-} \rightarrow Cu(s) \quad , at\ the\ Cathode\ surface \qquad (5.4)$$

The color of the copper sulfate solution in the middle compartment was bluish at the beginning and it turned to a colorless one at the end of the experiment. At the end, the copper ion concentration could be reduced from 955.0 ppm to few ppm, as anticipated.

5.3 The Parameters Affecting the Integrating Process:

The performance of the integrated process is influenced by many parameters including the following:

1. Membrane materials:

The membrane materials affect the diffusivity of the anions and cations existing in the system when potentials are applied. Each membrane has its own diffusivity coefficient and dielectric constant that can distinguish it from others. The effect can be investigated by using different types of membrane with different diffusivity coefficients and install them in the system.

2. Temperature:

The temperature of the system is the major factor that would affect the performance of the system because it directly influences the reaction rate constant. To investigate the temperature influence, the system content temperature has to be adjusted by either passing them in a water bath or surrounding the system with a jacket.

3. Effect of the supporting salt added to the synthetic wastewater:

When the supporting salt is added to the wastewater in the system, the conductivity of the system will improve. Subsequently, the current that passes through the system will be higher and the reaction rate will be improved. The supporting salts that could be added to the system should satisfy a condition that it shouldn't agglomerate and hinder movement of the diffusing species.

4. Electrode Materials:

When the cations diffuse through the cation exchange membrane installed in the system, they are first adsorbed on the surface of the cathode, receive the deficient charges and

finally they are reduced to the metallic form covering the surface of the cathode. The electrode materials affect the performance of the system because it directly influences the rate of the adsorption step. When the electrode is fabricated from a material that makes its surface rough, more surface area will be provided and subsequently the diffusing species will be able to locate more rooms to accommodate themselves.

5. Concentration of the cations in the middle compartment:

This factor will show the same effect of the supporting salt when it is added to the synthetic wastewater. At the same potential value, the current that passes through the system will be more as the concentration of the cations increase in the wastewater. The effect of this factor can be investigated by using different wastewater stocks with different concentrations and treat them in the system.

6. Electrode Potential:

The electrode potential is the potential applied across the system electrodes and causes the cations and anions existing in the wastewater compartment to diffuse through the cation-exchange membrane and anion-exchange membrane, respectively. Increasing the electrode potential will increase the rate of the migration of the diffusing species and the rate of the reduction reaction. However, at a very high potential the rate of the apparent reaction rate constant will decrease and rate of the side reaction will become dominant.

7. Concentration of the sulfuric acid in the side compartments:

To maintain the smooth flow of the current within the system, the side compartments were filled with sulfuric acid. The concentration of the sulfuric acid added is considered as one of the parameters that can affect the performance of the system. Its effect can be illustrated by using more than one stacks of sulfuric acid with different concentrations and investigate the performance of the migrating species at each concentration.

8. Distance between membranes:

When the distance between the membranes is reduced, the system efficiency in terms of removing the metal ions will increase. The influence can be investigated by fabricating a number of wastewater compartment with different dimensions and record the observations.

Among all of these parameters, some of them are related to the materials like membrane material, electrode material whereas the others are process parameters. Investigating the effects resulting from changing the composition of the wastewater like the adding supporting salt to the synthetic wastewater or altering the concentration of the metal ions in the wastewater is not appreciable because another quantity of contaminants has to be added. Subsequently, further treatment for the added contaminants should be done. Studying the effect of the temperature will complicate the system in this stage and this is beyond our scope, which is basically concerned with checking the functionality of the new process. We have selected to study the effect of the electrode potential, distance between membranes, and the sulfuric acid concentration in the side compartments.

5.3.1 Apparent Reaction Rate Constants:

The concentrations against time data collected under different operating conditions were plotted in Figure 5.1 to Figure 5.8 on a logarithmic scale. The plot of each set of experiments done at a certain operating condition is spilt into two figures to enhance the presentation of the plots. The data could be represented by the first order reaction equation:

$$\ln C(t) = \ln C_o - kt \qquad [5.1]$$

where :

C_o : Initial Copper ion concentration.

k : Apparent reaction rate constant.

The apparent reaction rate constant presented in equation [5.1] is a lumped parameter. The metal ions in the system will be subjected to three types of mass transfer. The first type is due to the movement of the anions and cations under the influence of the potential applied across the system electrodes. This type of movement is referred to as migration. The metal ions will keep on moving till they reach the cathode surface where they will be reduced to the metallic form. Subsequently, the concentration of the metal ions next to the cathode will drop down creating a concentration gradient. The created concentration gradient will cause the metal ions to move from the higher concentration region to the lower one. This type of mass transfer is called diffusion. Since, the integrated process was operated without using any thermal gradient or stirring, the effect of the third type of mass transfer, called convection, can be neglected.

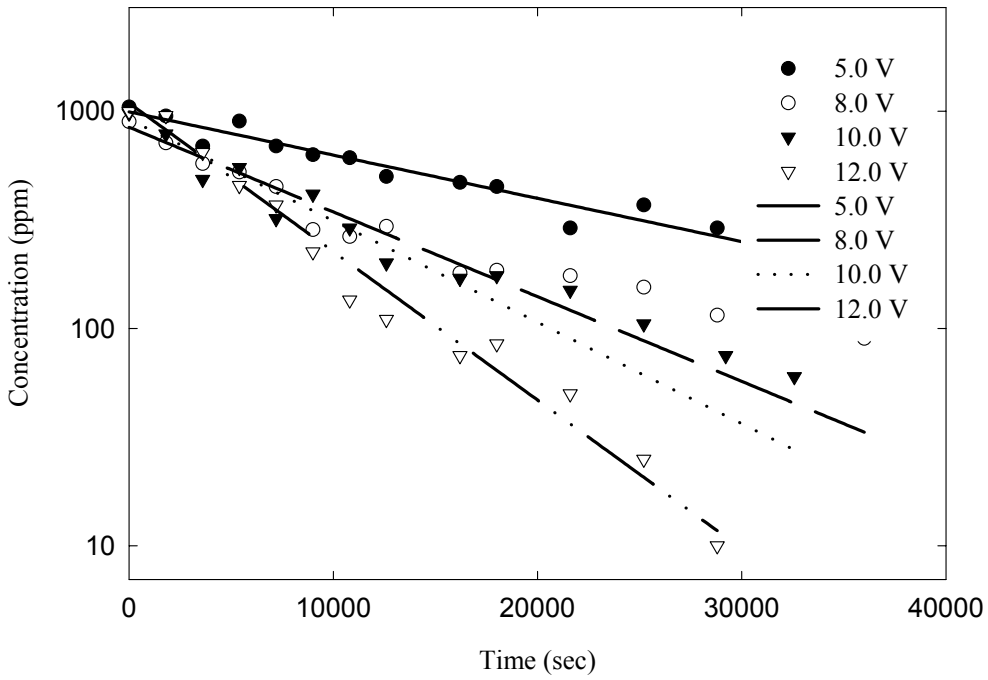

Figure 5.1: Copper Concentration versus Time at membrane spacing of 7.1 cm and side compartment concentration of 0.5 M

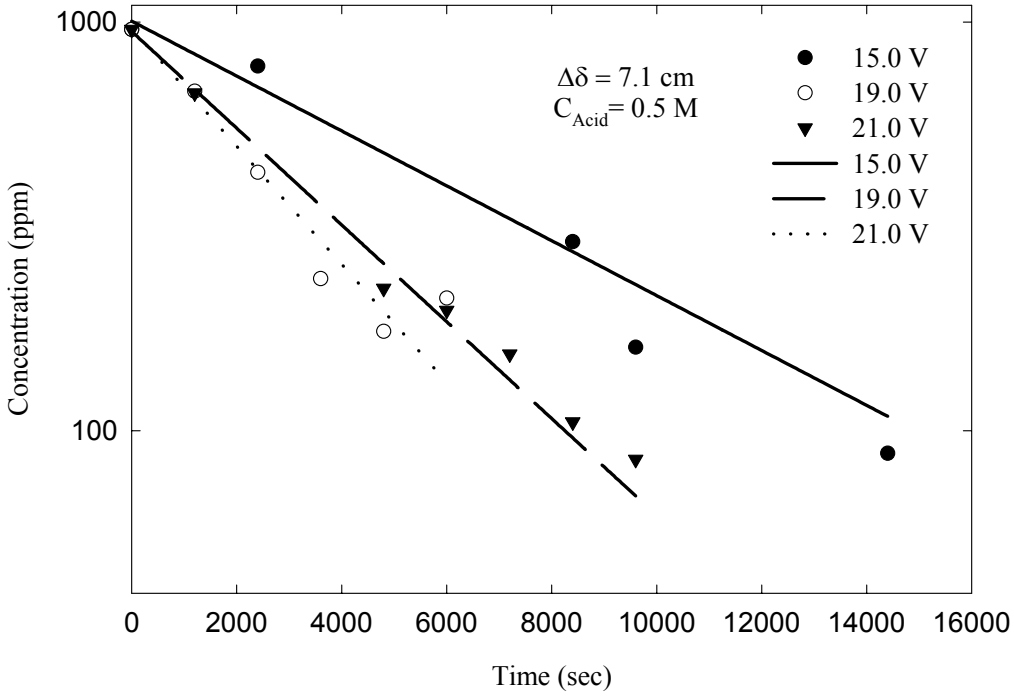

Figure 5.2 (Cont.): Copper Concentration versus Time at membrane spacing of 7.1 cm and side compartment concentration of 0.5 M

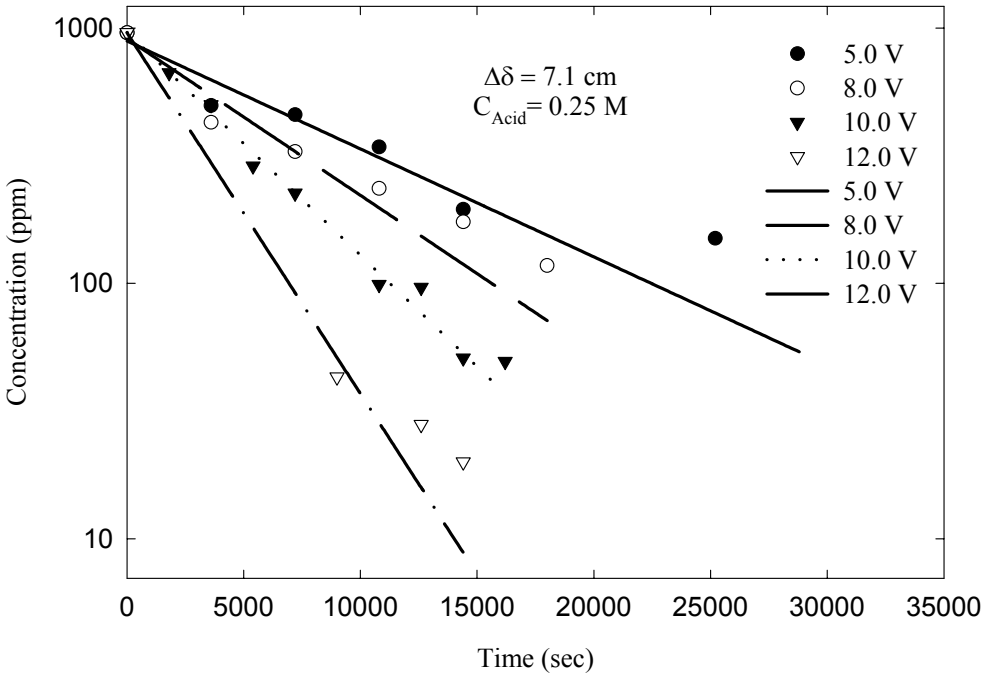

Figure 5.3: Copper Concentration versus Time at membrane spacing of 7.1 cm and side compartment concentration of 0.25 M

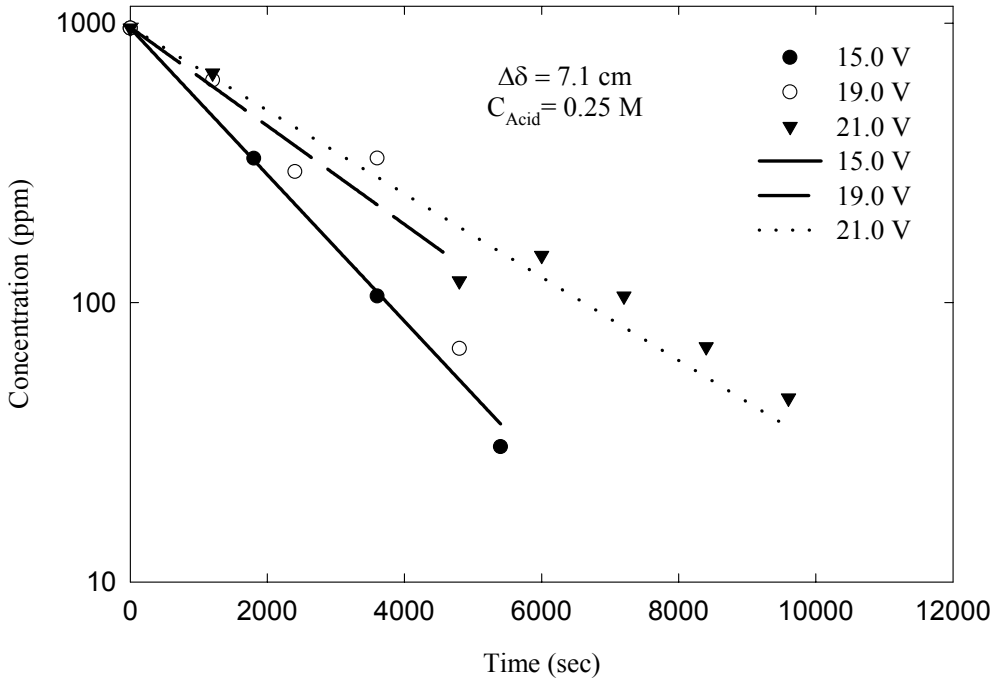

Figure 5.4 (Cont.): Copper Concentration versus Time at membrane spacing of 7.1 cm and side compartment concentration of 0.25 M

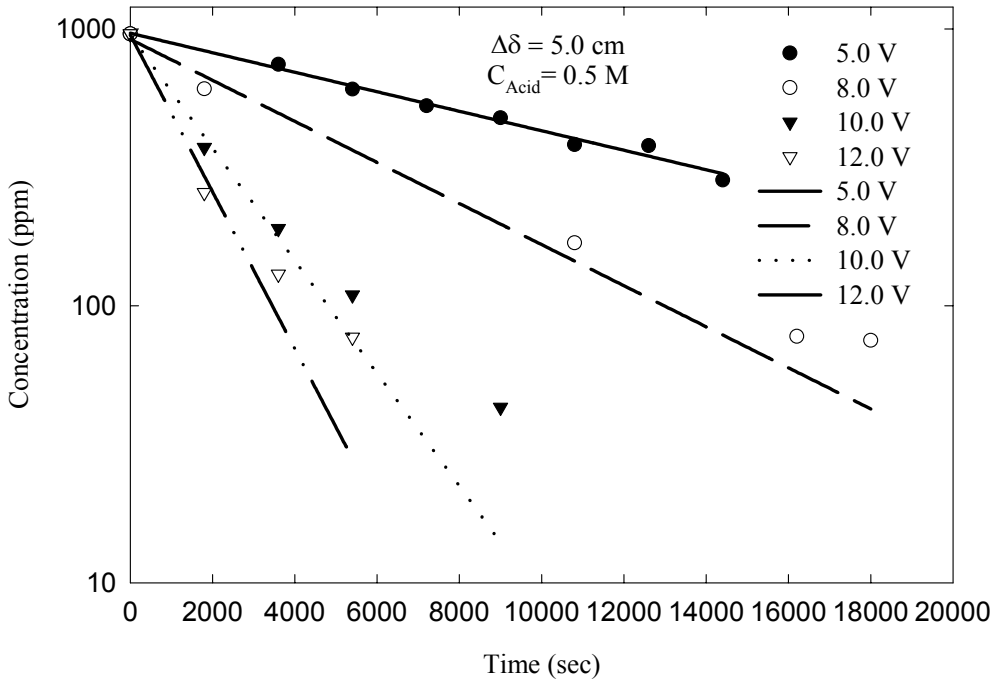

Figure 5.5: Copper Concentration versus Time at membrane spacing of 5.0 cm and side compartment concentration of 0.5 M

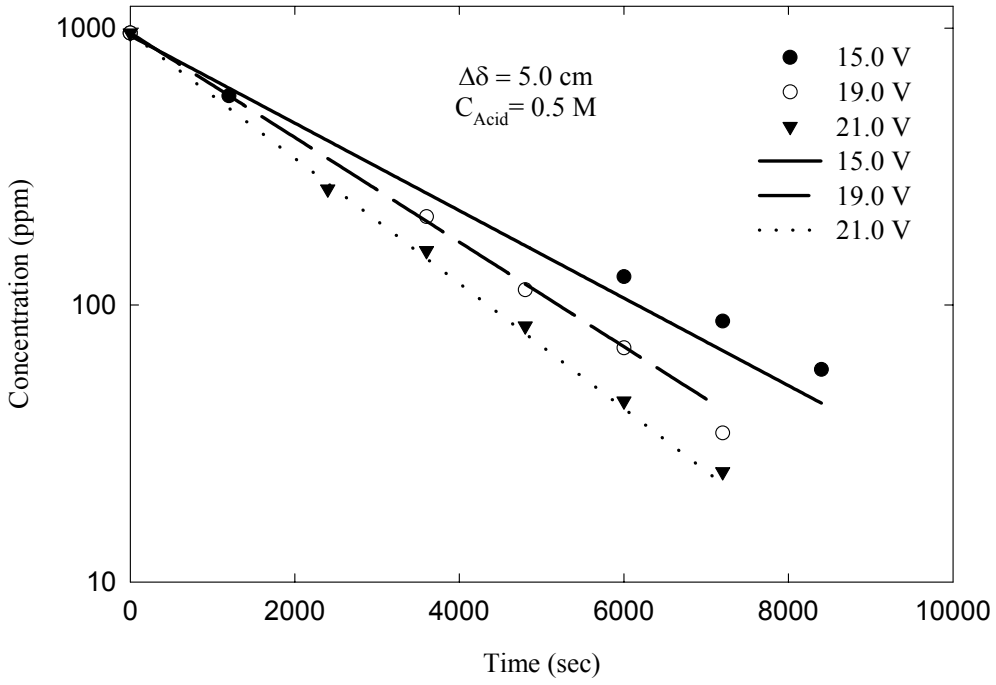

Figure 5.6 (Cont.): Copper Concentration versus Time at membrane spacing of 5.0 cm and side compartment concentration of 0.5 M

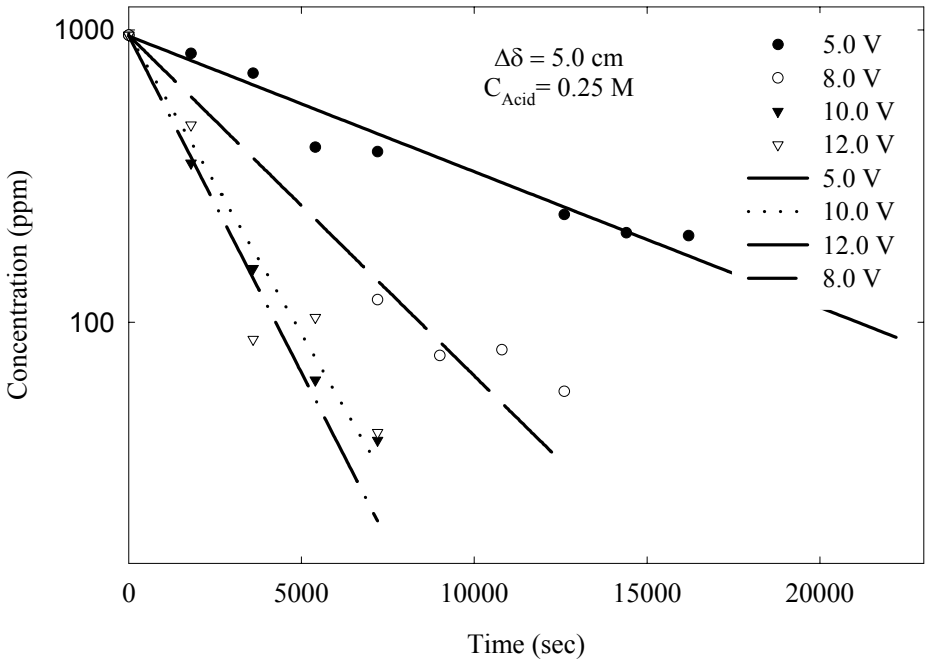

Figure 5.7: Copper Concentration versus Time at membrane spacing of 5.0 cm and side compartment concentration of 0.25 M

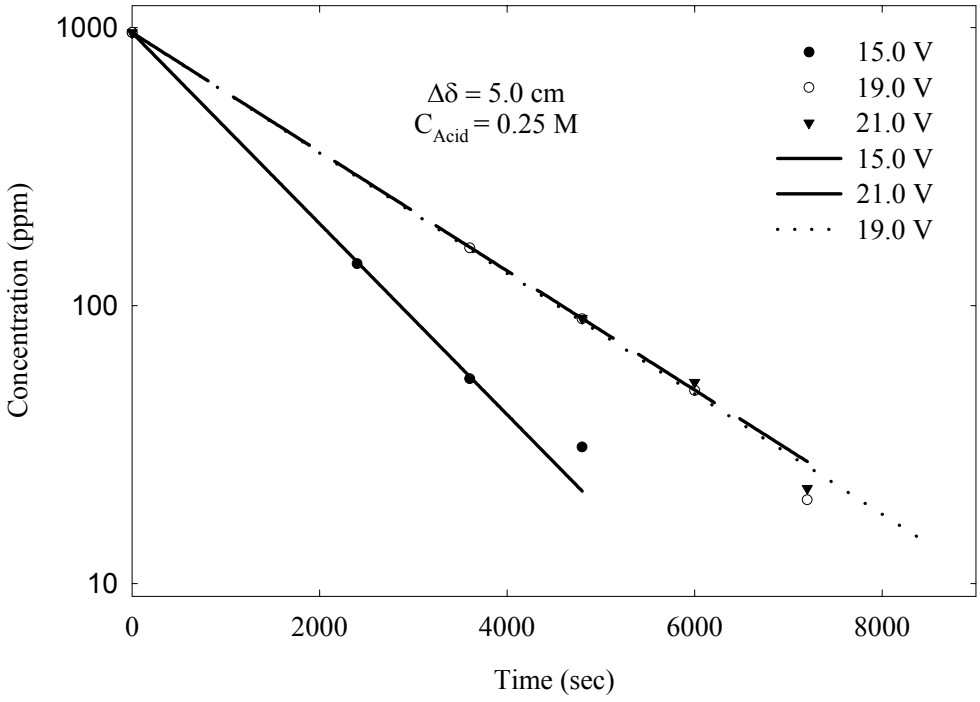

Figure 5.8 (Cont.): Copper Concentration versus Time at membrane spacing of 5.0 cm and side compartment concentration of 0.25 M

In conclusion, the apparent reaction rate constant calculated from equation [5.1] has a contribution from reaction rate constant, mass transfer coefficient and side reaction rate. It could be affected by cell voltages, membrane spacing, temperature and concentration of the sulfuric acid in the side compartments.

5.3.1.a Effect of the Applied Potential:

The apparent reaction rate constant derived from Figure 5.1 to 5.8 is plotted against cell potential in Figure 5.9 for the distance between the membranes of 7.1 cm and the sulfuric acid concentration in the side compartments of 0.5 M. The apparent reaction rate constant increases with the cell potentials till it reached a maximum then it drops down. The trend can be divided into two regimes. In the first regime, the apparent reaction rate constant increases as the potential of the cell increases and the process become kinetic controlled. Then, in the second regime, the apparent reaction rate constant decreases as the potential increases and the process becomes mass transfer controlled. The drop in the trend is because of the side reaction rate that becomes dominant as the cell potential increases.

The apparent reaction rate constant is plotted against cell potential in Figure 5.10 at a membrane distance of 7.1 cm and sulfuric acid concentration of 0.25 M. The apparent reaction rate constant increases as the cell potential increases, reaches a maximum then it drops down.

When the potential across the electrodes is increased, this action works in favor of the reduction reaction of the copper ions to the metallic form and the process at this stage becomes kinetic controlled. As the cell potential is increased, the process starts becoming mass transfer controlled till a drop in the apparent reaction rate constant occurs due to the dominance of the side reaction rates.

The apparent reaction rate constant is plotted against cell potentials in Figure 5.11 & 5.12 at a membrane distance of 5.0 cm and sulfuric acid concentration of 0.5 and 0.25, respectively. The apparent reaction rate constant increases as the cell potential increases till it reaches a maximum. Then, it goes down because the side reactions at high cell potential become dominant and the process becomes mass transfer controlled.

5.3.1.b Effect of the Membrane Spacing:

The apparent reaction rate constant is plotted against cell potential in Figure 5.13 and 5.14 at two different membrane spacing and sulfuric acid in the side compartments. In both figures and at the two different membrane spacing, the apparent reaction rate constant increases as the cell potential increase. However, the at a membrane spacing of 5.0 cm, the apparent reaction rate constant is higher than those at a membrane spacing of 7.1 cm. When the distance between the membranes is decreased, the ohmic resistance between the electrodes is also decreased. Subsequently, the apparent reaction rate constant becomes high. The numerical values of the apparent reaction rate constant are listed in tables 5.1 and 5.2 at sulfuric concentration of 0.5 M and 0.25 M, respectively.

The effect of the distance between the membranes was tried to be further investigated by decreasing the spacing from 5.0 cm to 2.0 cm. The test couldn't success because at that distance high current flowed in the system resulting in burning the fuses of the ammeter.

5.3.1.c Effect of the Sulfuric Acid Concentration in the Side Compartments:

Figures 5.15 and 5.16 show the effect of the concentration of the sulfuric acid in the side compartments on the apparent reaction rate constant. In these two figures, the apparent reaction rate constants are plotted against cell potentials at different concentration of the sulfuric acid in the side compartments. The trend in both figures shows that the apparent reaction rate constants increase as the cell potentials increase. Using a sulfuric acid concentration of 0.25 M in the side compartments could improve the apparent reaction rate constants much better than using a sulfuric acid concentration of 0.5 M in the side compartments. When highly concentrated sulfuric acid is used, the acid ions will accumulate on the membrane surfaces hindering the diffusion of the copper ions. This phenomenon is referred to as concentration polarization. Tables 5.3 and 5.4 list the numerical values of the apparent reaction rate constant at two different values of sulfuric acid concentration 0.5 M and 0.25 M.

5.3.2 The Power Consumption:

Energy consumed to remove a kilogram of copper ions was calculated by integrating the function resulting by multiplying the cell potential with the current equation between the

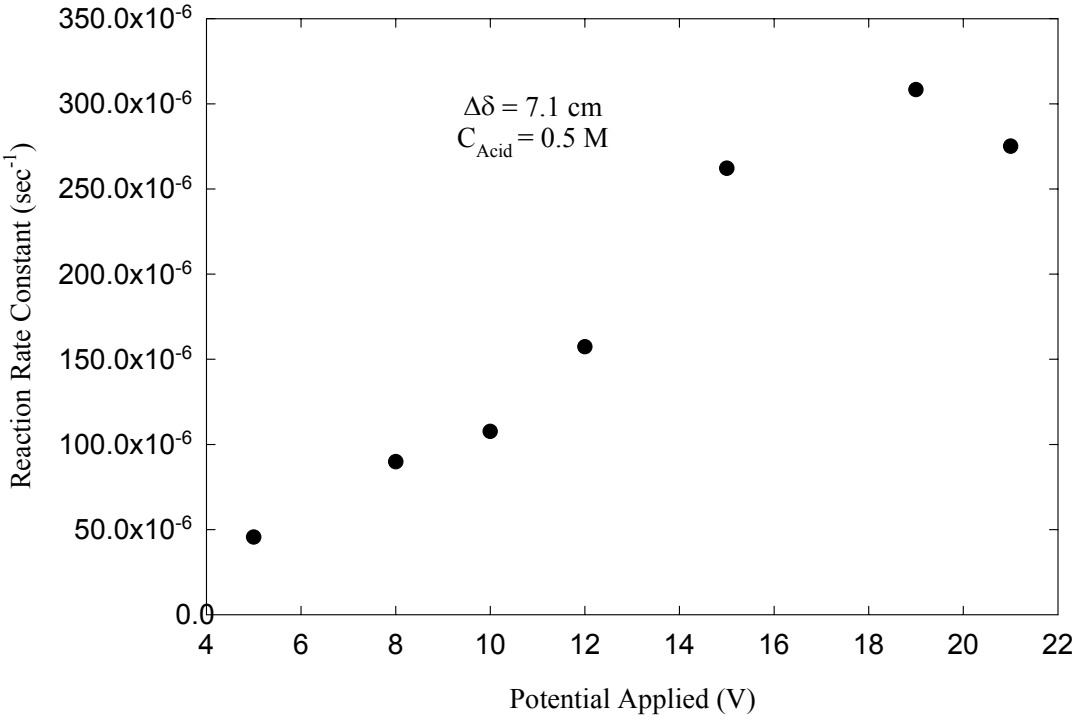

Figure 5.9: Reaction Rate Constant versus Potential at membrane spacing of 7.1 cm and side compartment concentration of 0.5 M

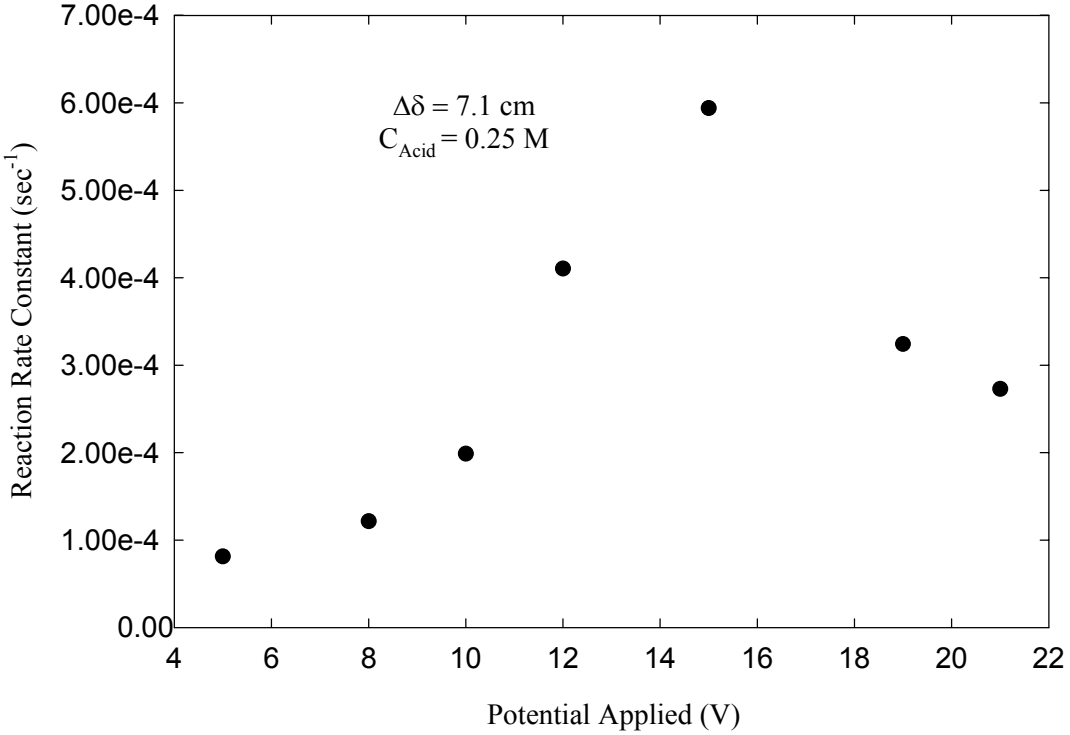

Figure 5.10: Reaction Rate Constant versus Potential at membrane spacing of 7.1 cm and side compartment concentration of 0.25 M

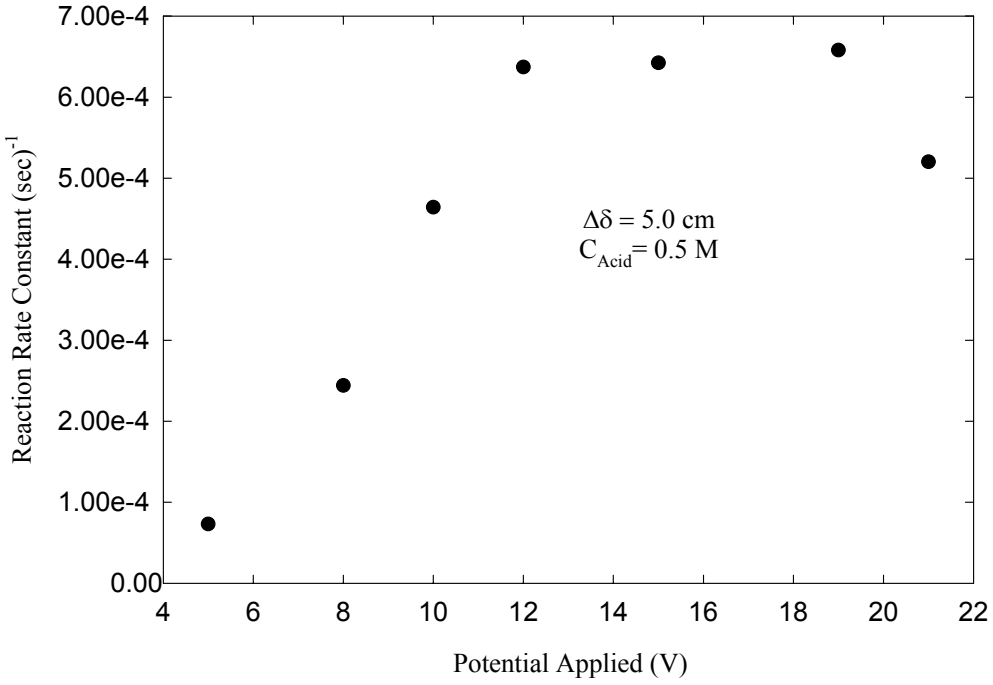

Figure 5.11: Reaction Rate Constant versus Potential at membrane spacing of 5.0 cm and side compartment concentration of 0.5 M

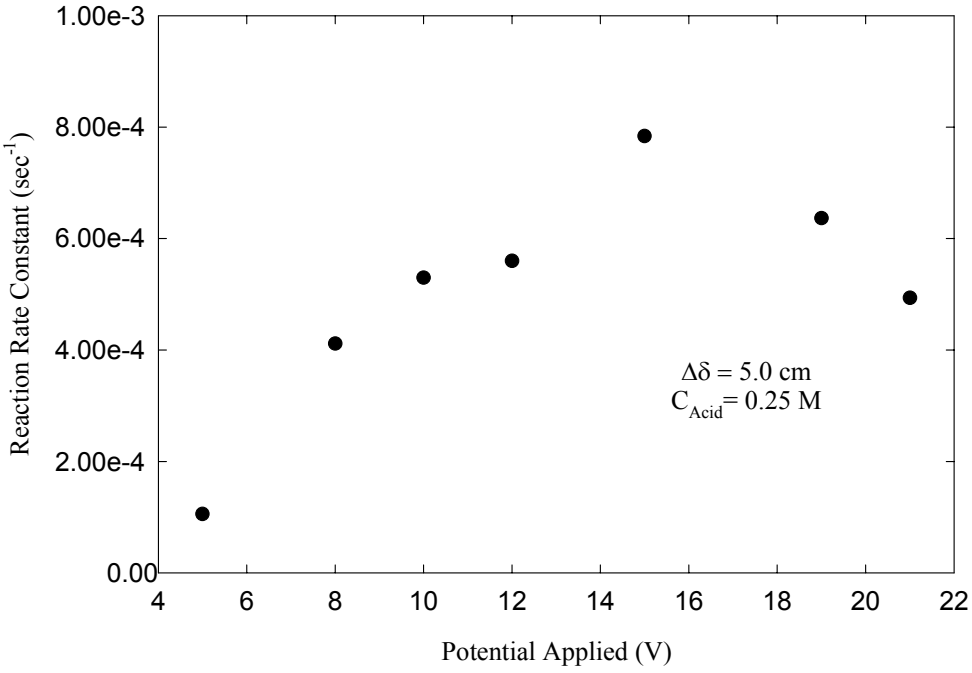

Figure 5.12: Reaction Rate Constant versus Potential at membrane spacing of 5.0 cm and side compartment concentration of 0.25 M

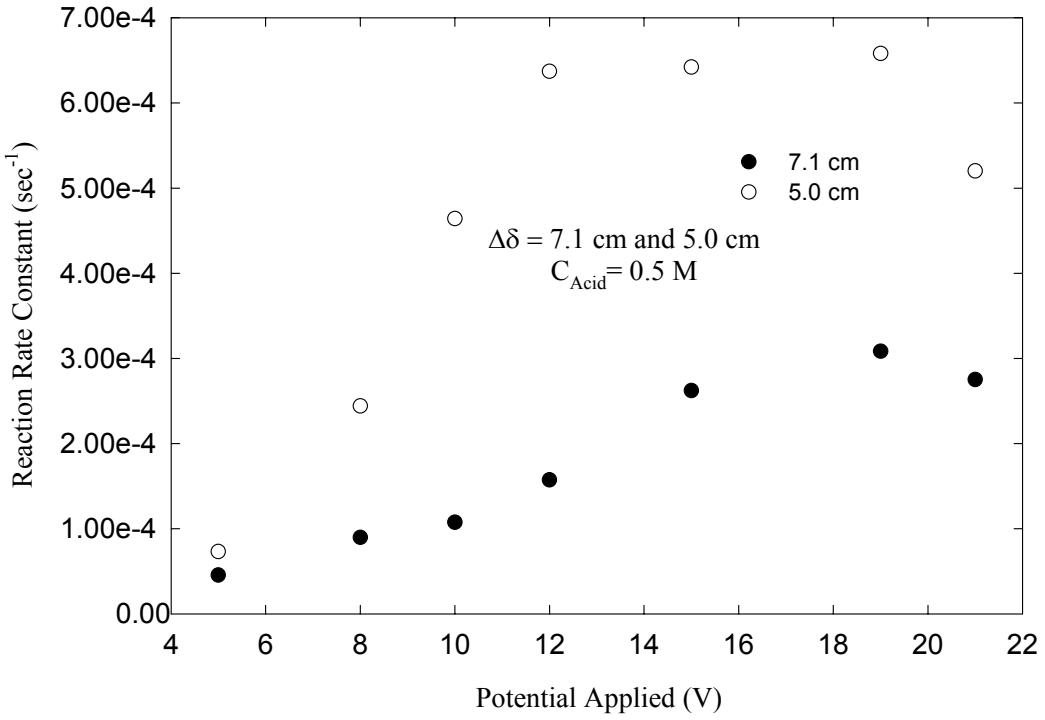

Figure 5.13: Reaction Rate Constant versus Potential at membrane spacing of 7.1 cm and 5.0 cm and side compartment concentration of 0.5 M

Table 5.1: Apparent reaction rate constant values at a sulfuric acid concentration of 0.5 M and two different distances between membranes

Cell Potential (V)	Distance Between Membranes=7.1 cm	Distance Between Membranes=5.0 cm
	Apparent reaction rate constant (sec^{-1})	Apparent reaction rate constant (sec^{-1})
5.0	4.5500×10^{-5}	7.3120×10^{-5}
8.0	8.9780×10^{-5}	2.4410×10^{-4}
10.0	1.0760×10^{-4}	4.6420×10^{-4}
12.0	1.5730×10^{-4}	6.3710×10^{-4}
15.0	2.6210×10^{-4}	6.4220×10^{-4}
19.0	3.0830×10^{-4}	6.5790×10^{-4}
21.0	2.7510×10^{-4}	5.2020×10^{-4}

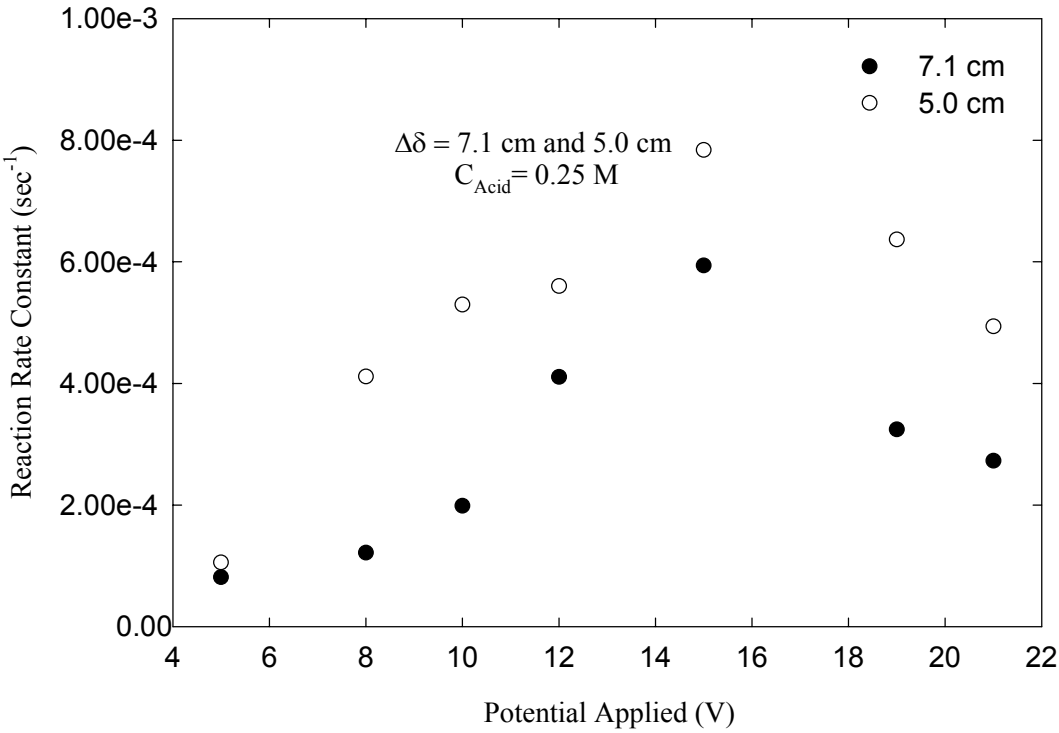

Figure 5.14: Reaction Rate Constant versus Potential at membrane spacing of 7.1 cm and 5.0 cm and side compartment concentration of 0.25 M

Table 5.2: Apparent reaction rate constant values at a sulfuric acid concentration of 0.25 M and two different distances between membranes

Cell Potential (V)	Distance Between Membranes=7.1 cm	Distance Between Membranes=5.0 cm
	Apparent reaction rate constant (sec^{-1})	Apparent reaction rate constant (sec^{-1})
5.0	8.1360×10^{-5}	1.0560×10^{-4}
8.0	1.2150×10^{-4}	4.1120×10^{-4}
10.0	1.9880×10^{-4}	5.2950×10^{-4}
12.0	4.1040×10^{-4}	5.5990×10^{-4}
15.0	5.9390×10^{-4}	7.8400×10^{-4}
19.0	3.2420×10^{-4}	6.3630×10^{-4}
21.0	2.7270×10^{-4}	4.9350×10^{-4}

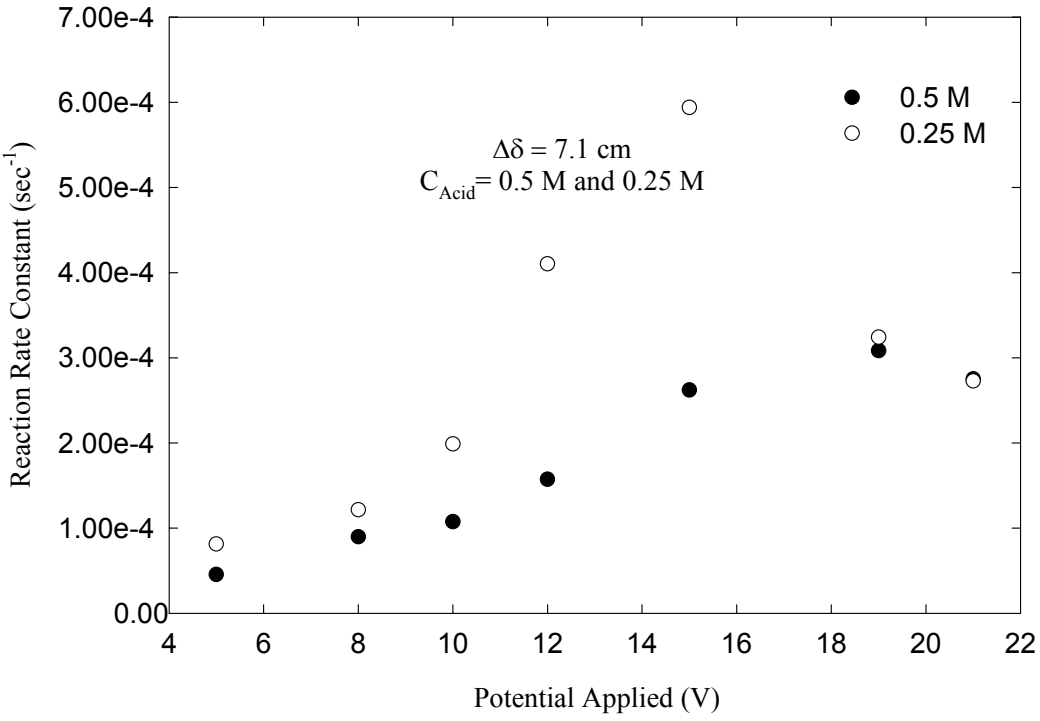

Figure 5.15: Reaction Rate Constant versus Potential at membrane spacing of 7.1 cm and side compartment concentration of 0.5 M and 0.25 M

Table 5.3: Apparent reaction rate constant values when the distance between the membranes is 7.1 cm and two different concentrations of sulfuric acid in the side compartments

Cell Potential (V)	H_2SO_4 concentration= 0.5 M	H_2SO_4 concentration= 0.25 M
	Apparent reaction rate constant (sec^{-1})	Apparent reaction rate constant (sec^{-1})
5.0	4.5500×10^{-5}	8.1360×10^{-5}
8.0	8.9780×10^{-5}	1.2150×10^{-4}
10.0	1.0760×10^{-4}	1.9880×10^{-4}
12.0	1.5730×10^{-4}	4.1040×10^{-4}
15.0	2.6210×10^{-4}	5.9390×10^{-4}
19.0	3.0830×10^{-4}	3.2420×10^{-4}
21.0	2.7510×10^{-4}	2.7270×10^{-4}

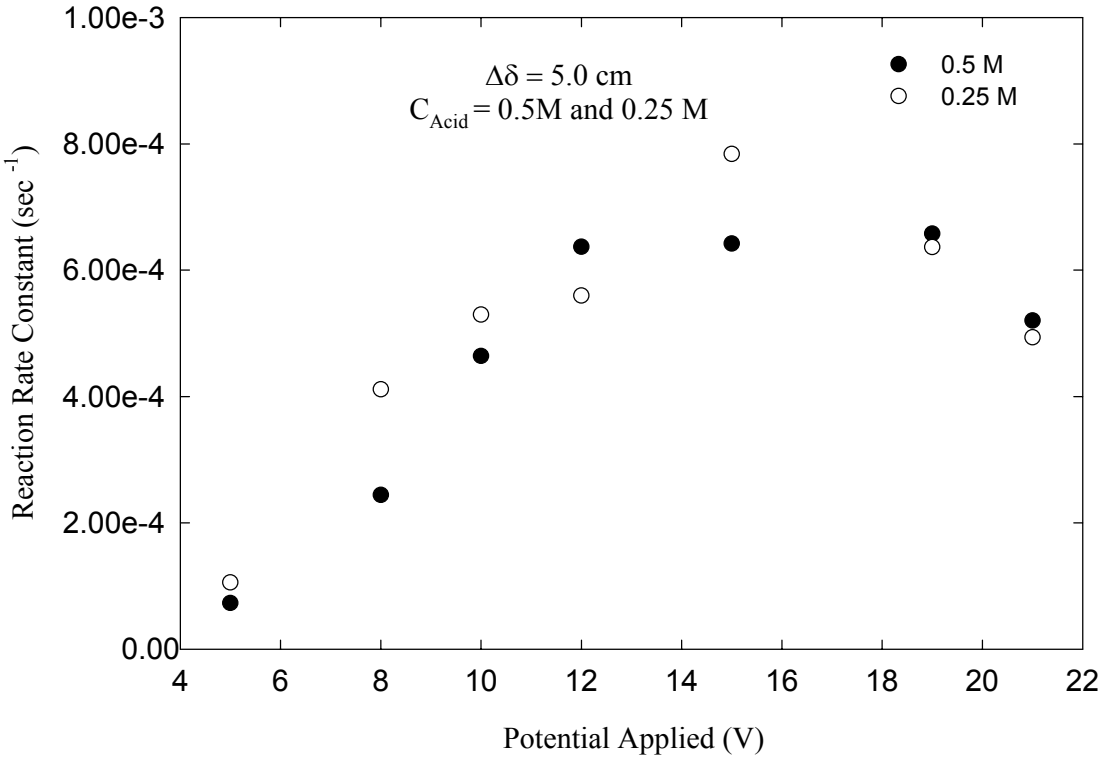

Figure 5.16: Reaction Rate Constant versus Potential at membrane spacing of 5.0 cm and side compartment concentration of 0.5 M and 0.25 M

Table 5.4: Apparent reaction rate constant values when the distance between the membranes is 5.0 cm and two different concentrations of sulfuric acid in the side compartments

Cell Potential (V)	H_2SO_4 concentration= 0.5 M	H_2SO_4 concentration= 0.25 M
	Apparent reaction rate constant (sec^{-1})	Apparent reaction rate constant (sec^{-1})
5.0	7.3120×10^{-5}	1.0560×10^{-4}
8.0	2.4410×10^{-4}	4.1120×10^{-4}
10.0	4.6420×10^{-4}	5.2950×10^{-4}
12.0	6.3710×10^{-4}	5.5990×10^{-4}
15.0	6.4220×10^{-4}	7.8400×10^{-4}
19.0	6.5790×10^{-4}	6.3630×10^{-4}
21.0	5.2020×10^{-4}	4.9350×10^{-4}

initial time and the moment of time at which the rate of reaction is almost constant. It can be represented mathematically by:

$$\frac{dC_{Cu}}{dt} \approx 0 \qquad [5.2]$$

Next, the resulting value is divided by the amount of copper removed in the period. The current and the time data were fitted into a third order polynomial. The equation representing the energy consumption is:

$$E(\frac{W}{Kg}) = \frac{\int_0^t VI(t)\,dt}{W} = \frac{V\int_0^t I(t)\,dt}{W} \qquad [5.3]$$

where:

E: Energy consumed to remove certain amount of copper (W/Kg)

V: Cell Potential (V)

t: Time (Seconds)

W: weight of copper amount (Kg)

A computer code using Matlab was used to calculate the energy consumed at each run (Appendix A3-1). The code was provided with the current equation, concentration equation, initial time and final time. This intensive quantity can be affected by a number of parameter. The effect of cell potential, distance between membranes and the concentration of the side compartments are illustrated as follows:

5.3.2.a Effect of Cell Potential:

The energy consumptions are plotted against the cell potentials in Figures 5.17, 5.18, 5.19, and 5.20. The energy consumptions decrease as the cell potential increase till they reach a minimum then they keep on increasing as the cell potentials increase. The energy consumptions decrease at the beginning because most of the energy provided to the system will be consumed in overcoming the ohmic resistance between the system electrodes as well as enhancing the rate of the reduction reaction of the copper ions. Subsequently, more copper ions will be recovered at low cell potentials. However, at high cell potentials; the energy supplied to the system will be used in overcoming the mass transfer resistance as well as in enhancing the rate of the side reactions involving the breakage of water.

5.3.2.b Effect of Membrane Spacing:

The energy consumption is plotted against cell potential in Figure 5.21 and Figure 5.22 at two different membrane spacing, namely 7.1 cm and 5.0 cm. In both trends, the energy consumption deceases as the cell potential increases till it reaches a minimum then after that it increases as the potential increases. When the distance between the membranes is reduced from 7.1 cm to 5.0 cm, the energy consumption also decreased due to the reduction in the ohmic resistance between the system electrodes.

5.3.2.c Effect of the Sulfuric Acid Concentration in the Side Compartments:

The effect of the sulfuric acid concentration in side compartments on the energy consumption is presented in Figure 5.23 and 5.24. The energy consumption is plotted against the cell potentials. The data points follow a certain trend in which the energy consumption decreases as the cell potentials increase because of insignificant of the mass transfer effect and ohmic resistance between the electrodes. Then, it gets increased as the cell potentials increase because the energy spent at this stage enhance the rate of the side reactions and decelerate the rate of copper depletion.

5.3.3 The Current Efficiency:

The current efficiency is obtained by comparing the mass of copper recovered from the wastewater at the end of the run to the total charge passed during the run. It can be interpreted mathematically as:

$$Current\ Efficiency = \frac{W}{\frac{M}{nF}\int_0^{\theta} Idt} \times 100 \qquad [5.3]$$

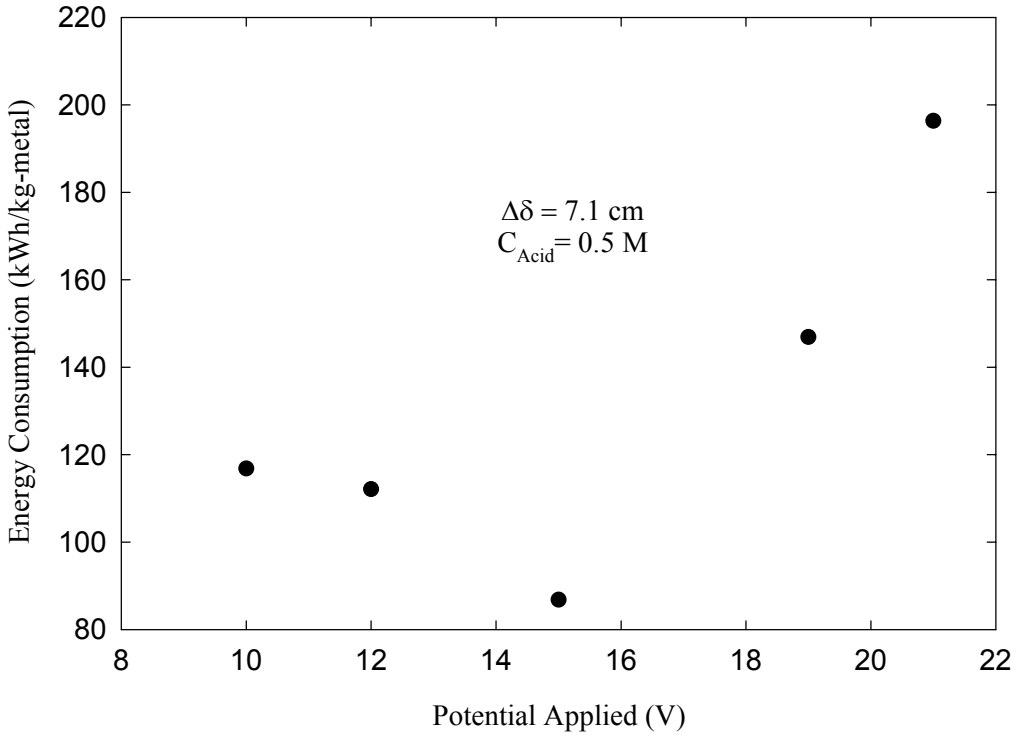

Figure 5.17: Energy consumption versus potential applied at membrane spacing of 7.1 cm and side concentration of sulfuric acid of 0.5 M

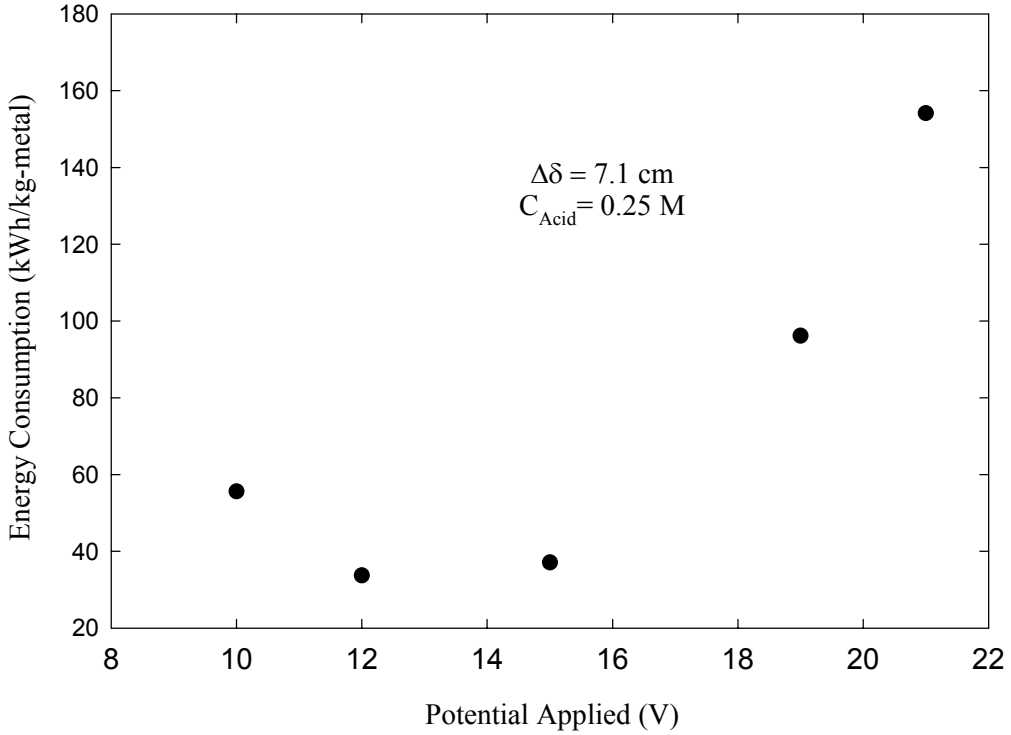

Figure 5.18: Energy consumption versus potential applied at membrane spacing of 7.1 cm and side concentration of 0.25 M

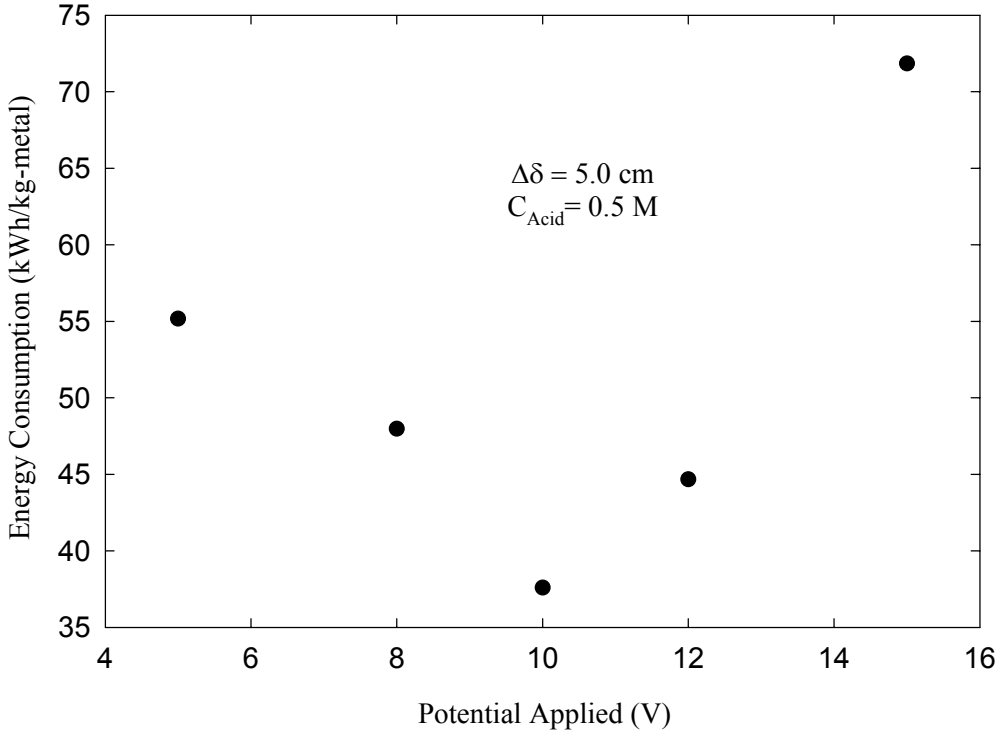

Figure 5.19: Energy consumption versus potential applied at membrane spacing of 5.0 cm and side concentration of 0.5 M

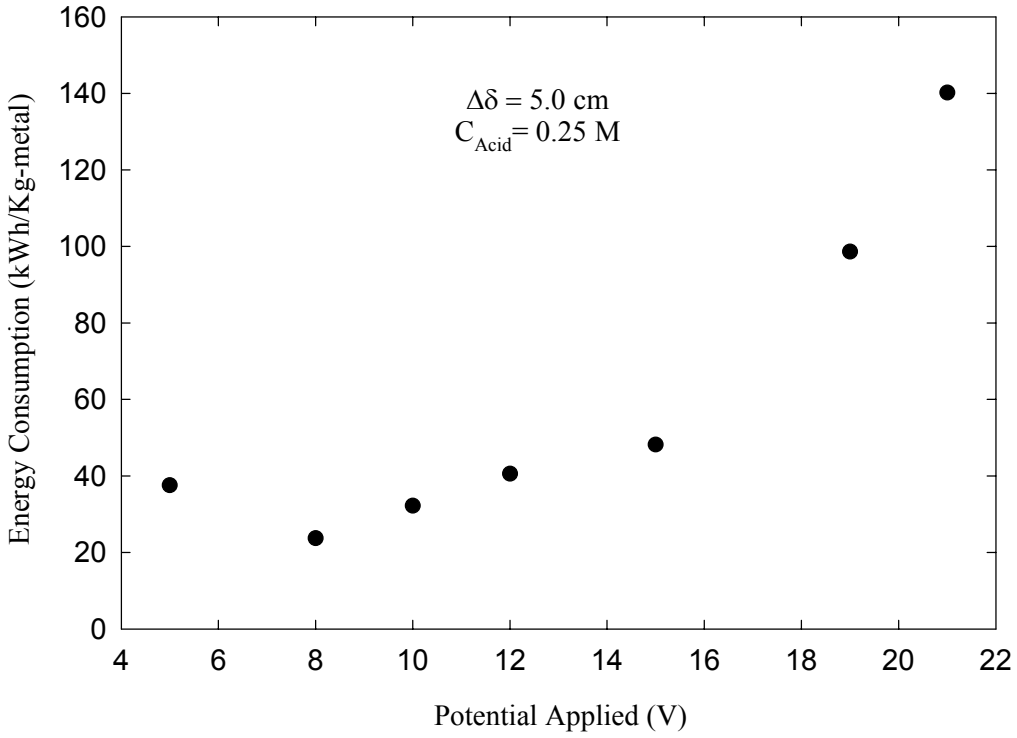

Figure 5.20: Energy consumption versus potential applied at membrane spacing of 5.0 cm and side concentration of 0.25 M

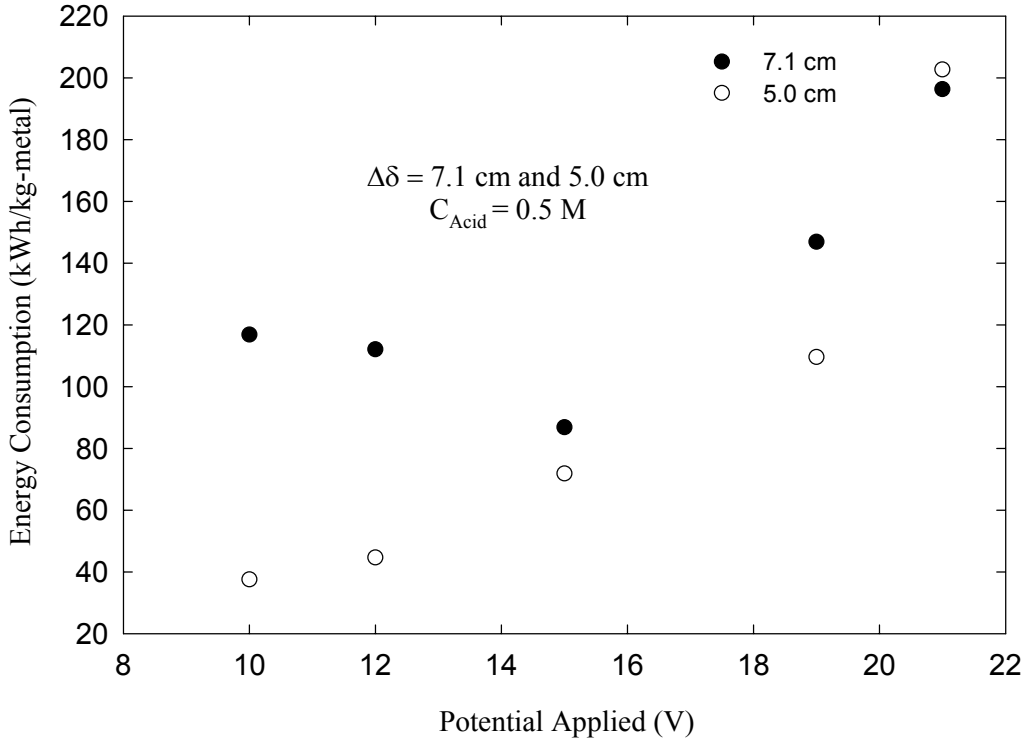

Figure 5.21: Energy consumption versus potential applied at membrane spacing of 7.1 cm and 5.0 cm and side concentration of 0.5 M

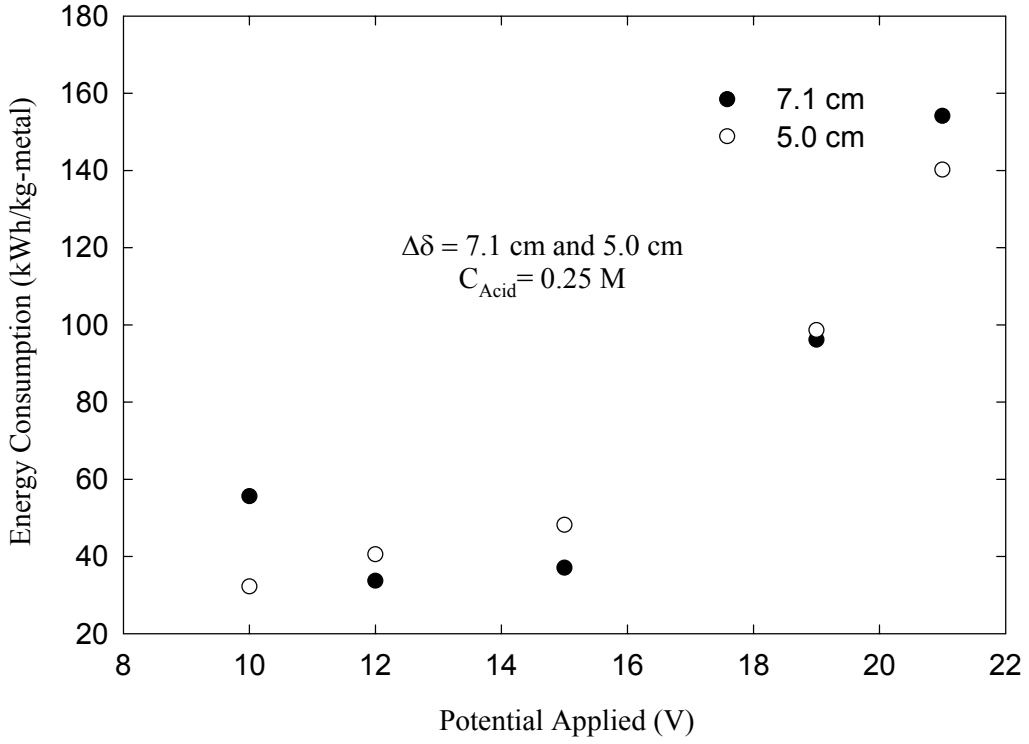

Figure 5.22: Energy consumption versus potential applied at membrane spacing of 7.1 cm and 5.0 cm and side concentration of 0.25 M

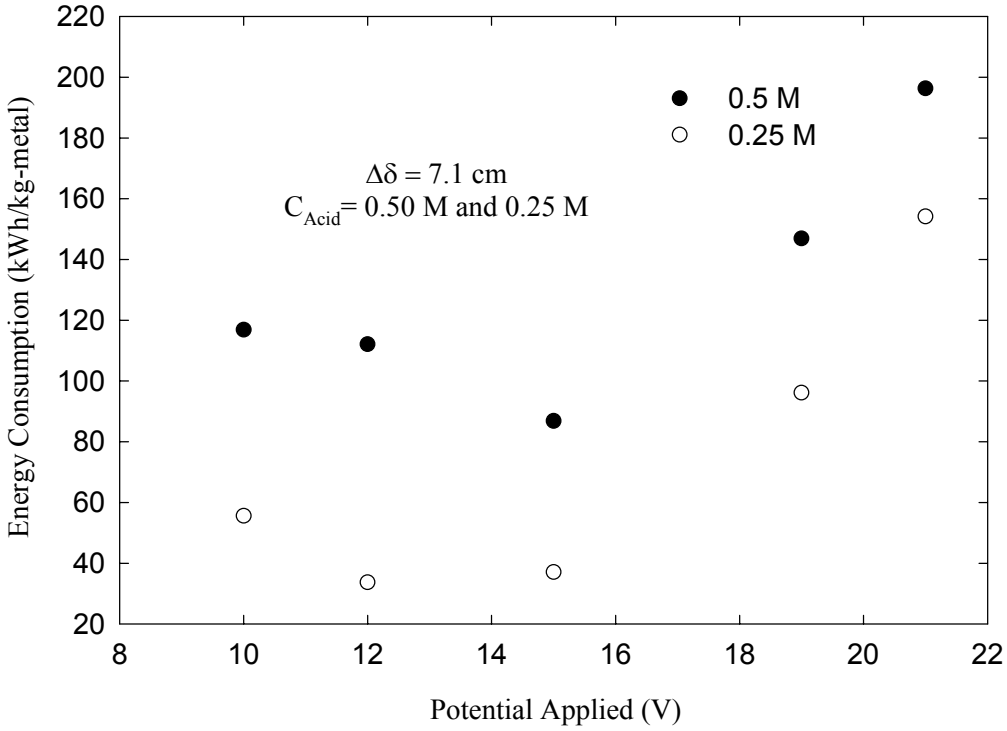

Figure 5.23: Energy consumption versus potential applied at membrane spacing of 7.1 cm and side concentration of 0.5 M and 0.25 M

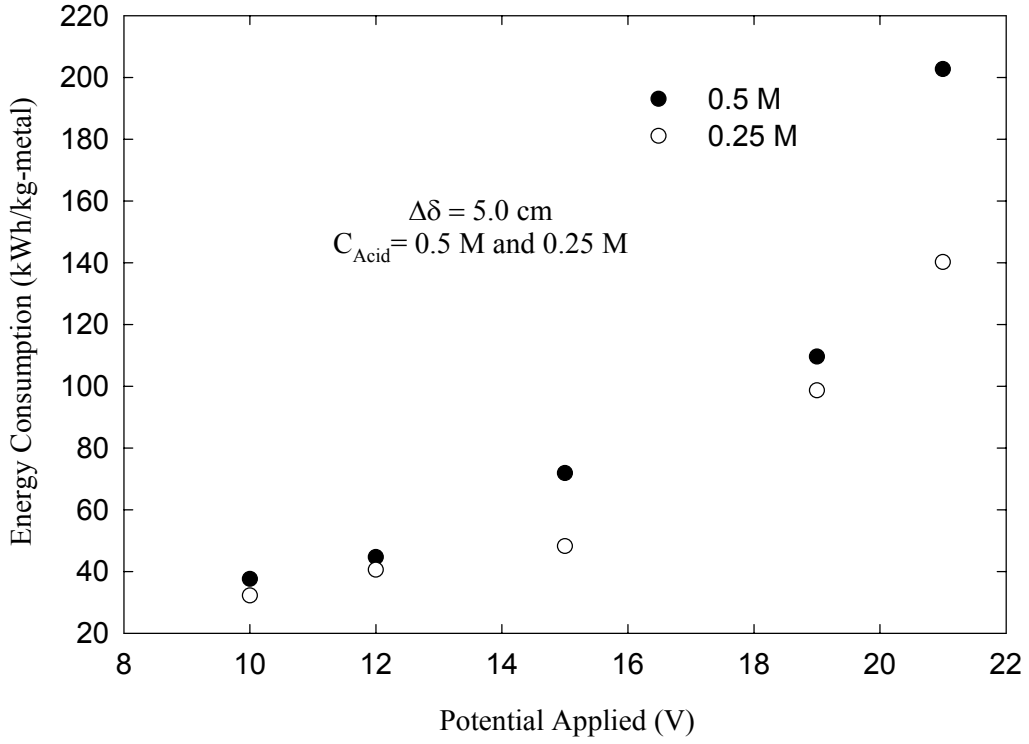

Figure 5.24: Energy consumption versus potential applied at membrane spacing of 5.0 cm and side concentration of 0.5 M and 0.25 M

where:

W: weight of copper recovered from the solution (g).

M: Molecular weight of copper (g-mole/g).

n: number of exchange electrons.

F: Faraday's Constant.

I: Current-time relation (Ampere).

A computer code using MATLAB was written to calculate this quantity in which the experimental data collected from the experiments were supplied (Appendix A3-2). The current efficiency gets affected by a number of parameters such as cell potential, distance between membranes, and the concentration of the sulfuric acid in the side compartments. The effect of these parameters can be discussed as follows:

5.3.3.a Effect of Cell Potentials:

The current efficiency is plotted against the final concentration of copper ions in wastewater in figures 5.25, 5.26, 5.27, 5.28, 5.29, and 5.30 at different cell potentials. The current efficiency curves increases as the final concentration of the copper increases and cell potentials increase. As the copper concentration in the system decreases, the current efficiency decreases because of the drop in the rate of the reduction reaction of the copper ions.

The current efficiency keeps on increasing as the cell potential increases due to the enhancement in the copper recovery rate. However, when the cell potential exceed 15.0 V, it becomes low because the rate of the side reaction which includes the breakage of water molecules become significant and the amount of the copper recovered becomes low at this of stage.

5.3.3.b Effect of the Membrane Spacing:

The current efficiency is plotted against final concentration of copper ions in Figures 5.32, 5.33 and 5.34 at two different membrane spacing. As the final concentration of the copper ions increases the current efficiency increases or the distance between membranes decreases. When the distance between the membranes is reduced, the ohmic resistance between the electrodes decreases. Subsequently, the current efficiency gets improved because more copper is deposited at the cathode.

5.3.3.c Effect of the Sulfuric Acid Concentration in the Side Compartments:

The effect of the sulfuric acid concentration in the side compartments on the current efficiency is given in the Figures 5.35, 5.36 and 5.37. In these Figures, the current efficiency is plotted against the final concentration of the copper in the system at two different values of sulfuric acid concentration in the side compartments 0.5 M and 0.25 M.

Decreasing the concentration of the sulfuric acid in the side compartments could greatly help in improving the current efficiency because it minimize the effect of the concentration polarization. By such an action, more copper ions could be recovered in the metallic form causing an appreciable improvement in the current efficiency of the system.

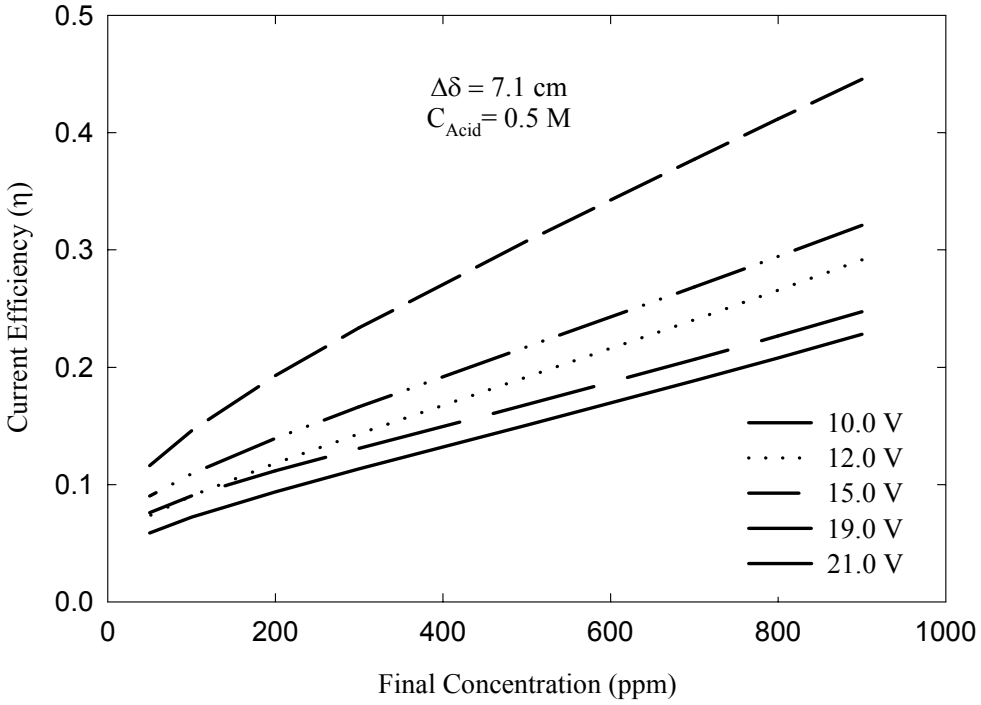

Figure 5.25: Current efficiency versus final concentration at membrane spacing of 7.1 cm and side concentration of 0.5 M

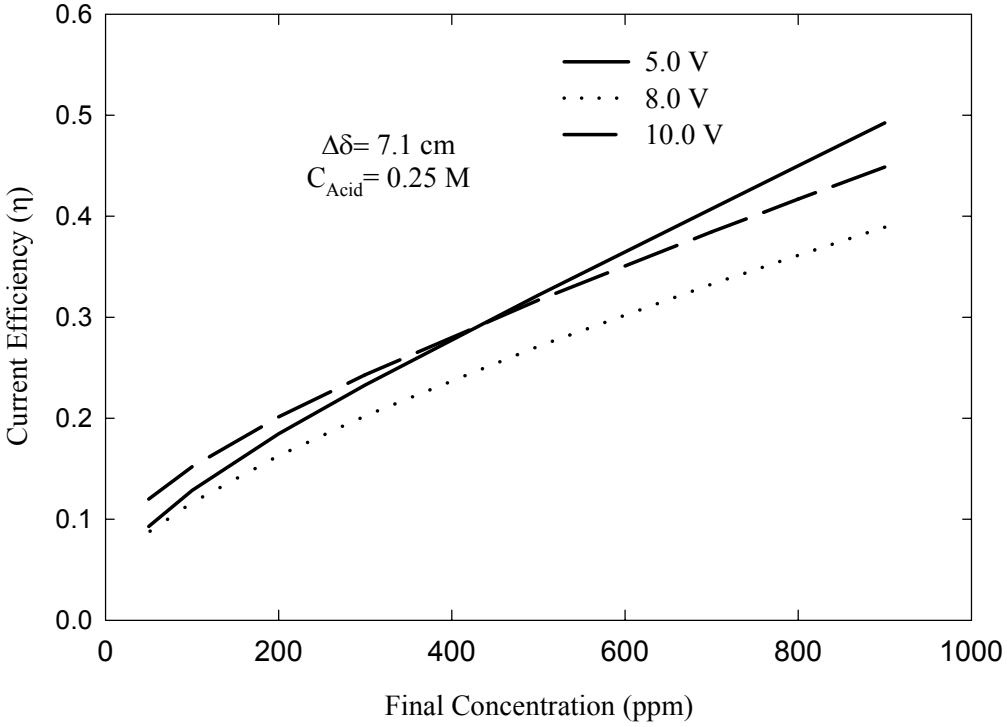

Figure 5.26: Current efficiency versus final concentration at membrane spacing of 7.1 cm and side concentration of 0.25 M

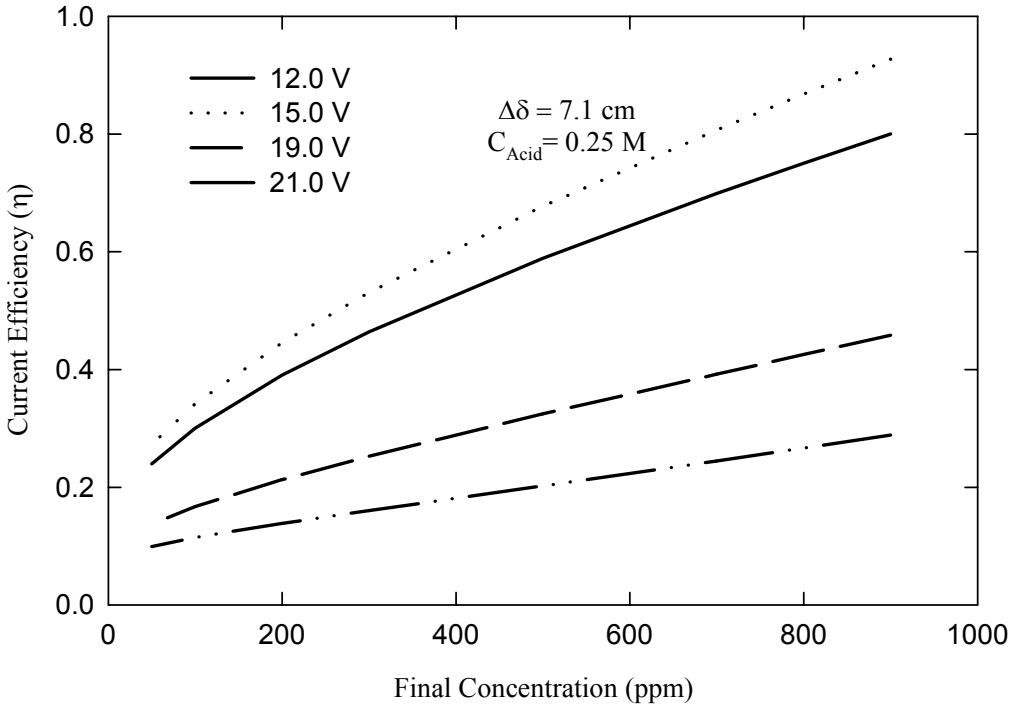

Figure 5.27 (Cont.): Current efficiency versus final concentration at membrane spacing of 7.1 cm and side concentration of 0.25 M

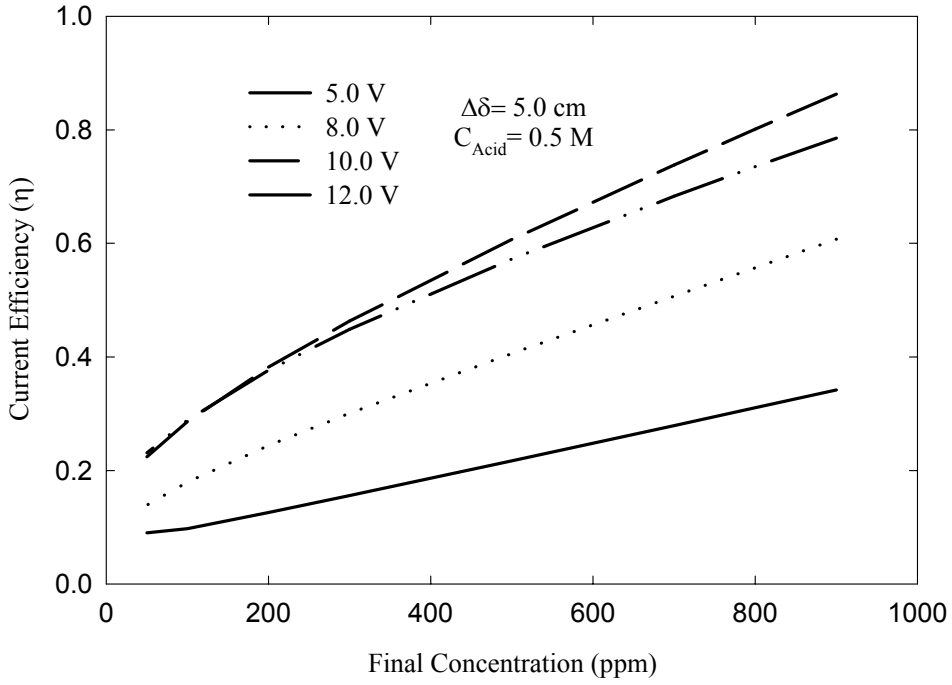

Figure 5.28: Current efficiency versus final concentration at membrane spacing of 5.0 cm and side concentration of 0.5 M

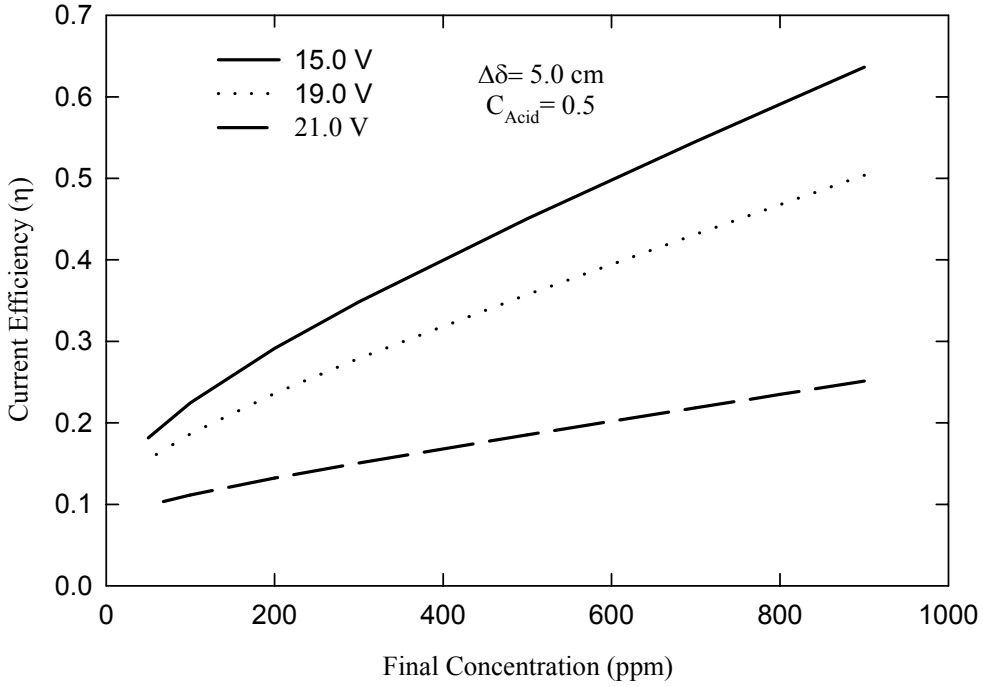

Figure 5.29 (Cont.): Current efficiency versus final concentration at membrane spacing of 5.0 cm and side concentration of 0.5 M

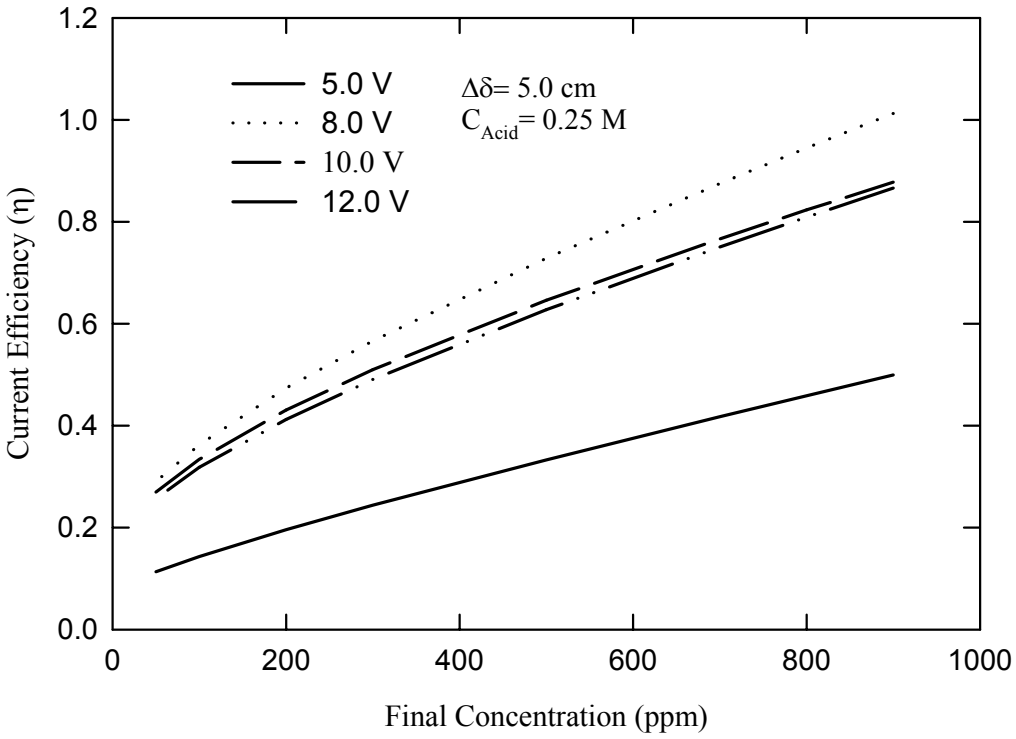

Figure 5.30: Current efficiency versus final concentration at membrane spacing of 5.0 cm and side concentration of 0.25 M

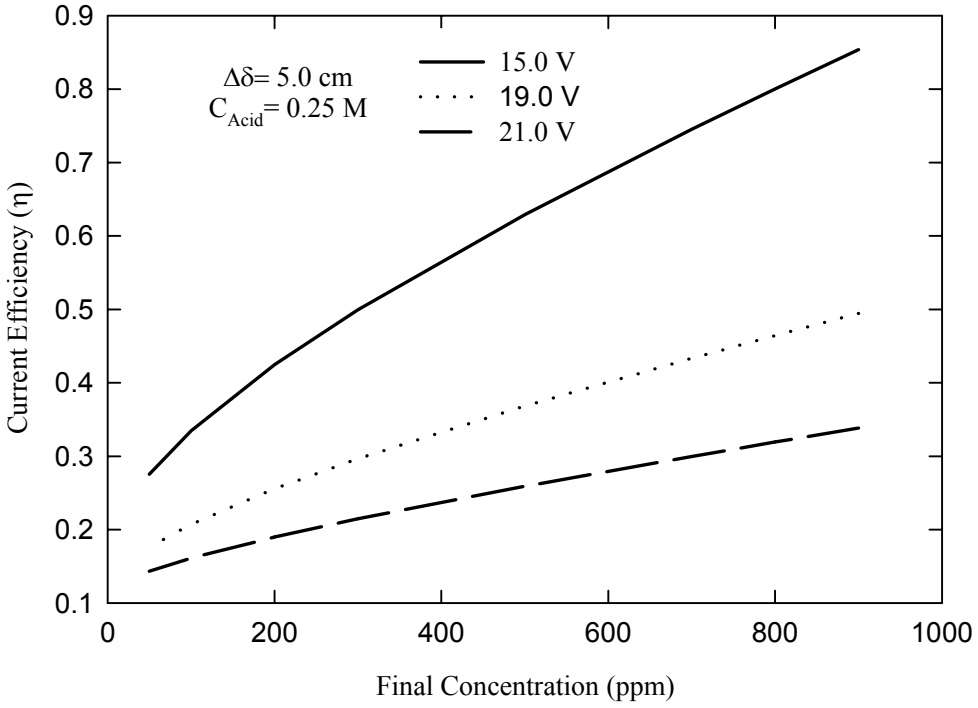

Figure 5.31 (Cont.): Current efficiency versus final concentration at membrane spacing of 5.0 cm and side concentration of 0.25 M

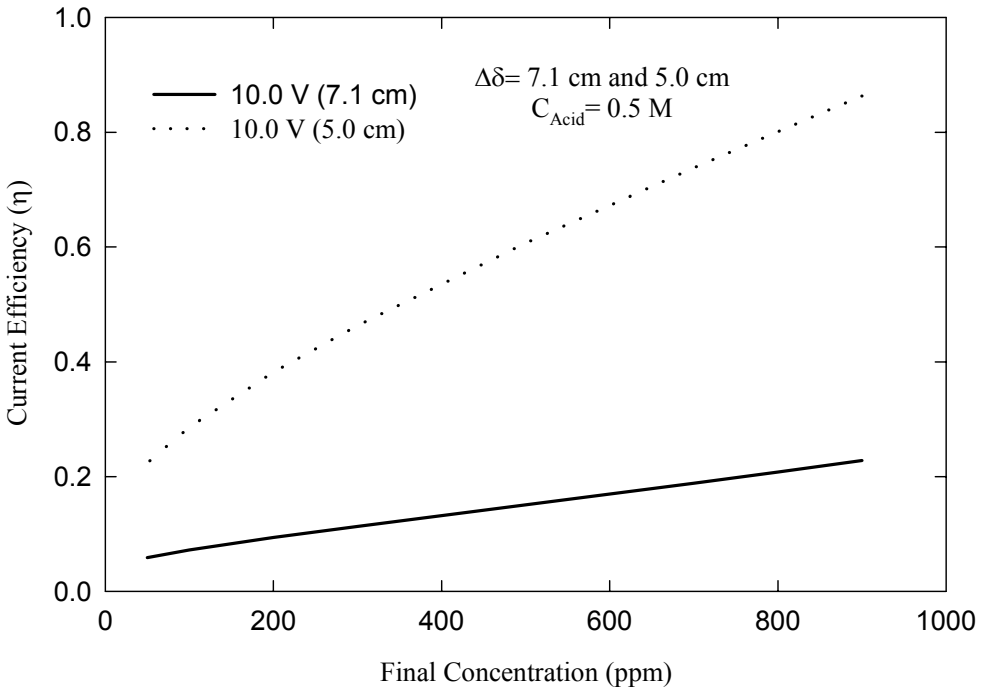

Figure 5.32: Current efficiency versus final concentration at a potential of 10.0 V, side concentration of 0.5 M and membrane spacing of 7.1 cm and 5.0 cm

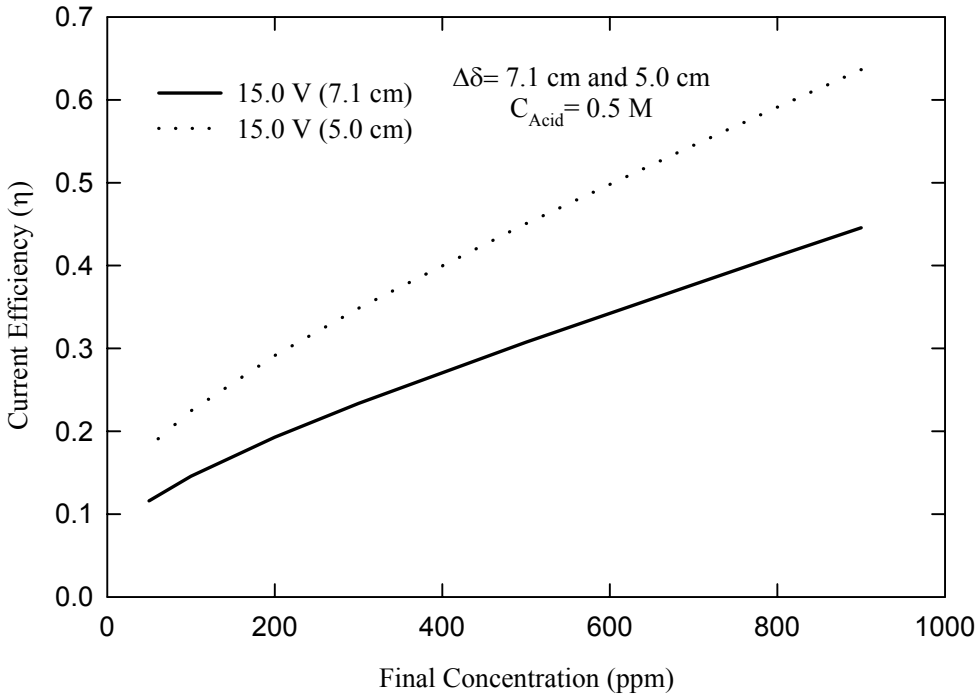

Figure 5.33: Current efficiency versus final concentration at a potential of 15.0 V, side concentration of 0.5 M and membrane spacing of 7.1 cm and 5.0 cm.

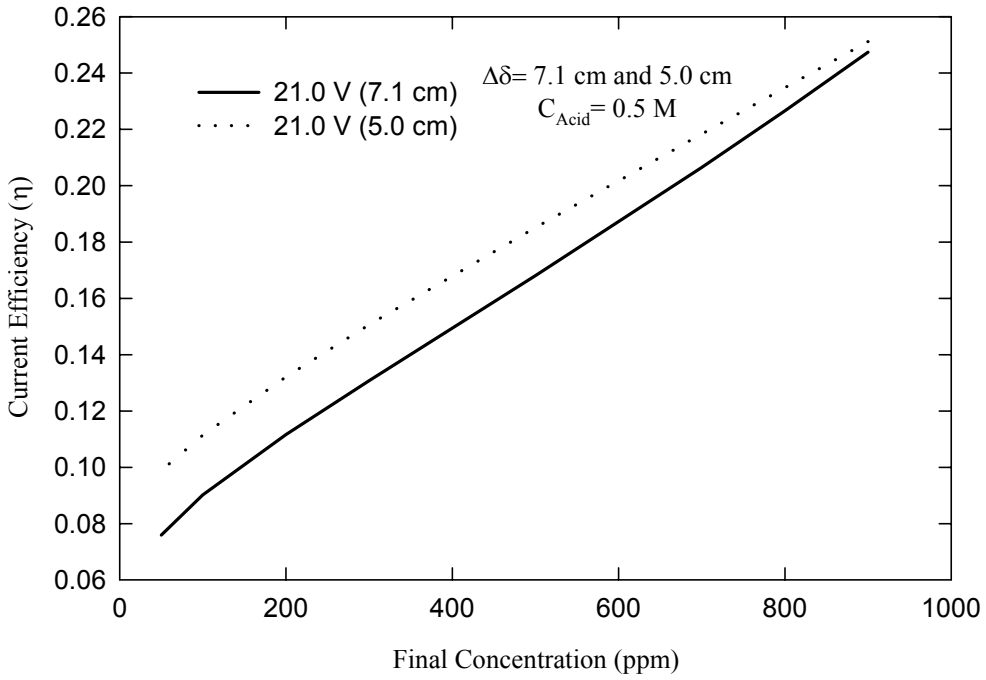

Figure 5.34: Current efficiency versus final concentration at a potential of 21.0 V, side concentration of 0.5 M and membrane spacing of 7.1 cm and 5.0 cm

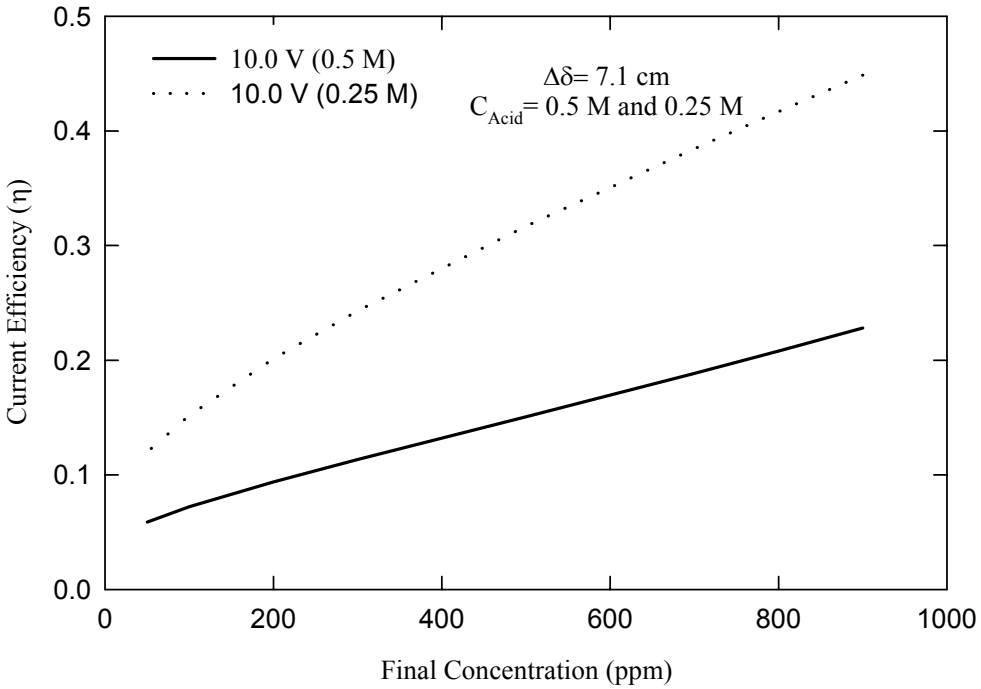

Figure 5.35: Current efficiency versus final concentration at a potential of 10.0 V, membrane spacing of 7.1 cm and side concentration of 0.5 M and 0.25 M

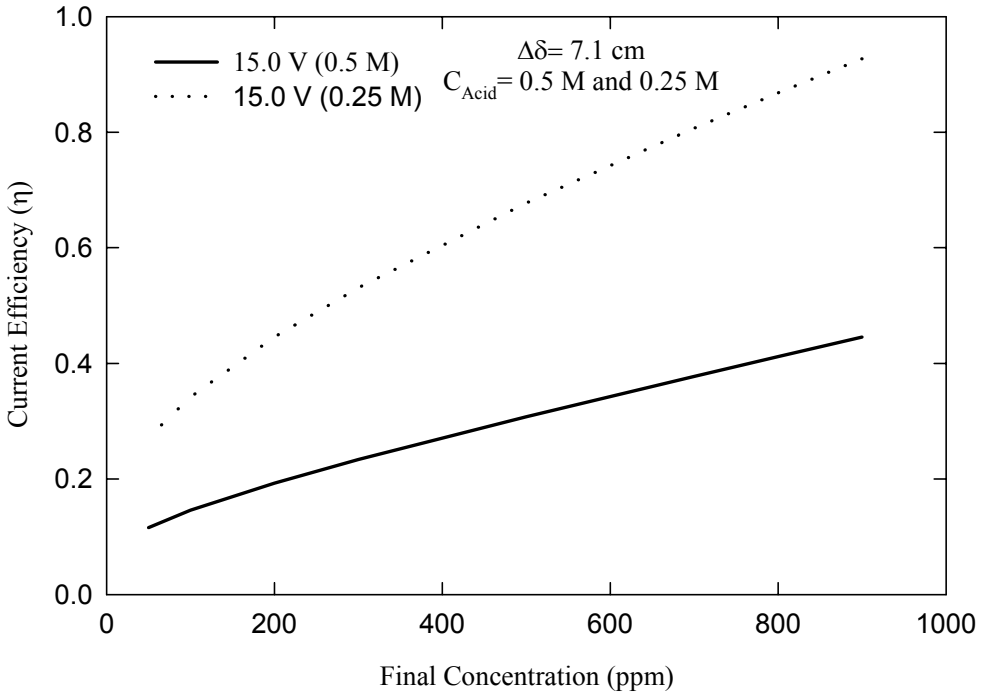

Figure 5.36: Current efficiency versus final concentration at a potential of 15.0 V, membrane spacing of 7.1 cm and side concentration of 0.5 M and 0.25 M

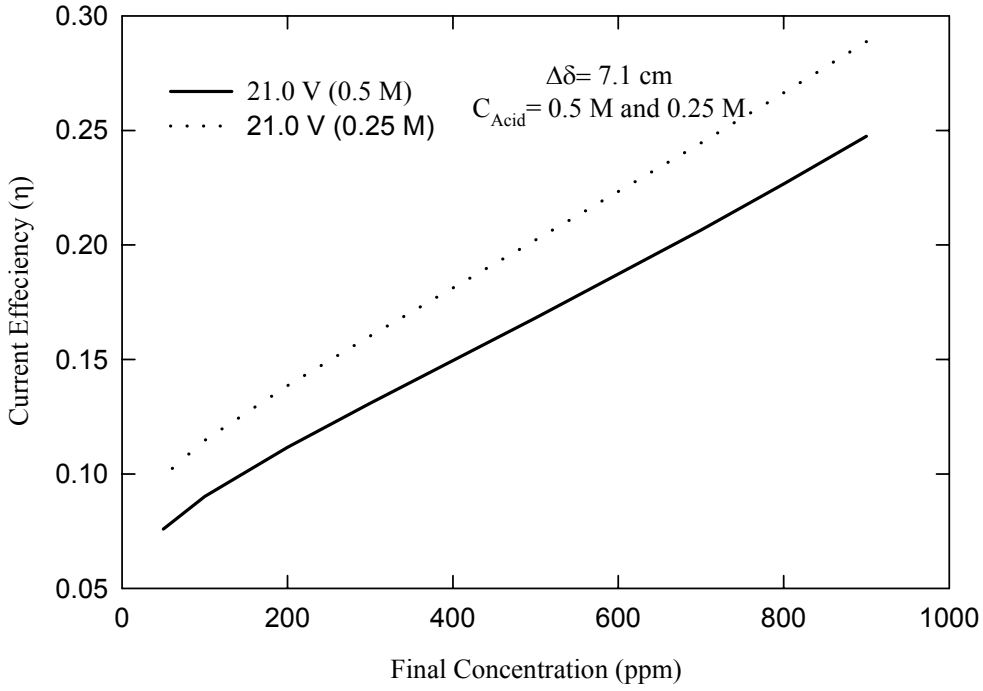

Figure 6.37: Current efficiency versus final concentration at a potential of 21.0 V, membrane spacing of 7.1 cm and side concentration of 0.5 M and 0.25 M

CHAPTER 6

CONCLUSIONS AND RECOMMENDATIONS

6.1 Conclusions:

This study has successfully demonstrated an integrated electrolytic-electrodialytic process, which eliminates which the shortcomings of both electrolytic and electrodialytic process for the removal of heavy metal ions from wastewater. The copper ions from the incoming stream could be removed in the metallic form, which then can be utilized later. The effect of the process operation variables on the apparent reaction rate constant was investigated. Energy consumption of copper recovery process was evaluated. A parametric study was undertaken. The main conclusions of the present study can be summarized as:

1. The copper ion concentration of 1000 ppm in wastewater placed in the middle compartments decreased logarithmically with time. Almost complete removal of copper ions could be obtained at cell potentials 5.0, 8.0, 10.0, 12.0, 15.0, 19.0, and 21.0 V.
2. At the beginning, the process was kinetic controlled and the combined reaction rate constant and mass transfer coefficient kept on increasing till a certain potential range. Beyond that range, the process became mass transfer rate controlled and the combined constant decreased because of the dominate of side reaction rates.

3. The distance between the membranes has a strong influence on the apparent reaction rate constant. This parameter could increase the constant when the distance was reduced from 7.1 cm to 5.0 cm. At a cell potential of 8.0 and side concentration of sulfuric acid of 0.5 M, the apparent reaction rate constant is 8.9780×10^{-5} sec^{-1} at a membrane distance of 7.1 cm while it is 2.4410×10^{-4} sec^{-1} at a membrane distance of 5.0 cm.
4. When the concentration of the sulfuric acid in the side compartments was decreased from 0.5 M to 0.25, the apparent reaction rate constant increased. At a cell potential of 8.0 and membrane spacing of 7.1 cm, the apparent reaction rate constant is 8.9780×10^{-5} sec^{-1} at a side concentration of sulfuric acid of 0.5M while it is 1.2150×10^{-4} sec^{-1} at a side concentration of sulfuric acid of 0.5 M
5. For a specific membrane spacing and sulfuric acid concentration in the side compartments, the energy consumed to remove copper ions decreases as the cell potential increases from 5.0 V till 15.0 V is reached. After that, the energy consumption increases as the cell potential increases.
6. Energy consumed to remove the copper ions could be minimized by decreasing the distance between the membranes from 7.1 cm and 5.0 cm.
7. Energy consumed to remove one kilogram of copper decreased when the concentration of the sulfuric acid in the side compartment was decreased from 0.5 M to 0.25 M.

6.2 Recommendations:

It is recommended to carry out the following:

1. An elaborate parametric study should be undertaken to understand fully the effect of the membrane materials, electrode materials, temperature and the concentration of the supporting salt. The system should be also tested for other values of membrane spacing and acid concentrations to see the trend.
2. The data obtained from this parametric study of the integrated process should be compared with the data obtained from a combination of commercial electrolytic cell and electrodialytic cell.
3. A mathematical model should be developed. Subsequently, the kinetic data obtained from the parametric study should be used in conjunction with the mathematical model to retrieve kinetic parameters. This will enable us to scale up the proposed method for possible industrial applications.

NOMENCLATURE

C (t)	copper concentration at any time, ppm.
C_o	initial concentration of copper, ppm.
C_{Acid}	sulfuric acid concentration in the side compartments of the cell, M.
E	energy spent to recover one kilogram of copper, kW/kg-copper removed.
F	Faraday constant, 96500 C/equiv.
I	cell current, A.
M	atomic weight of copper, 63.5 g/mol.
n	number of electron transferred in the cathode deposition reaction, equal to 2 equiv/mol for copper deposition reaction.
k	apparent reaction rate constant, sec^{-1}.
t	time, sec
W	mass of copper removed, kg
V	cell potential, V
η	current Efficiency, %
$\Delta\delta$	Distance between membranes, cm

REFERENCE

Amor, Z., Malki S., Taky, M., Bariou, B., Mameri, N., and Elmidaoui, A., "Optimization of fluoride removal from brakish water by electrodialysis", Desalination, 120, 263-271 (1998).

Bal, A.S., and Vaidya, A.N., "Application of membrane technology in wastewater management", Chem. Eng. World, 33, 1, 5 (1998).

Bennion, D.N., Newman, J., "Electrochemical removal of copper ions from very dilute solutions", J. Appl. Electrochem., 2, 113 (1972).

Cartwright, P.S., "Zero discharge/water reuse – The opportunities for membrane technologies in pollution control", Desalination, 83, 225-241 (1991).

Cedrone, N.J., "Silver recovery cells", J. SMPTE., 65, 429 (1956).

Chaudary, A.J., Donaldson, J.D., Grimes, S. M., and Yasri, N.G. "Separation of nickel and cobalt using elecrodialysis in the presence of EDTA", J. Appl. Electrochem., 30, 439-445 (2000).

Cherif, A. T., Molenat, J., Elmidaoui, A., "Nitric acid and sodium hydroxide generation by elecrodialysis using biopolar membranes", J. Appl. Electrochem., 27, 1069-1074 (1997).

Chin, D. -T., "Electrolytic recovery of metals from wastewater", Report to the U.S. National Science Foundation, Grant DUE965008 (2000).

Chin, K.K. and Ong S.L., "water conservation through reclamation of sewage for reuse", Pro 2nd Annual Conf. Integr. Water Res. Plan for 21 Century, ASCE, p 73-76 (1995).

Davis, M., "Use advanced methods to treat wastewater", Hydrocarbon Proc., 73, 43-46 (1994).

Fleishmann, M., Jansson, R.E.W., and Marshall, R.J., "Improvement in and relating to electrochemical cells", Br. Pat. 1522872, (1976).

Fleishmann, M., King, C.J.H., Oldfield, J.W., Plimley, R.E., and Tennakkoon, C.L.K., "Improvement in and relating to electrochemical cells", Br. Pat. 1419246, (1971b).

Fleishmann, M., Oldfield, J.W., and Tennakkoon, L., "Electrochemical removal of copper ions by use of fluidized Bed Electrode", J. Appl. Electrochem., 1, 103 (1971a).

ESE Cell, U.S. Patent 3859195, 7 Jan. (1975), assigned to Du Pont.

Grib, H., Belhocine, D., Lounici, H., Pauss, H., and Mameri, N., "Desalting of phenylalanine solutions by electrolysis with ion-exchange membrane", J. Appl. Electrochem., 30, 259-262 (2000).

Hertwing, K., Bergmann, H., and Nieber, F. "The rotating cylinder cathode – A novel electrochemical reactor for electrochemical effluent treatment", Galvanotech., 83, 1696 (1992).

Hickman, K., Weyerts, W., and Goehler, O.E., "Recovery of silver", Ind. Eng. Chem., 25, 202 (1933).

Holland, F.S., "The development of eco-cell Process", Chem. Ind., 453, (July, 1978).

Itoi, S., Nakamura, I., and Kawahara, T., "Electrodialytic recovery process of metal finishing watewater", Desalination, 32, 383-389 (1980).

Kedem, O., Schechtmann, L., Mirsky, Y., Savelieve, G., and Daltrophe, N., "Low-Polarization electrodialysis membranes", Water Supply, 17, 305-314 (1999).

Khristoskova, S., Lazavou, D., "Electrochemical purification of chromium (VI) in wastewater", Nauchni Tr. Plovdivski Univ., 22, 153 (1984).

Korngold, E., "Electrodialysis in advanced wastewater treatment", Desalination, 24, 129-139 (1978).

Kuhn, A.T., and Houghton, R.W., "The design and optimization of industrial electrochemical cells", Topics in pure and applied electrochemistry, SAEST, Karaikudi, India, (1979) 133.

Lopez-Cacicedo, C.L., "The recovery of metals from rinse waters in 'Chemelec' electrolytic cell", Trans. Inst. Met. Fin., 53, 74 (1975).

Ogutveren, U.B., Koparal, S., and Ozel, E., "Electrodialysis for the removal of copper ions from wastewater", J. Environ. Sci. Health, A32(3), &49-761 (1997).

O'Keefee, T. J. and Ettel, V. A., "The electrolytic recovery of metals from aqueous solution", Electrochem. Soc. Symp. Proceeding Volume PV87-7, 103 (1997).

Palmer, S.A.K., Breton, M.A., Nunno, T.J., and Sullivan, D.M., "Metal/Cyanide containing wastes treatment technologies" pp 10-100, Noyes Data Corporation, Park Ridge, NJ, 1988.

Reed, A.K., Shea, J.F., Tewksbury, T.L., Cherry, R.H., and Smithson, G.R., "An investigation of techniques for removal of cyanide from electroplating wastes",

Report for project No. 12010EIE, Battelle Columbus Laboratory, Columbus, Ohio, 1971.

Resbeut, S., Pourcelly, G., Sandeaux, R., and Gavach, C., "Electromembrane Processes for waste treatment: electrodialysis applied to the demineralization of phenylalnine solutions", Desalination, 120, 235-245 (1998).

Ribeiro, A.B., Mateus, E.P., Ottesen, L.M., Bech-Nielsen, G., "Electrodialytic removal of Cu, Cr, and As from chromated copper arsenate-treated timber waste", Environ. Sci. & Tech., 34, 784-788 (2000).

Robertson, P.M., and Dossenbach, O., "Stirring by gas introduction and its application in the electroplating industry", oberflaeche-Surf., 22(9), 282 (1981).

Robertson, P.M., Leudolph, J., and Mauret, H., "Improvement in rinse water treatment by electrolysis", Plat. and Surf. Fin., 70(10), 48 (1983).

Rodrigues, M.A.S., Bernardes, A.M., and Ferreira, J.Z., "Application of electrodialysis on the treatment of effluents with chromium hexavalent", TMS Annual meeting, Minerals, Metals and Materials Soc. (TMA), Warrendale, PA, USA, p 659-672 (1999).

Saito, K., "Recovery of bromide ion by electrodialysis", Japan Pat. 7938794, 1979.

Saracco, G., Zanetti, C.Z., and Onofrio, M., "Novel application of monovalent ion-permselective membranes to the recovery treatment of an industrial wastewater by electrodialysis", Ind. Eng. Chem. Res., 32, 657-662 (1993).

Seto, T., Ehara , L., Komori, R., Yamaguchi, A., and Miwa, T., "Seawater desalination by electrodialysis", Desalination, 25, 1-7 (1987).

Shifrin, S. M., Varygin, V.S., Golyshev, V.K., Krasnobrod, I.G., and Khosid, E.V., "Selection of anode material for electrochemical treatment of wastewater", Zh. Prikl. Krim., 52(7), 1648 (1979).

Shim, J-B., Oh, W-Z., Lee, B-J, and Park, H-S., "Electrodialysis of vanadium (III) and Iron (II) ions from a simulated decontamination solution", Separation Science and Technology, 34 (10), 1963-1979 (1999).

Tison, R.P., "Copper Recovery Using a Tumbled-Bed electrochemical reactor", J. Electrochem. Soc., 128, 317 (1981).

Tokumyama Corp. Brochure, "Neosepta Ion-exchange membranes", Brochure, 1999.

Toshio, S., Yasou, H., Yoshinori I., Atsushi, T., Kazuhico, W., and Hiroshi, H., "Development of electrochemical denitrification from wastewater containing

ammonium nitrate", Proc: Int. Conf. Radioactive waste management and environmental remediation, ICEM v2, ASME, New York, NY, USA, p 1089-1093 (1995).

U.S. Environmental Protection Agency Regulation, "Identification and listings of hazardous wastes" guideline 40, CFR 413 (1992).

Weinginger, J. L., "Electrochemical recovery of metals from wastewater", AIChE symp. Series, 79, 179(1987).

Wisniewski, J.A., and Wisniewska, G., "Application of electrodialysis to wastewater and acid recovery", Environ. Protection Eng., 25, 145-150 (1999).

Xue, Z., Hua, Z., Li. Q., and Yao, N., "Reuse and treatment of electrochemical industrial wastewater by electrodialysis", Proc: National Conference on Environmental Engineering, "Saving a Threatened Resource- In Search of Solutions", ASCE, New York, NY, USA, p 376-381 (1992).

Yu, Z., and Admassu, W., "Modeling of electrodialysis of metalion removal from pulp and paper mill process stream", Chem. Eng. Sci., 55, 4629-4641, (2000).

Yun, L., Guo, Q., Hao, J., Jiang, W., "Recovery of acetic acid from dilute wastewater by means of biopolar membrane electrodialysis", Desalination, 129, 283-288 (2000).

Zartwright, P.S., "Zero discharge/water reuse- The opportunities for membrane technologies in pollution control", Desalination, 83, 225-241 (1991).

Zhou, C. -D. and Chin, D. –T., "Continuous electrolytic treatment of complex metal cyanides with a rotating barrel plater as the cathode and a packed-bed as the anode", Plat. and Surf. Fin., 81(6), 70 (1994).

Zhou, C. -D. and Chin, D. –T., "Copper recovery and cyanide destruction with a plating barrel cathode and a packed-bed anode", Plat. and Surface Fin., 80(6), 69(1993).

Zhou, K., Zhang, Q., Luo, A., Fu, C., Shang, J., Li, M., Huang, W., Zhu, X., "Treatment of industrial wastewater from an alumina plant by membrane technology (I)-measurement of limiting current density of electrodialysis", J. Central South University of Technology, 6, 82-85 (1999).

Zhou, K., Zhang, Q., Luo, A., Fu, C., Xiang, J., Li, M., Zhu, X., Huang, W., "Treatment of industrial wastewater from an alumina plant by membrane technology (II)-Study of technological process", J. Central South University of Technology, 6, 86-89 (1999).

Appendix

A1. Part One: Raw Date

In this part, only raw data representing the concentration of the copper ions against time and the current against are listed in form of tables. The principle equation relating the concentration of the diluted samples of wastewater to the actual concentrations is derived. It is located in the pages: 98-132.

A2. Part Two: Concentration versus Time and Current versus Time Plots

The basic plots of the copper concentration against time and current running in the system against time are listed. It is located in the pages: 133-190

A3. Part Three: Computer Code

The computer codes used to make the calculation of the energy consumption and the current efficiency are placed. It is located in the pages: 191-196

A1. Part One:

Raw Data

The data collected in the experiments can be divided into two sets: concentration against time and current against time. While they are presented in this section, both sets of data are listed in a single table in which only a single list of time is used. The operating conditions at which the experiment done is mentioned at the beginning in the form of tables. These tables preset include the parameters and their values.

The concentration data of the wastewater listed in the tables below represent the concentration of the copper ions in the diluted samples. As it was mentioned earlier, a sample of 0.2 ml of wastewater was taken and diluted in the 100 ml volumetric flask by adding 10 ml of 10% vol. nitric acid and deionized water till the mark of 100 ml was reached. The concentration of the copper ions was revealed by the help of atomic absorption spectrometer. The actual concentration of the copper ions in the wastewater compartment can be evaluated by:

$$\left(C_{Cu}\right)_{unknown} V_{unknown} = \left(C_{Cu}\right)_{diluted} V_{diluted}$$

where:

$(C_{Cu})_{unknown}$: concentration of the copper ions in wastewater.

$V_{unknown}$: volume of sample of the wastewater dilutes .

$(C_{cu})_{diluted}$: concentration of the copper ions in the diluted samples measured by atomic absorption spectrometer.

$V_{diluted}$: the volume of the diluted samples

So, substitute in the above equation:

$0.2\ (C_{Cu})_{unknown}=100\ (C_{cu})_{diluted}$

Finally, $(C_{Cu})_{unknown}=500\ (C_{Cu})_{diluted}$

In conclusion, each sample taken was diluted five hundred times before they were measured by atomic absorption spectrometer.

As far as current flowing in the circuit is concerned, it was recorded at different time while the cell potential was maintained. In the first ten minutes of the experiments, it was changing dramatically then after that the increment in the current got stabilized.

Phase I: Fixed operation parameters for tables A1-1 to A1-7

Parameters	Value
Distance Between Membranes (cm)	7.1
Side Concentration of sulfuric acid (M)	0.5
Volume of wastewater in the middle compartment (ml)	650

Table A1-1: Experimental Data

Cell Potential =5.0 V

Time (min)	Concentration of the diluted Samples (ppm)	Current (A)
0	2.09	0.277
1	----	0.339
3	----	0.355
4	----	0.359
7	----	0.368
9	----	0.372
12	----	0.376
15	----	0.375
25	----	0.391
30	1.90	0.406
60	1.38	0.457
90	1.80	0.49
120	1.38	0.526
150	1.26	0.56
180	1.22	0.541
210	1.00	0.572
270	0.94	0.616
300	0.90	0.647
360	0.58	0.681
420	0.74	0.702
480	0.58	0.703
600	0.51	0.728
1642	0.18	----

Table A1-2: Experimental Data

Cell Potential =8.0 V

Time (min)	Concentration of the diluted Samples (ppm)	Current (A)
0	1.79	0.816
2	----	0.795
4	----	0.799
6	----	0.800
8	----	0.801
10	----	0.804
30	1.43	0.856
60	1.15	0.906
90	1.05	0.944
120	0.90	0.992
150	0.57	1.035
180	0.53	1.062
210	0.59	1.070
270	0.36	1.082
300	0.37	1.078
360	0.36	1.055
420	0.31	1.048
480	0.23	1.037
540	----	1.015
600	0.18	1.000

Table A1-3: Experimental Data

Cell Potential =10.0 V

Time (min)	Concentration of the diluted Samples (ppm)	Current (A)
0	1.96	0.904
1	----	0.854
2	----	0.86
4	----	0.869
6	----	0.876
8	----	0.876
10	----	0.894
30	1.57	0.920
60	0.96	0.979
90	1.10	1.172
120	0.64	1.14
150	0.83	1.200
180	0.58	1.233
210	0.40	1.253
270	0.34	1.217
300	0.35	1.198
360	0.30	1.164
420	0.21	1.128
487	0.15	1.086
543	0.12	1.066

Table A1-4: Experimental Data

Cell Potential =12.0 V

Time (min)	Concentration of the diluted Samples (ppm)	Current (A)
0	1.99	1.053
1	----	0.988
2	----	0.968
3	----	0.965
4	----	1.001
6	----	1.005
8	----	1.022
10	----	1.032
30	1.91	1.117
60	1.29	1.274
90	0.91	1.379
120	0.74	1.428
150	0.45	1.462
180	0.27	1.457
210	0.22	1.427
270	0.15	1.34
300	0.17	1.295
360	0.10	1.221
420	0.05	1.166
480	0.02	1.149

Table A1-5: Experimental Data

Cell Potential =15.0 V

Time (min)	Concentration of the diluted Samples (ppm)	Current (A)
0	1.919	1.34
2	----	1.36
4	----	1.38
6	----	1.39
8	----	1.40
10	----	1.42
20	----	1.49
30	----	1.57
40	1.561	1.65
50	----	1.71
60	0.671	1.76
72	----	1.81
80	0.351	1.84
94	----	1.87
100	0.233	1.87
120	0.190	1.87
130	----	1.86
140	0.335	1.85
160	0.268	1.80
240	0.176	----
270	----	1.54

Table A1-6: Experimental Data

Cell Potential =19.0 V

Time (min)	Concentration of the diluted Samples (ppm)	Current (A)
0	1.919	1.85
2	----	1.88
4	----	1.92
6	----	1.94
8	----	1.98
10	----	2.01
20	1.356	2.18
30	----	2.30
40	0.858	2.38
50	----	2.42
60	0.471	----
72	----	2.42
80	0.350	2.40
90	----	2.33
100	0.422	2.31
110	----	2.26
120	0.319	2.21
150	----	2.06
160	0.204	2.03
170	----	1.99
180	0.153	1.95

Table A1-7: Experimental Data

Cell Potential =21.0 V

Time (min)	Concentration of the diluted Samples (ppm)	Current (A)
0	1.919	1.99
2	----	2.03
4	----	2.07
6	----	2.11
8	----	2.15
10	----	2.19
20	1.342	2.37
30	----	2.46
40	1.235	2.49
50	----	2.52
60	0.512	2.50
70	----	2.50
80	0.446	2.42
90	----	2.38
100	0.394	2.32
102	----	2.24
120	0.308	2.19
130	----	2.13
140	0.210	2.07
150	----	2.02
160	0.170	1.97
170	----	1.92

Phase II: Fixed operation parameters for tables A1-8 to A1-14

Parameters	Value
Distance Between Membranes (cm)	7.1
Side Concentration of sulfuric acid (M)	0.25
Volume of wastewater in the middle compartment (ml)	650

Table A1-8: Experimental Data

Cell Potential =5.0 V

Time (min)	Concentration of the diluted Samples (ppm)	Current (A)
0	1.919	0.301
2	----	0.301
4	----	0.302
6	----	0.304
8	----	0.306
10	----	0.308
60	0.994	0.360
120	0.915	0.401
180	0.685	0.439
240	0.390	0.493
300	----	0.532
420	0.360	0.614
480	0.260	0.650
450	0.312	0.717
600	0.291	0.816

Table A1-9: Experimental Data

Cell Potential =8.0 V

Time (min)	Concentration of the diluted Samples (ppm)	Current (A)
0	1.919	0.589
2	----	0.569
4	----	0.570
6	----	0.575
8	----	0.580
10	----	0.586
30	----	0.627
60	0.854	0.666
90	----	0.699
120	0.656	0.737
150	----	0.823
180	0.471	0.827
210	----	0.904
240	0.348	0.924
270	----	0.943
300	0.235	1.009
360	0.255	----
420	0.292	1.156
450	----	1.157
480	0.188	1.176
510	----	1.186
540	0.115	1.152
570	----	1.121
600	0.156	1.102

Table A1-10: Experimental Data

Cell Potential =10.0 V

Time (min)	Concentration of the diluted Samples (ppm)	Current (A)
0	1.919	0.821
2	----	0.836
4	----	0.849
6	----	0.849
8	----	0.850
10	----	0.850
25	----	0.876
30	----	0.885
60	1.002	0.930
76	----	0.974
90	0.576	1.017
108	----	1.046
120	0.451	1.065
180	0.198	1.130
195	----	1.144
210	0.193	1.150
225	----	1.152
240	0.102	1.153
255	----	1.137
270	0.099	1.13
300	0.111	1.129
330	----	1.111
360	----	1.094
435	----	1.050
450	0.077	1.040
465	----	1.034
480	0.081	1.022
540	----	0.996

Table A1-11: Experimental Data

Cell Potential =12.0 V

Time (min)	Concentration of the diluted Samples (ppm)	Current (A)
0	1.919	0.989
2	----	0.974
4	----	0.968
6	----	0.968
8	----	0.968
10	----	0.968
15	----	0.969
60	0.419	1.075
90	----	1.125
150	0.086	1.155
210	0.056	1.115
240	0.066	1.084
270	----	1.057
300	0.047	1.019
330	----	0.988
360	0.066	0.957
420	0.050	0.905

Table A1-12: Experimental Data

Cell Potential =15.0 V

Time (min)	Concentration of the diluted Samples (ppm)	Current (A)
0	1.919	1.21
2	----	1.21
4	----	1.22
6	----	1.22
8	----	1.23
10	----	1.24
30	0.657	1.34
60	0.211	1.44
90	0.061	1.46
98	----	1.45
120	0.070	1.43
150	0.089	1.38
180	0.104	1.30
210	0.124	1.22
240	0.144	1.15

Table A1-13: Experimental Data

Cell Potential =19.0 V

Time (min)	Concentration of the diluted Samples (ppm)	Current (A)
0	1.919	1.65
2	----	1.67
4	----	1.72
6	----	1.75
8	----	1.78
10	----	1.80
15	----	1.86
20	1.251	1.91
30	----	1.97
40	0.589	2.00
50	----	2.01
60	0.658	1.99
80	0.137	1.92
90	----	1.87
100	0.153	1.80
110	----	1.76
120	0.209	1.70
130	----	1.63
140	0.176	1.57
150	----	1.52
160	0.113	1.47
180	0.089	1.38
190	----	1.34
200	0.054	----

Table A1-14: Experimental Data

Cell Potential =21.0 V

Time (min)	Concentration of the diluted Samples (ppm)	Current (A)
0	1.919	1.95
2	----	1.99
4	----	2.03
6	----	2.06
8	----	2.10
10	----	2.13
15	----	2.19
20	1.327	2.26
26	----	2.28
35	----	2.32
40	0.439	2.31
45	----	2.30
50	----	2.28
60	0.237	2.23
71	----	2.16
80	0.239	2.07
90	----	1.98
100	0.295	1.88
110	----	1.79
120	0.211	1.70
130	----	1.63
140	0.139	1.55
150	----	1.50
160	0.091	1.44

Phase III: Fixed operation parameters for tables A1-15 to A1-28

Parameters	Value
Distance Between Membranes (cm)	5.0
Side Concentration of sulfuric acid (M)	0.5
Volume of wastewater in the middle compartment (ml)	510

Table A1-15: Experimental Data

Cell Potential =5.0 V

Time (min)	Concentration of the diluted Samples (ppm)	Current (A)
0	1.919	0.531
2	----	0.486
4	----	0.476
6	----	0.479
8	----	0.486
10	----	0.493
30	1.354	0.453
45	----	0.613
60	1.488	0.657
75	----	0.694
90	1.212	0.721
105	----	0.745
120	1.055	0.757
135	----	0.767
150	0.955	0.786
160	----	0.803
165	----	0.811
170	----	0.817
180	0.764	0.829
195	----	0.845
210	0.757	0.862
225	----	0.88
240	0.569	0.897
270	----	0.919
280	----	0.918
300	0.669	0.924
315	----	0.923

Table A1-16: Experimental Data

Cell Potential =8.0 V

Time (min)	Concentration of the diluted Samples (ppm)	Current (A)
0	1.919	0.78
2	----	0.747
4	----	0.755
6	----	0.766
8	----	0.778
10	----	0.789
15	----	0.819
30	1.216	0.872
45	----	0.923
60	0.594	0.976
90	0.474	1.083
120	0.372	1.207
135	----	1.239
150	0.530	1.255
165	----	1.271
175	----	1.273
180	0.338	1.273
185	----	1.272
270	0.155	1.223
300	0.150	----
330	0.168	----
360	0.132	1.199

Table A1-17: Experimental Data

Cell Potential =10.0 V

Time (min)	Concentration of the diluted Samples (ppm)	Current (A)
0	1.919	1.009
2	----	1.013
4	----	1.035
6	----	1.055
8	----	1.065
10	----	1.075
15	----	1.094
30	0.746	1.170
45	----	1.253
60	0.380	1.338
80	----	1.449
90	0.219	1.473
127	----	1.492
140	----	1.489
150	0.086	1.475
165	----	1.449
180	0.088	1.423
195	----	1.393
200	0.057	1.384
300	0.016	1.230
315	----	1.215
330	0.01	1.199

Table A1-18: Experimental Data

Cell Potential =12.0 V

Time (min)	Concentration of the diluted Samples (ppm)	Current (A)
0	1.919	1.53
2	----	1.54
4	----	1.54
6	----	1.55
8	----	1.56
10	----	1.57
15	----	1.6
30	0.513	1.7
45	----	1.77
60	0.260	1.82
75	----	1.84
87	----	1.83
102	----	1.76
120	0.115	1.72
135	----	1.66
150	0.104	1.6
165	----	1.53
180	0.074	1.48
210	0.061	1.37
315	----	1.26
330	0.035	1.25

Table A1-19: Experimental Data

Cell Potential =15.0 V

Time (min)	Concentration of the diluted Samples (ppm)	Current (A)
0	1.919	1.89
2	----	1.92
4	----	1.94
6	----	1.96
8	----	2.00
10	----	2.04
20	1.138	2.19
25	----	2.24
30	----	2.28
35	----	2.31
40	0.200	2.33
50	----	2.32
53	----	2.31
60	0.169	2.28
80	0.162	2.14
90	----	2.06
100	0.253	1.98
110	----	1.89
120	0.175	1.81
130	----	1.74
140	0.117	1.68

Table A1-20: Experimental Data

Cell Potential =19.0 V

Time (min)	Concentration of the diluted Samples (ppm)	Current (A)
0	1.919	2.41
2	----	2.45
4	----	2.50
6	----	2.56
8	----	2.63
10	----	2.68
20	0.632	2.84
24	----	2.85
26	----	2.84
30	----	2.83
40	0.350	2.80
50	----	2.67
60	0.417	2.52
70	----	2.35
80	0.227	2.18
90	----	2.05
100	0.140	1.92
110	----	1.83
120	0.069	1.75

Table A1-21: Experimental Data

Cell Potential =21.0 V

Time (min)	Concentration of the diluted Samples (ppm)	Current (A)
0	1.919	3.61
2	----	3.75
4	----	3.89
6	----	4.01
8	----	4.10
10	----	4.19
15	----	4.21
20	0.301	4.15
25	----	4.05
30	----	3.93
35	----	3.79
40	0.525	3.68
45	----	3.52
50	----	3.32
60	0.314	3.00
65	----	2.76
70	----	2.67
75	----	2.53
80	0.168	2.41
85	----	2.31
90	----	2.22
95	----	2.12
100	0.09	2.06
105	----	1.99
110	----	1.94
115	----	1.89
120	0.05	1.68

Phase IV: Fixed operation parameters for Tables A1-22 to A1-28

Parameters	Value
Distance Between Membranes (cm)	5.0
Side Concentration of sulfuric acid (M)	0.25
Volume of wastewater in the middle compartment (ml)	510

Table A1-22: Experimental Data

Cell Potential =5.0 V

Time (min)	Concentration of the diluted Samples (ppm)	Current (A)
0	1.919	0.389
2	----	0.386
4	----	0.39
6	----	0.395
8	----	0.400
10	----	0.403
30	1.662	0.410
60	1.423	0.456
90	0.794	0.496
120	0.767	0.529
210	0.467	0.620
240	0.405	0.638
270	0.396	0.650
300	0.433	0.658
370	0.334	0.665

Table A1-23: Experimental Data

Cell Potential =8.0 V

Time (min)	Concentration of the diluted Samples (ppm)	Current (A)
0	1.919	0.803
2	----	0.752
4	----	0.759
6	----	0.763
8	----	0.769
10	----	0.771
30	0.743	0.821
60	0.130	0.902
90	0.234	0.928
120	0.239	0.942
135	----	0.937
150	0.154	0.928
180	0.161	0.868
210	0.116	0.825
240	0.113	0.800

Table A1-24: Experimental Data

Cell Potential =10.0 V

Time (min)	Concentration of the diluted Samples (ppm)	Current (A)
0	1.919	1.18
2	----	1.14
4	----	1.14
6	----	1.14
8	----	1.14
10	----	1.15
20	----	1.17
30	0.701	1.20
50	----	1.26
60	0.306	1.27
75	----	1.28
80	----	1.27
85	----	1.26
90	0.127	1.25
100	----	1.24
120	0.079	1.18
140	----	1.13
150	0.032	1.10
180	0.017	1.03
210	0.25	0.97

Table A1-25: Experimental Data

Cell Potential =12.0 V

Time (min)	Concentration of the diluted Samples (ppm)	Current (A)
0	1.919	1.21
2	----	1.22
4	----	1.23
6	----	1.24
8	----	1.25
10	----	1.26
30	0.946	1.38
60	0.175	----
66	----	1.42
70	----	1.41
80	----	1.40
90	0.208	1.37
120	0.084	1.27
150	0.84	1.17
180	0.078	1.07

Table A1-26: Experimental Data

Cell Potential =15.0 V

Time (min)	Concentration of the diluted Samples (ppm)	Current (A)
0	1.919	1.71
2	----	1.72
4	----	1.75
6	----	1.76
8	----	1.77
10	----	1.80
15	----	1.83
20	0.248	1.86
27	----	1.87
29	----	1.86
40	0.283	1.81
50	----	1.73
60	0.109	1.64
70	----	1.55
80	0.062	1.45
90	----	1.37
100	0.057	1.29
140	0.033	1.03

Table A1-27: Experimental Data

Cell Potential =19.0 V

Time (min)	Concentration of the diluted Samples (ppm)	Current (A)
0	1.919	2.39
2	----	2.42
4	----	2.44
6	----	2.48
8	----	2.51
10	----	2.54
15	----	2.59
20	0.720	2.58
25	----	2.54
30	----	2.48
40	0.162	2.36
60	0.322	2.03
70	----	1.87
80	0.179	1.70
90	----	1.56
100	0.099	1.44
110	----	1.35
120	0.04	1.28
130	----	1.21
140	0.013	1.17

Table A1-28: Experimental Data

Cell Potential =21.0 V

Time (min)	Concentration of the diluted Samples (ppm)	Current (A)
0	1.919	2.65
2	----	2.67
4	----	2.70
6	----	2.74
8	----	2.77
10	----	2.79
15	----	2.78
18	----	2.77
20	0.435	2.75
30	----	2.58
40	0.327	2.40
50	----	2.17
70	----	1.77
80	0.180	1.60
90	----	1.46
100	0.106	1.35
110	----	1.26
120	0.044	1.19
130	----	1.12
140	0.250	1.09

A2. Part Two:

Concentration versus Time and Current versus Time Plots

In this section of appendix, all the plots of concentration against time and current against time are listed as the data arrangement in the previous part. These plots represent the key elements of the results obtained from this work. Concentration against time plots were used to obtain the apparent reaction rate constant at different operation conditions. On the same way, it could be used to evaluate the amount of the copper remains in solution at any time.

The current against time plots were used to evaluate the power consumed to remove certain quantity of copper ion and the current efficiency of the system. The current data were nicely correlated to the time using third order polynomials. These expressions, namely current polynomials can be also used to evaluate the amount of the current running in the system at specific time. In all the curves generated, sigma plot 5.0 package was used

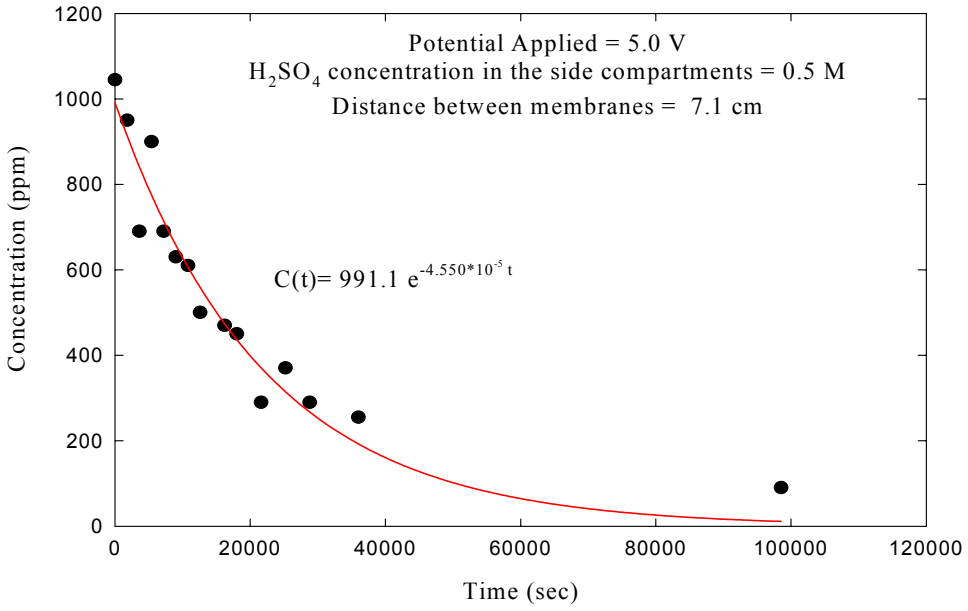

Figure A2- 1: Concentration versus Time at a potential of 5.0 V, membrane spacing of 7.1 cm and side concentration of 0.5 M

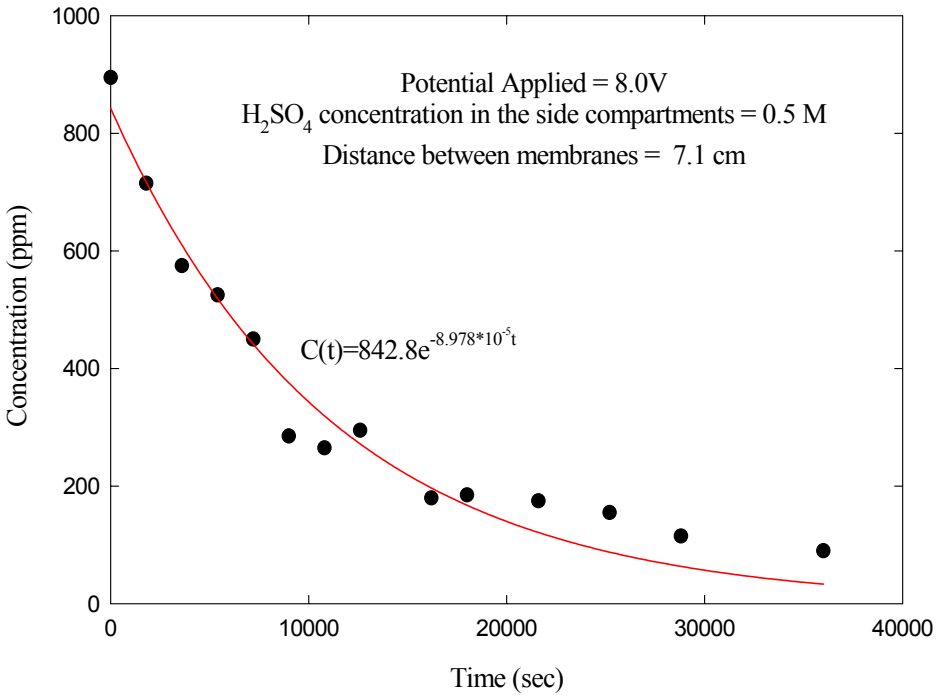

Figure A2- 2: Concentration versus Time at a potential of 8.0 V, membrane spacing of 7.1 cm and side concentration of 0.5 M

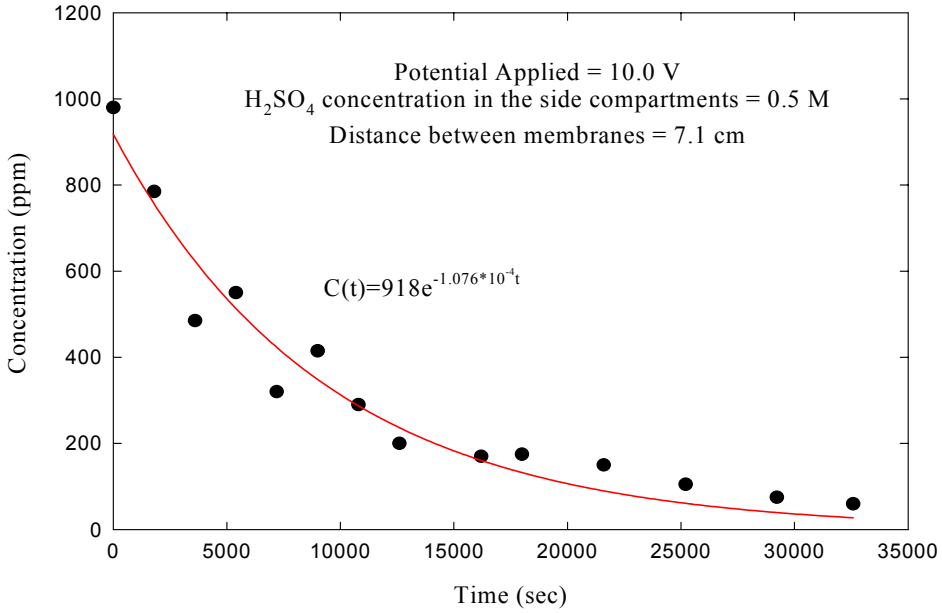

Figure A2- 3: Concentration versus Time at a potential of 10.0 V, membrane spacing of 7.1 cm and side concentration of 0.5 M

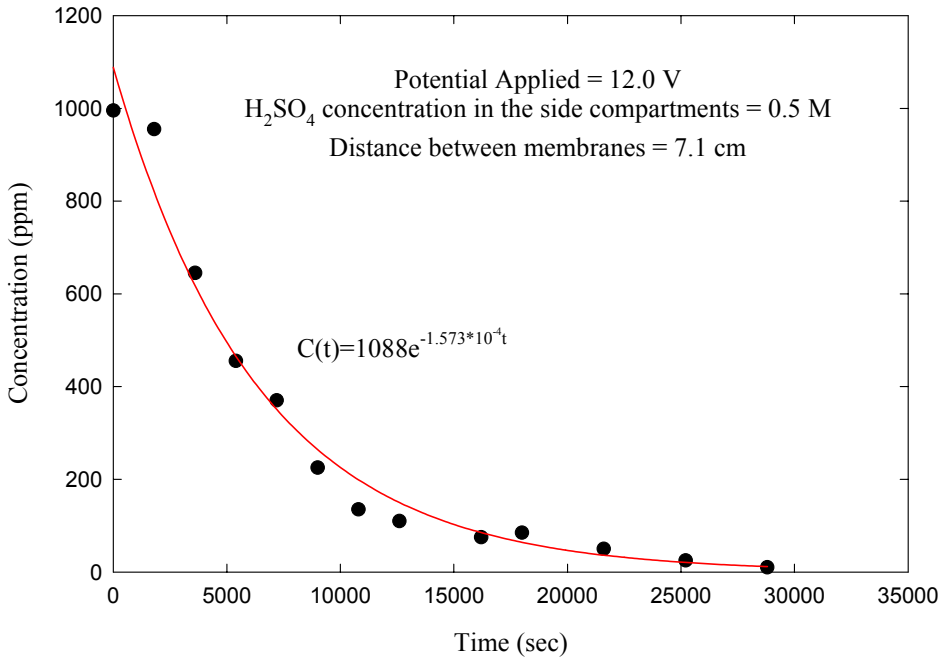

Figure A2- 4: Concentration versus Time at a potential of 12.0 V, membrane spacing of 7.1 cm and side concentration of 0.5 M

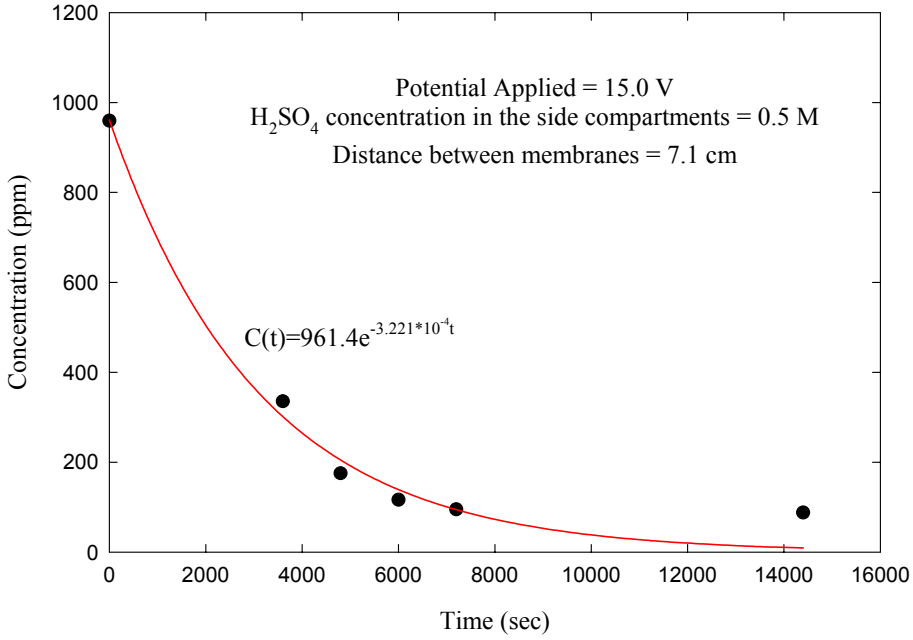

Figure A2- 5: Concentration versus Time at a potential of 15.0 V, membrane spacing of 7.1 cm and side concentration of 0.5 M.

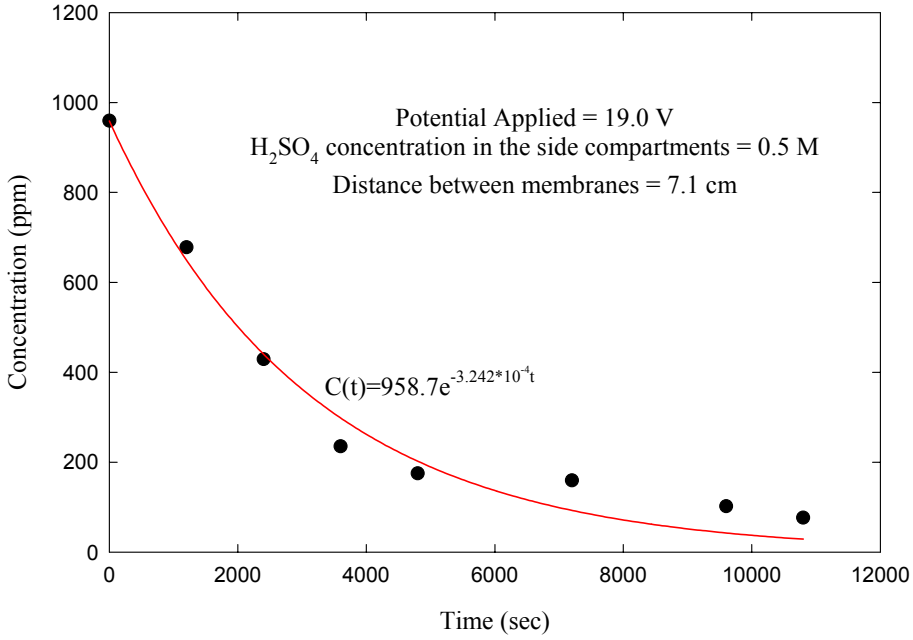

Figure A2- 6: Concentration versus Time at a potential of 19.0 V, membrane spacing of 7.1 cm and side concentration of 0.5 M

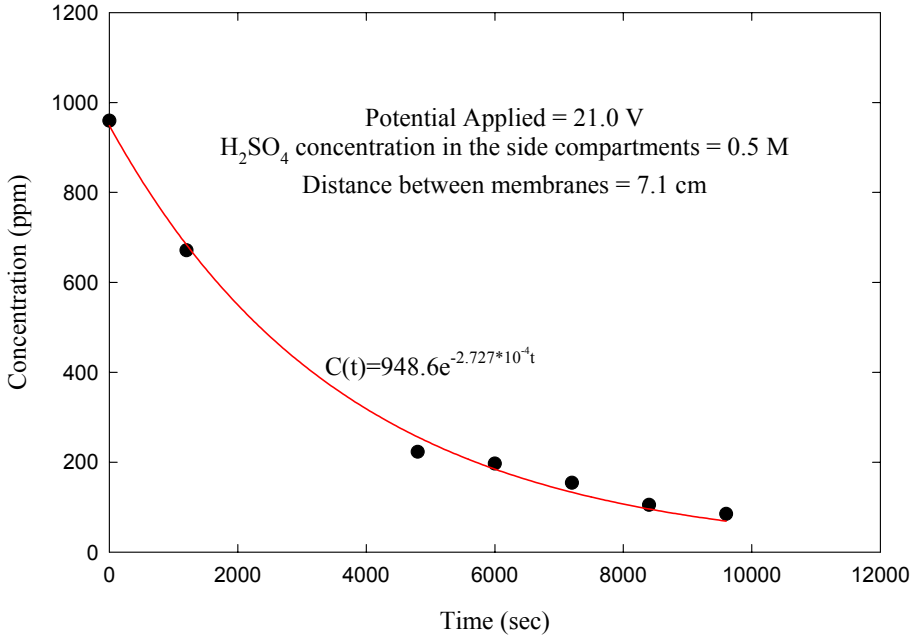

Figure A2- 7: Concentration versus Time at a potential of 21.0 V, membrane spacing of 7.1 cm and side concentration of 0.5 M

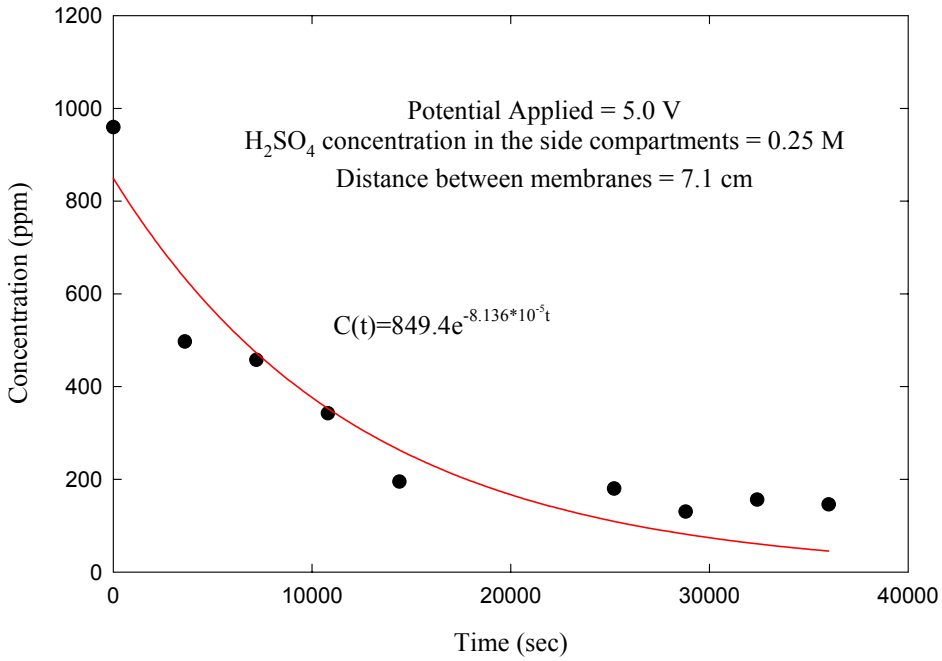

Figure A2- 8: Concentration versus Time at a potential of 5.0 V, membrane spacing of 7.1 cm and side concentration of 0.25 M

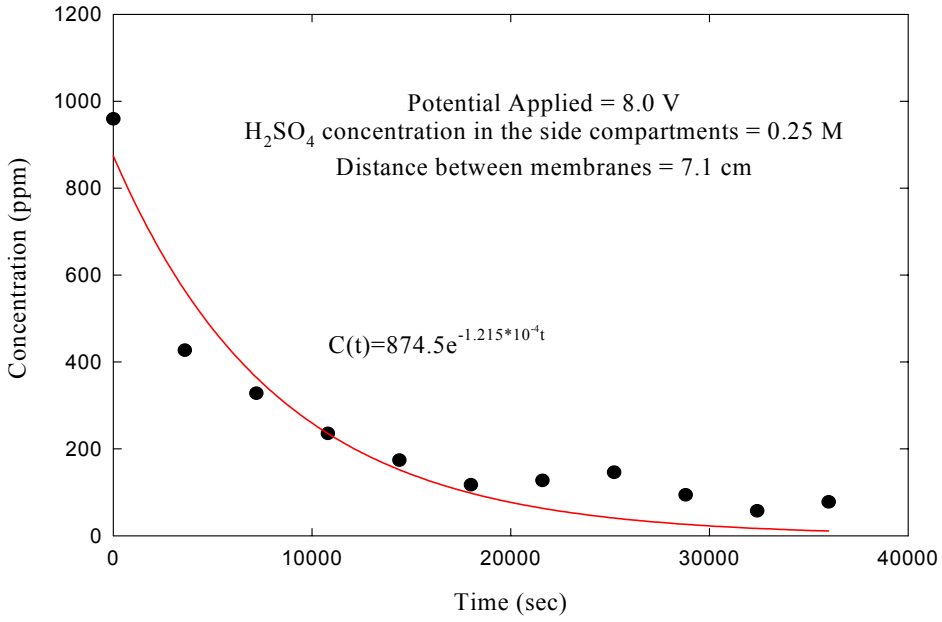

Figure A2- 9: Concentration versus Time at a potential of 8.0 V, membrane spacing of 7.1 cm and side concentration of 0.25 M

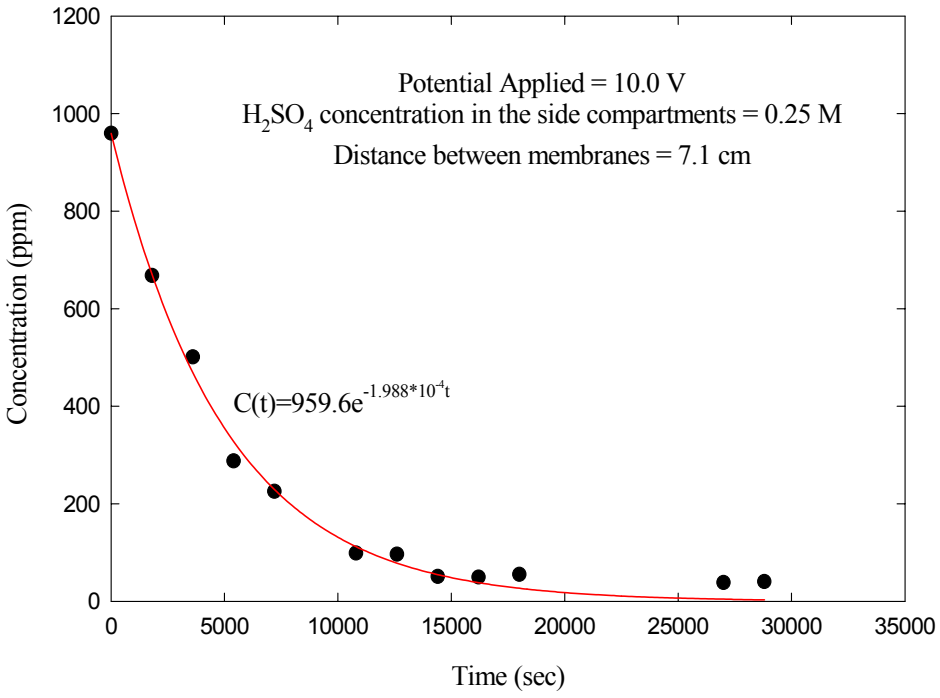

Figure A2- 10: Concentration versus Time at a potential of 10.0V, membrane spacing of 7.1 cm and side concentration of 0.25 M

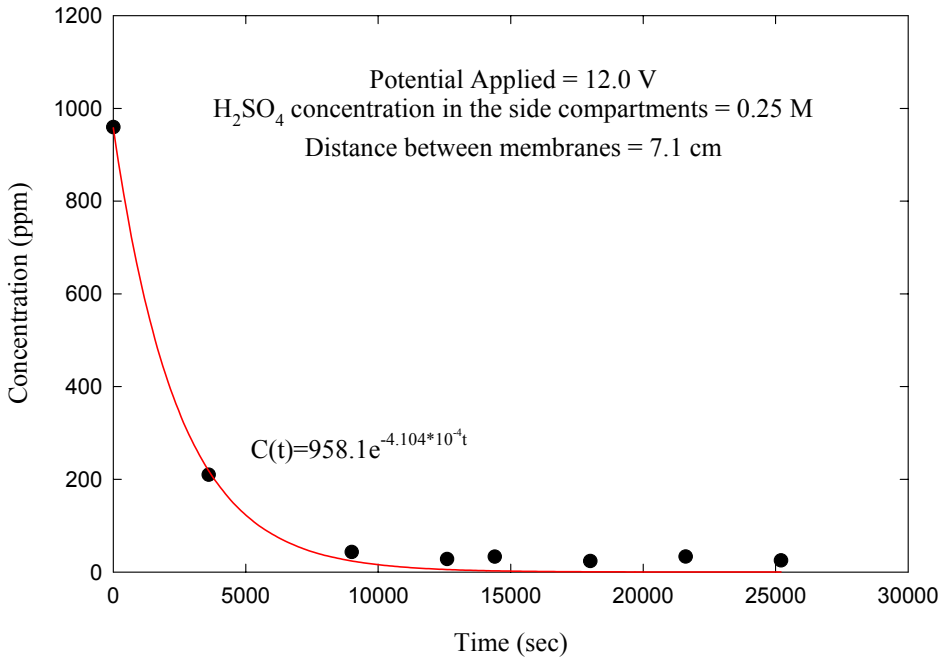

Figure A2- 11: Concentration versus Time at a potential of 12.0 V, membrane spacing of 7.1 cm and side concentration of 0.25 M

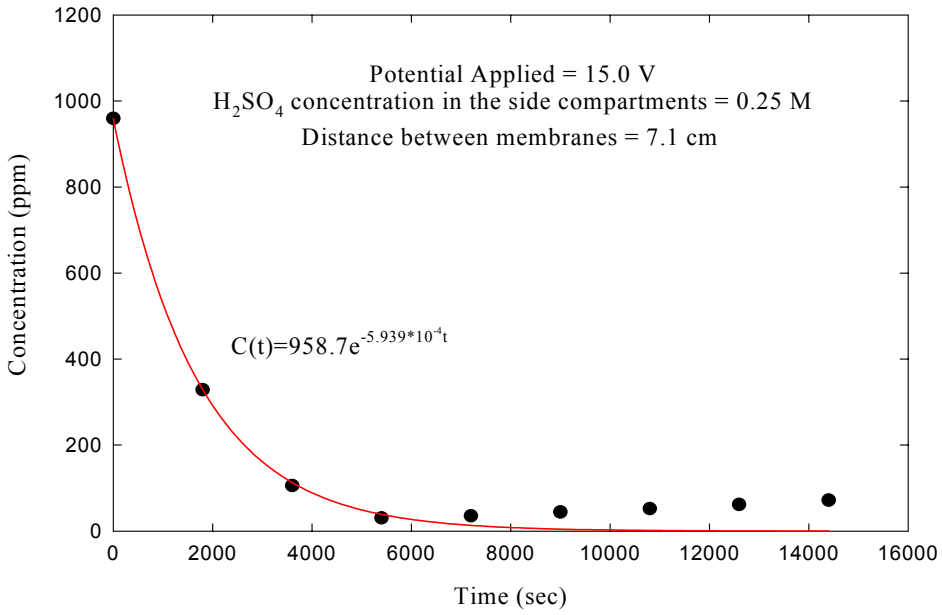

Figure A2- 12: Concentration versus Time at a potential of 15.0 V, membrane spacing of 7.1 cm and side concentration of 0.25 M

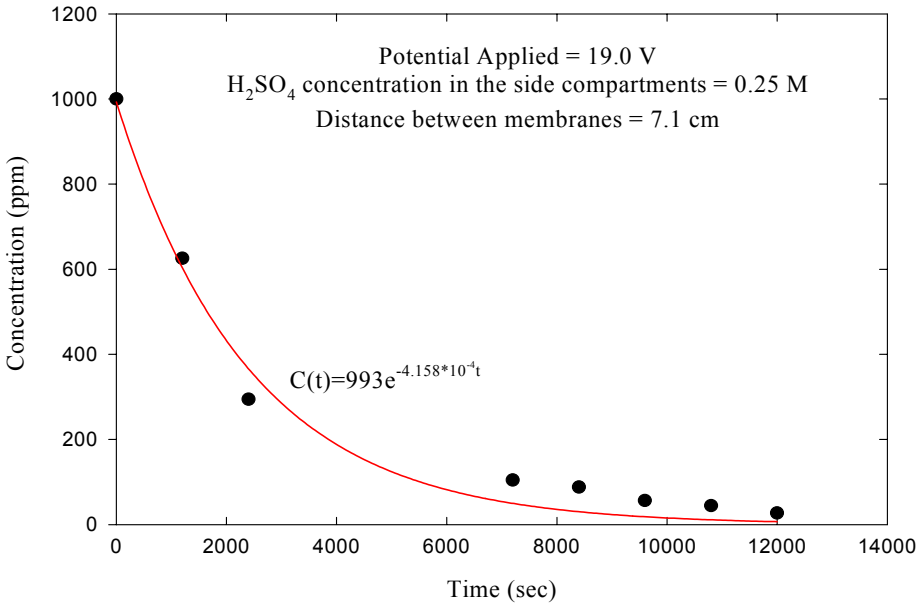

Figure A2- 13: Concentration versus Time at a potential of 19.0 V, membrane spacing of 7.1 cm and side concentration of 0.25 M

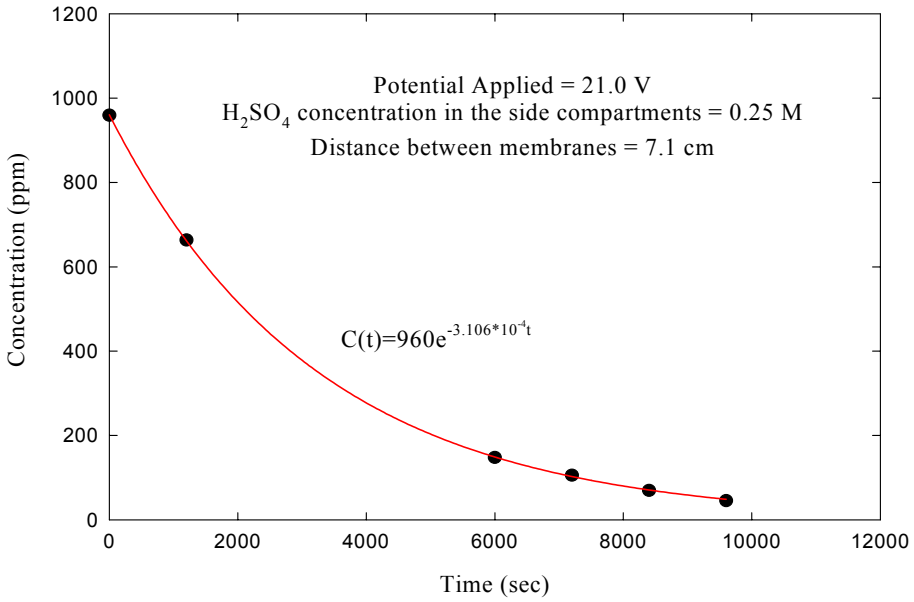

Figure A2- 14: Concentration versus Time at a potential of 21.0 V, membrane spacing of 7.1 cm and side concentration of 0.25 M

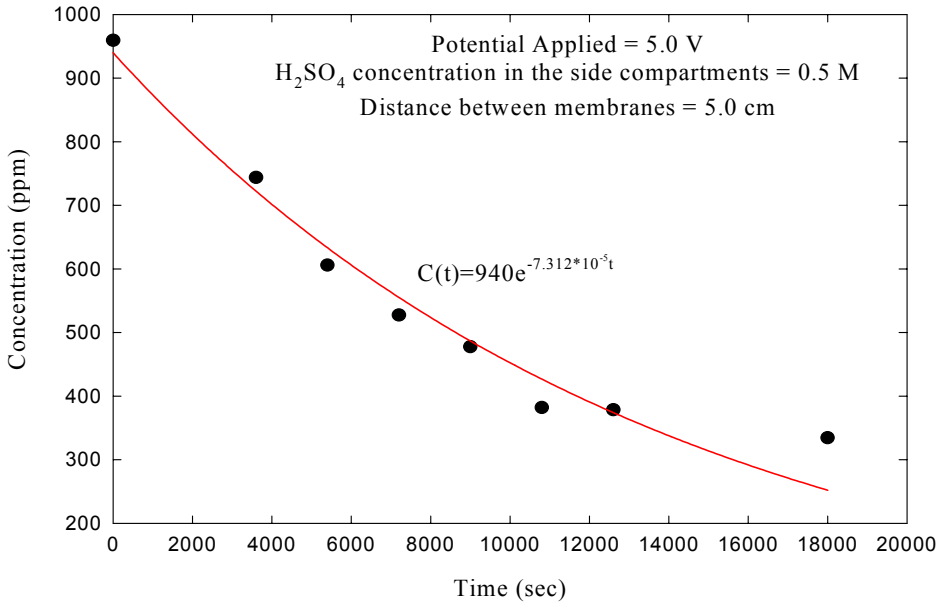

Figure A2- 15: Concentration versus Time at a potential of 5.0 V, membrane spacing of 5.0 cm and side concentration of 0.5 M

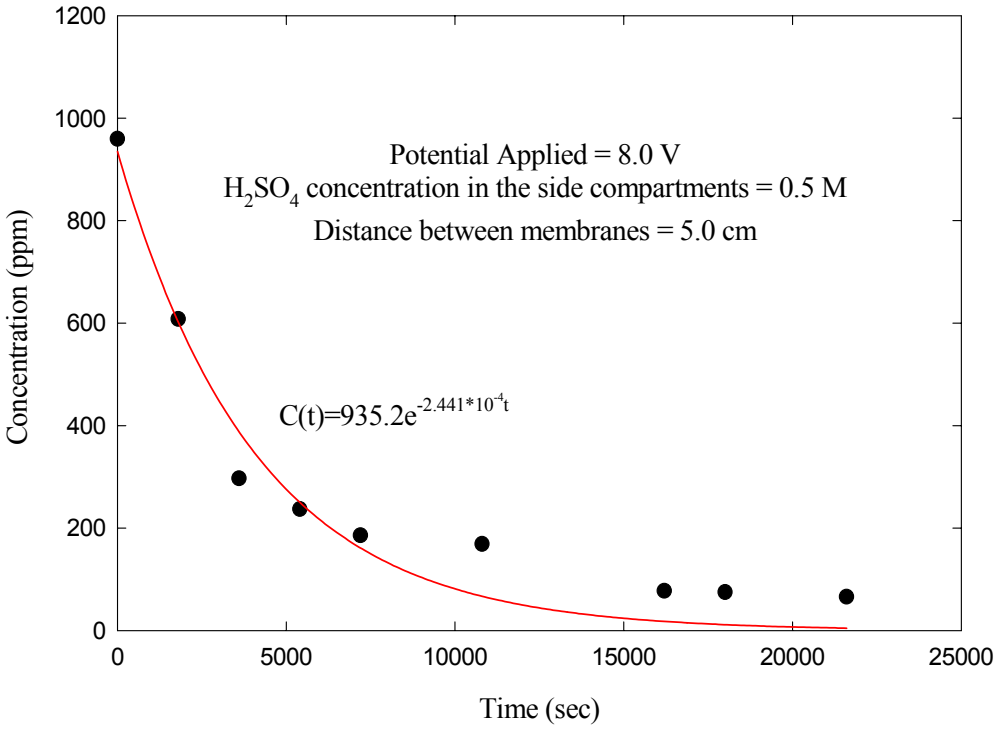

Figure A2- 16: Concentration versus Time at a potential of 8.0 V, membrane spacing of 5.0 cm and side concentration of 0.5 M

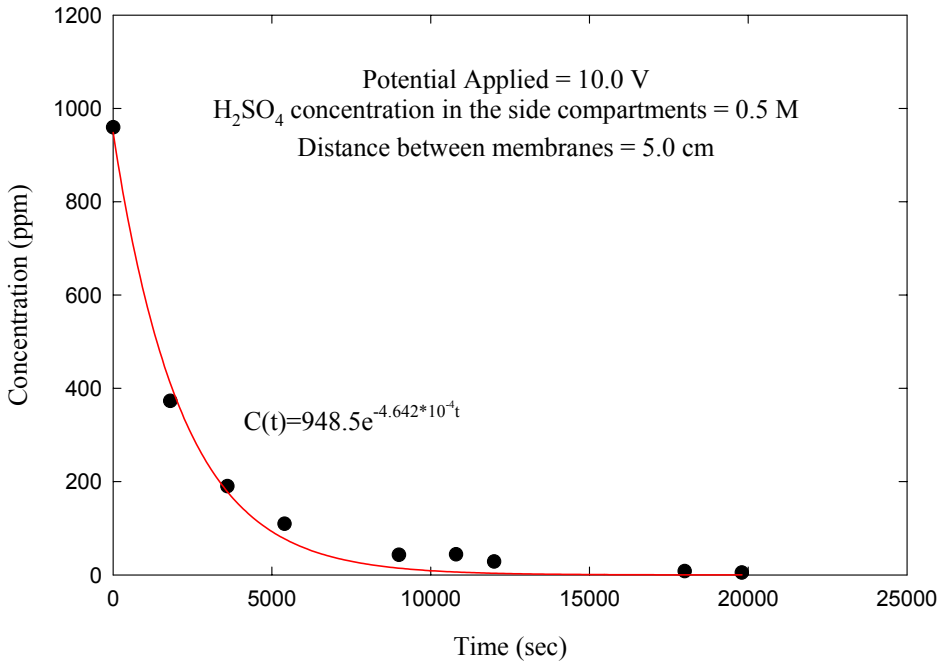

Figure A2- 17: Concentration versus Time at a potential of 10.0 V, membrane spacing of 5.0 cm and side concentration of 0.5 M

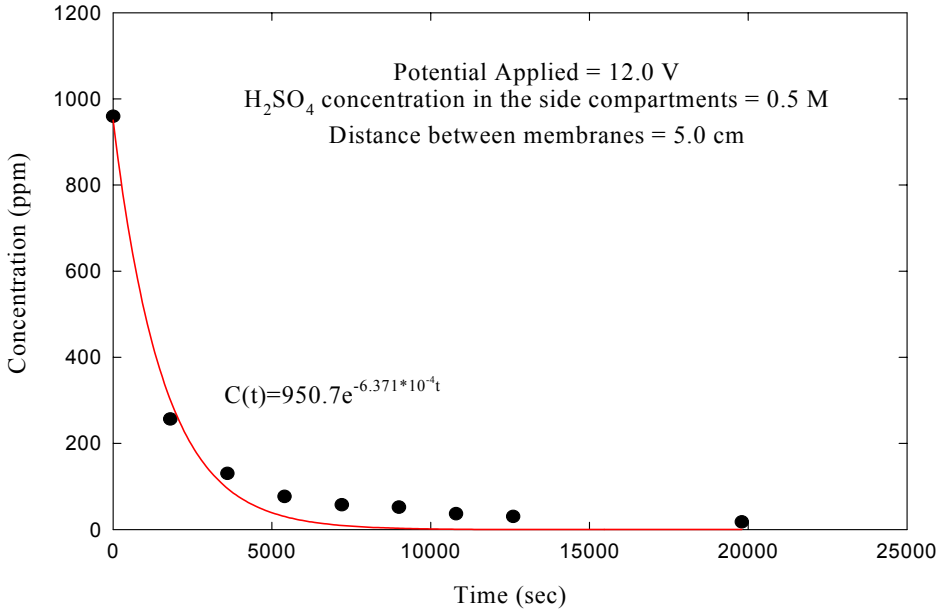

Figure A2- 18: Concentration versus Time at a potential of 12.0 V, membrane spacing of 5.0 cm and side concentration of 0.5 M

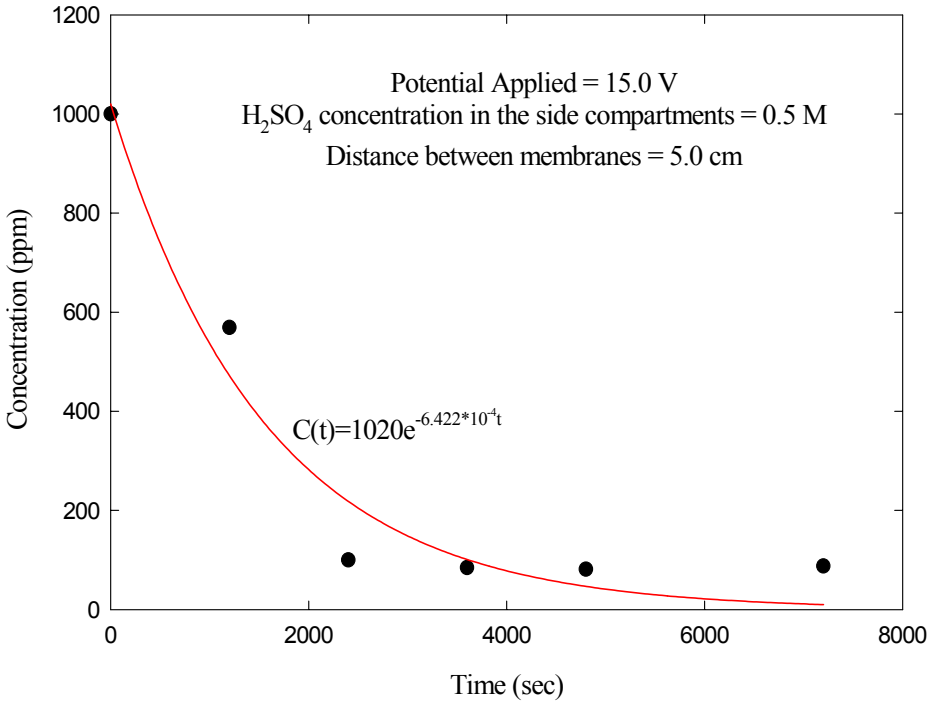

Figure A2- 19: Concentration versus Time at a potential of 15.0 V, membrane spacing of 5.0 cm and side concentration of 0.5 M

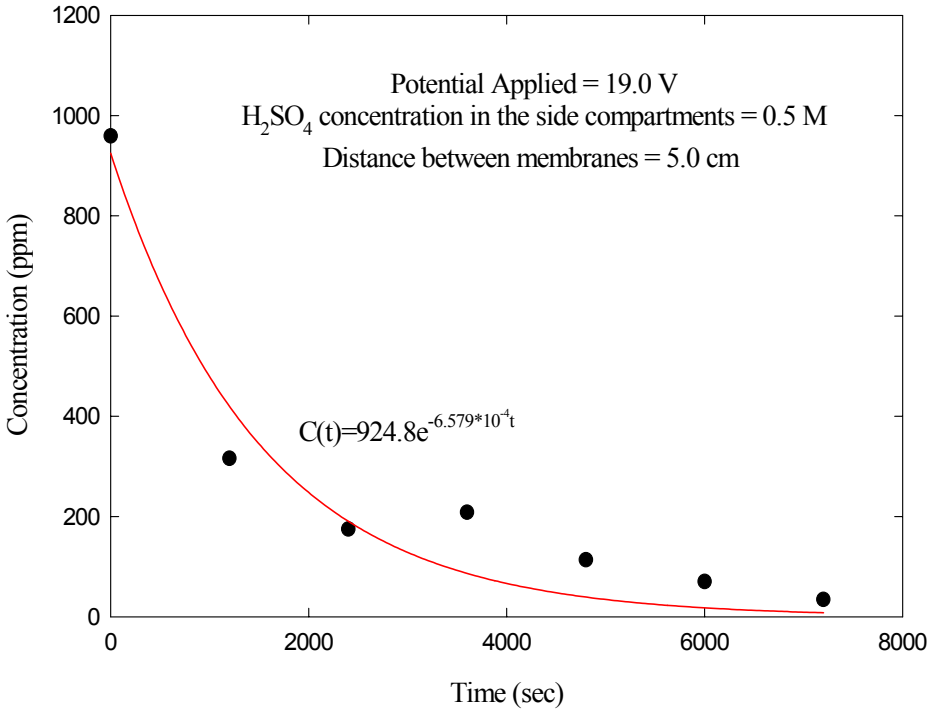

Figure A2- 20: Concentration versus Time at a potential of 19.0 V, membrane spacing of 5.0 cm and side concentration of 0.5 M

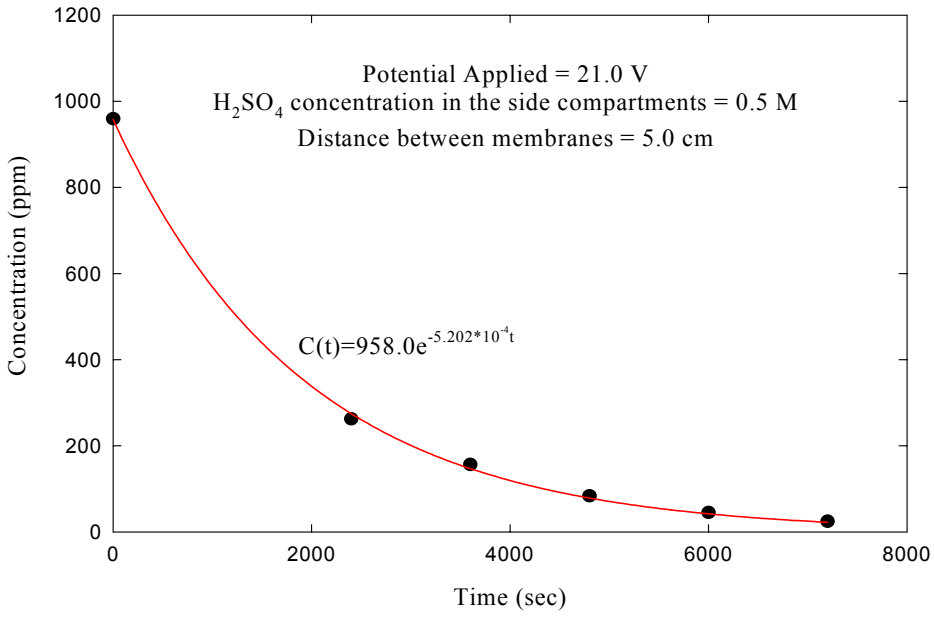

Figure A2- 21: Concentration versus Time at a potential of 21.0 V, membrane spacing of 5.0 cm and side concentration of 0.5 M

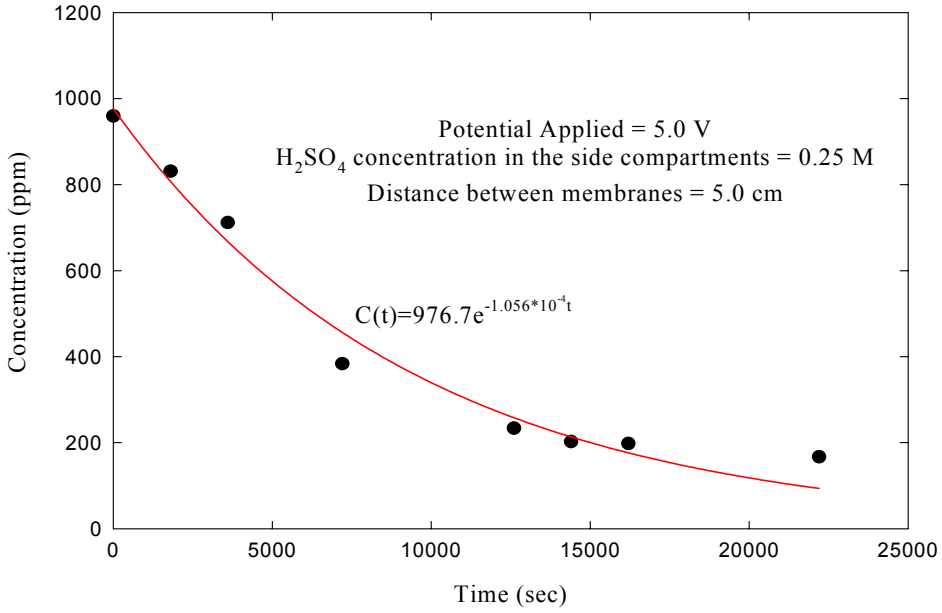

Figure A2- 22: Concentration versus Time at a potential of 5.0 V, membrane spacing of 5.0 cm and side concentration of 0.25 M

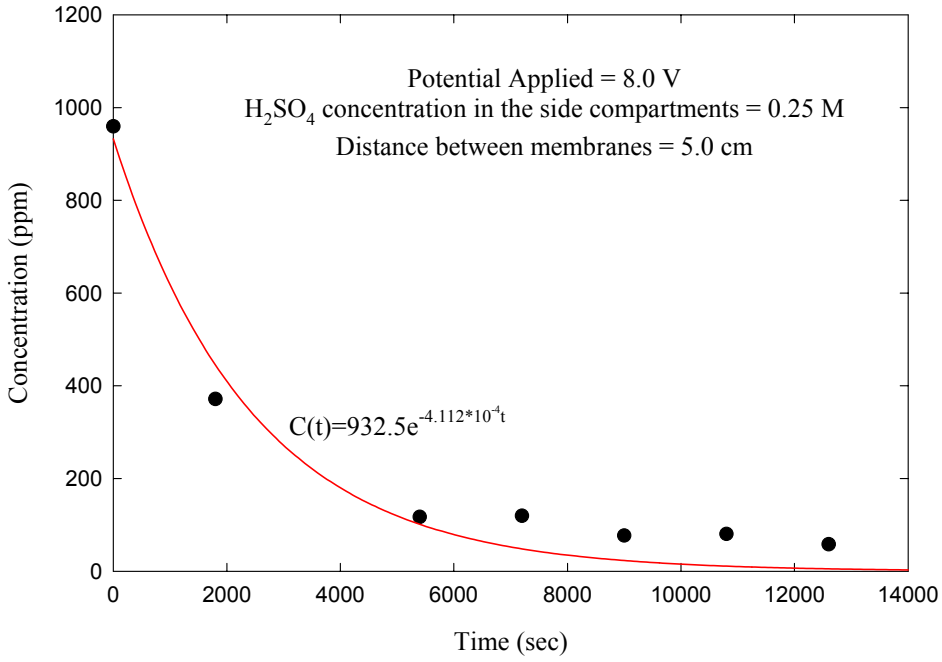

Figure A2- 23: Concentration versus Time at a potential of 8.0 V, membrane spacing of 5.0 cm and side concentration of 0.25 M

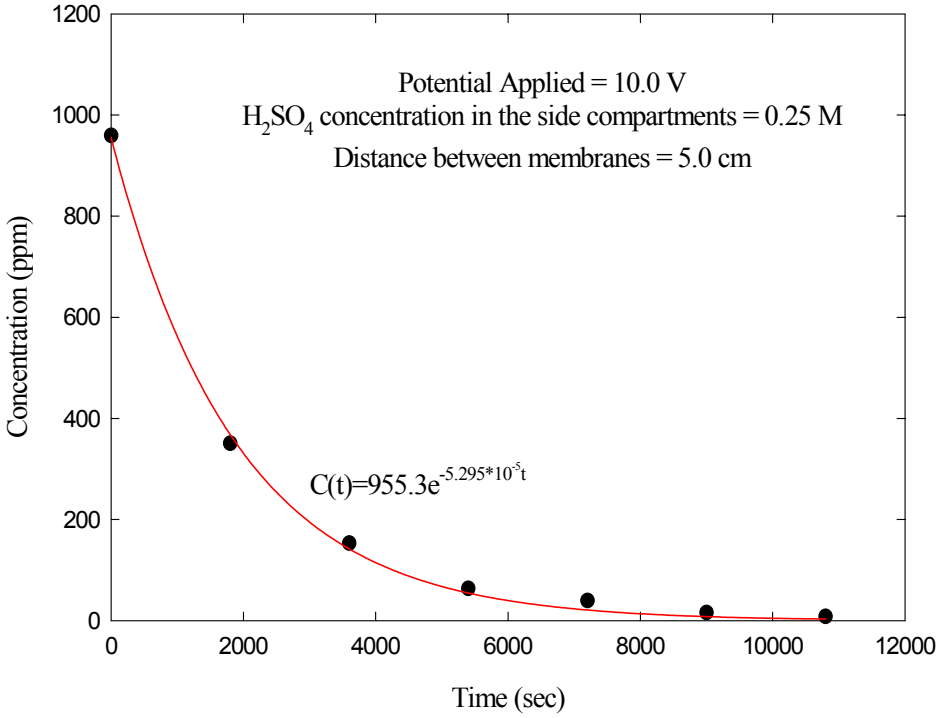

Figure A2- 24: Concentration versus Time at a potential of 10.0 V, membrane spacing of 5.0 cm and side concentration of 0.25 M

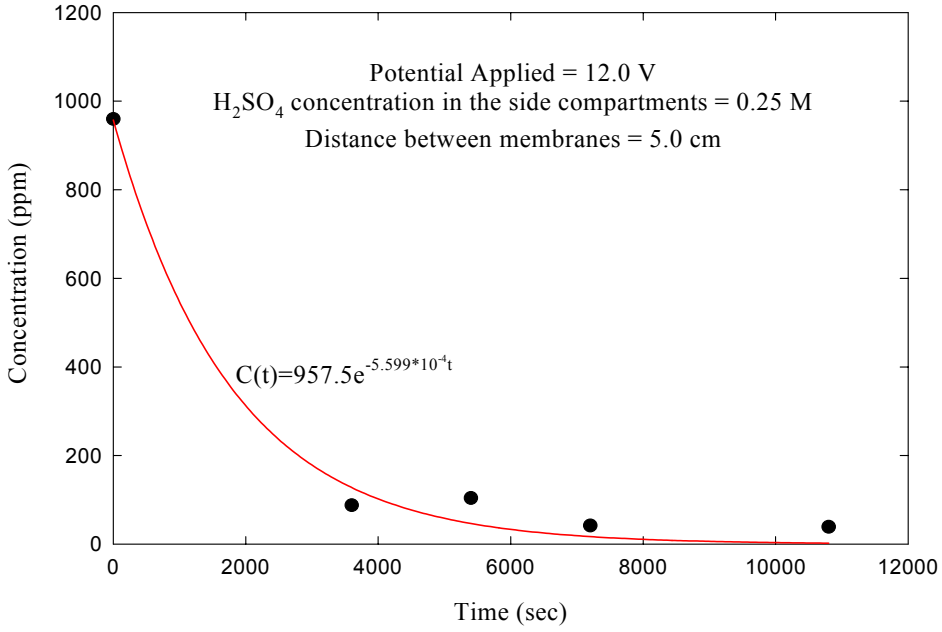

Figure A2- 25: Concentration versus Time at a potential of 12.0 V, membrane spacing of 5.0 cm and side concentration of 0.25 M

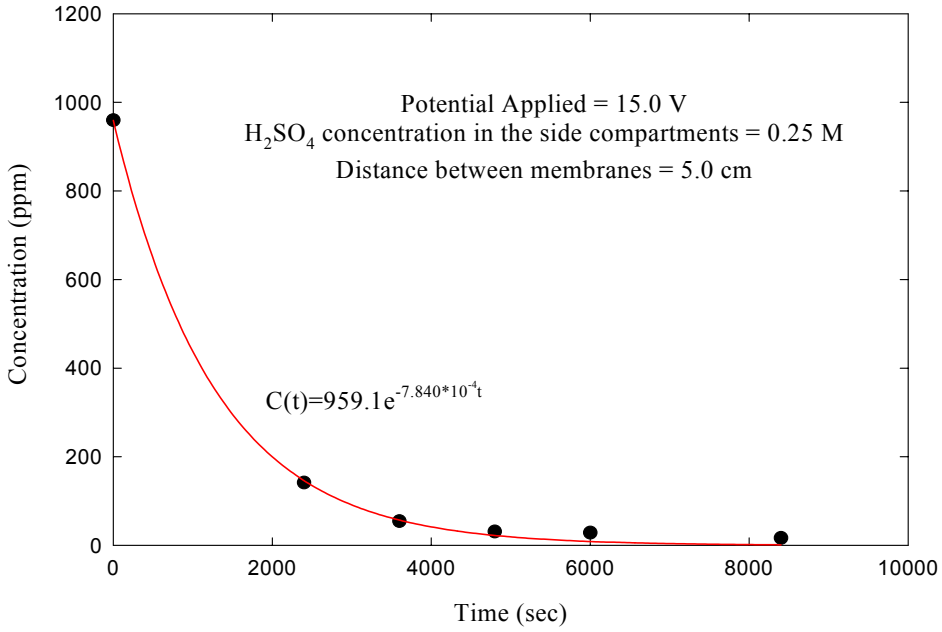

Figure A2- 26: Concentration versus Time at a potential of 15.0 V, membrane spacing of 5.0 cm and side concentration of 0.25 M

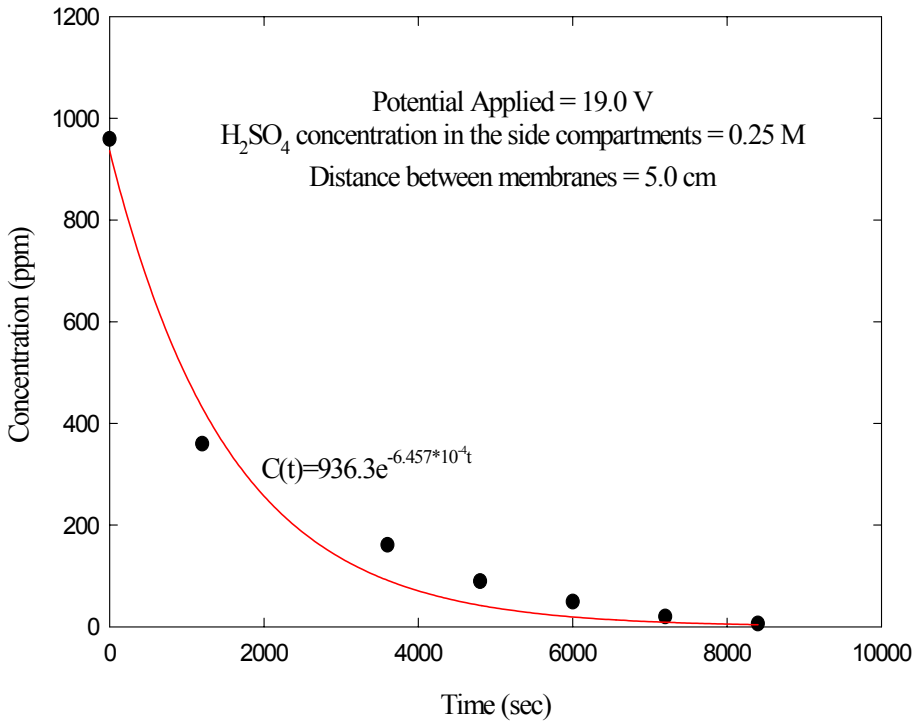

Figure A2- 27: Concentration versus Time at a potential of 19.0 V, membrane spacing of 5.0 cm and side concentration of 0.25 M

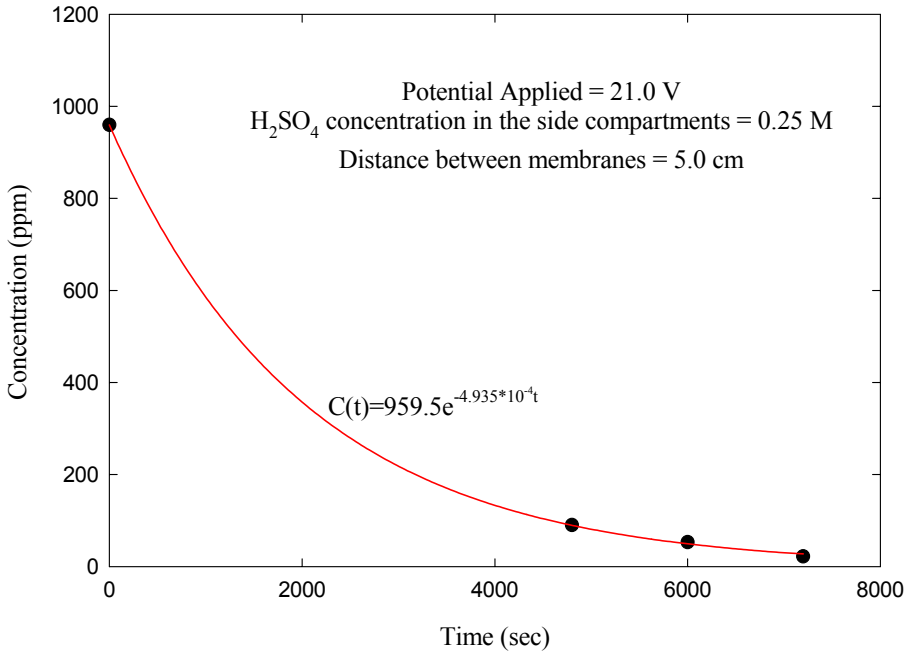

Figure A2- 28: Concentration versus Time at a potential of 21.0 V, membrane spacing of 5.0 cm and side concentration of 0.25 M

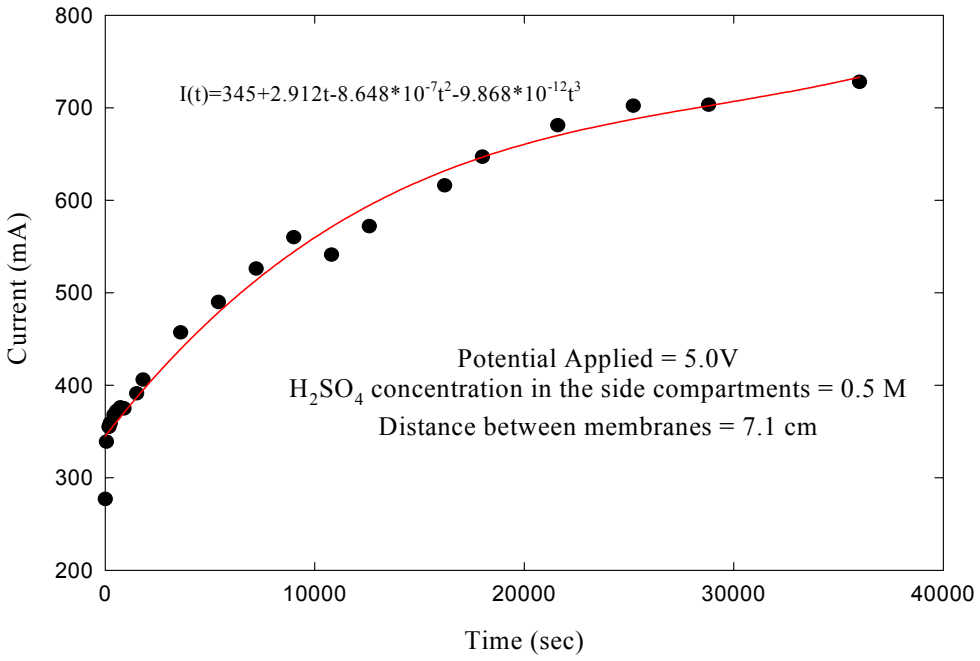

Figure A2- 29: Current versus Time at a potential of 5.0 V, membrane spacing of 7.1 cm and side concentration of 0.5 M

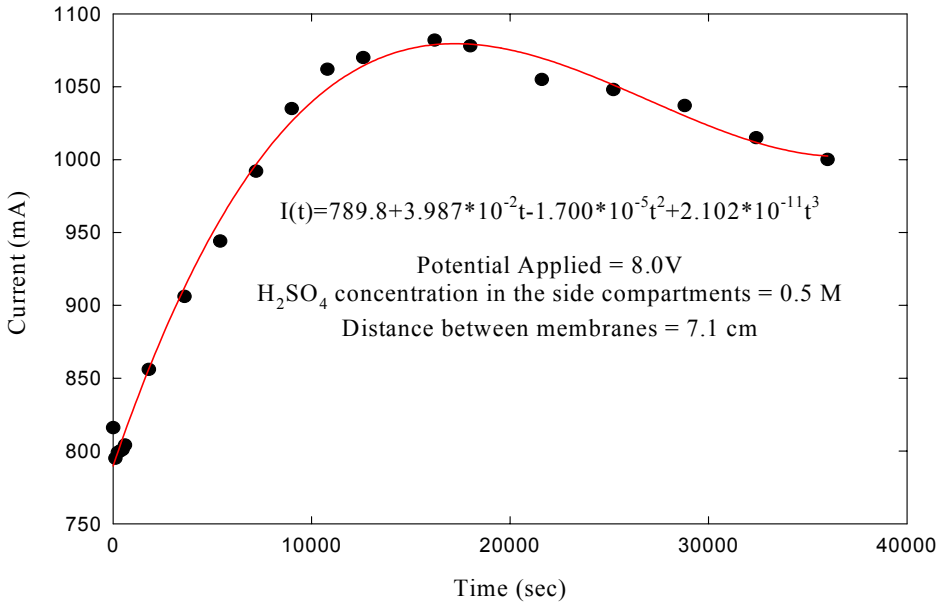

Figure A2- 30: Current versus Time at a potential of 8.0 V, membrane spacing of 7.1 cm and side concentration of 0.5 M

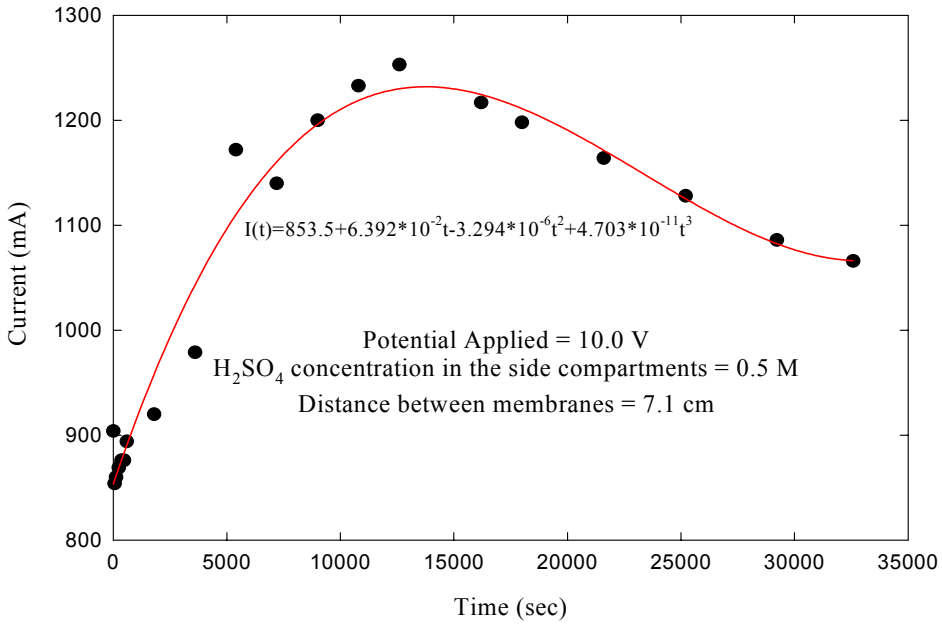

Figure A2- 31: Current versus Time at a potential of 10.0 V, membrane spacing of 7.1 cm and side concentration of 0.5 M

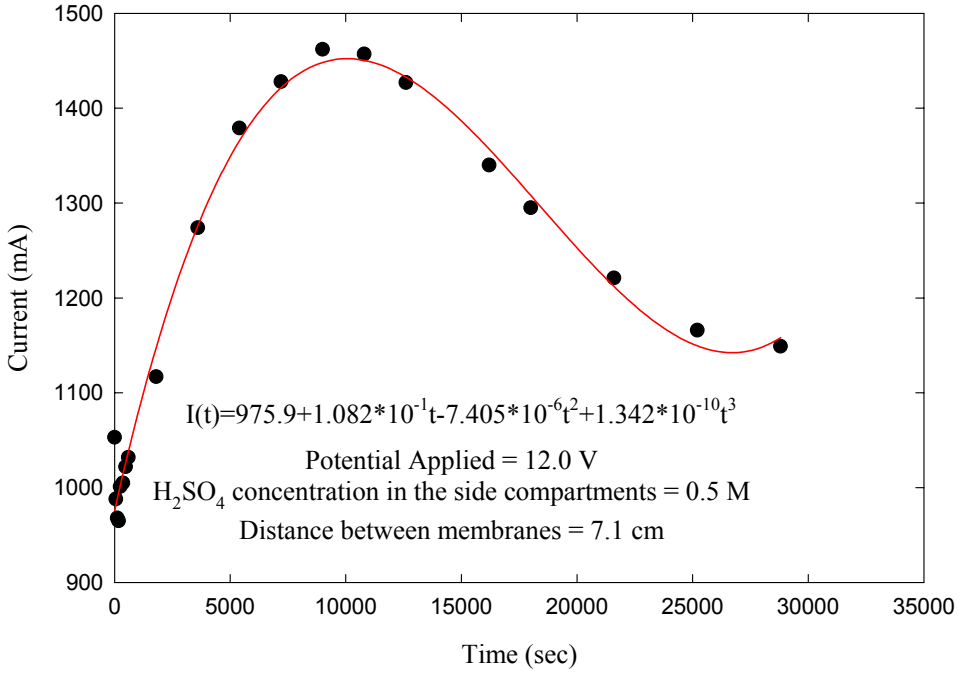

Figure A- 32: Current versus Time at a potential of 12.0 V, membrane spacing of 7.1 cm and side concentration of 0.5 M

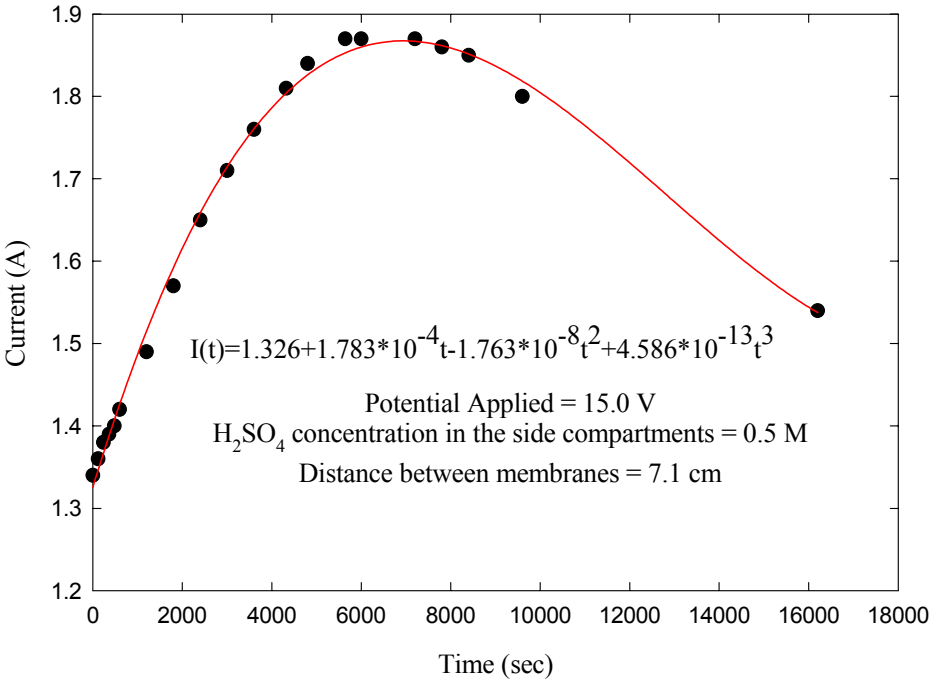

Figure A2- 33: Current versus Time at a potential of 15.0 V, membrane spacing of 7.1 cm and side concentration of 0.5 M

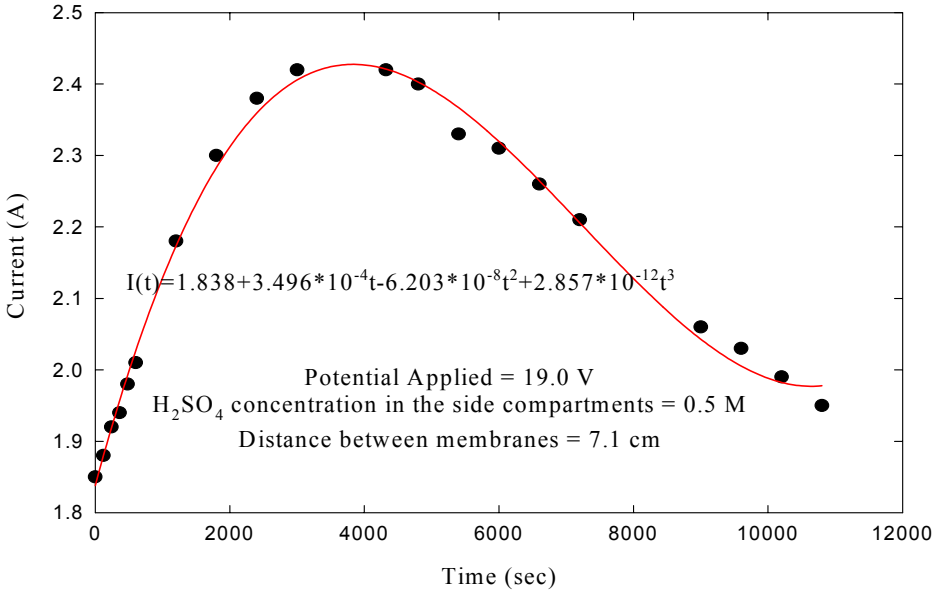

Figure A2- 34: Current versus Time at a potential of 19.0 V, membrane spacing of 7.1 cm and side concentration of 0.5 M

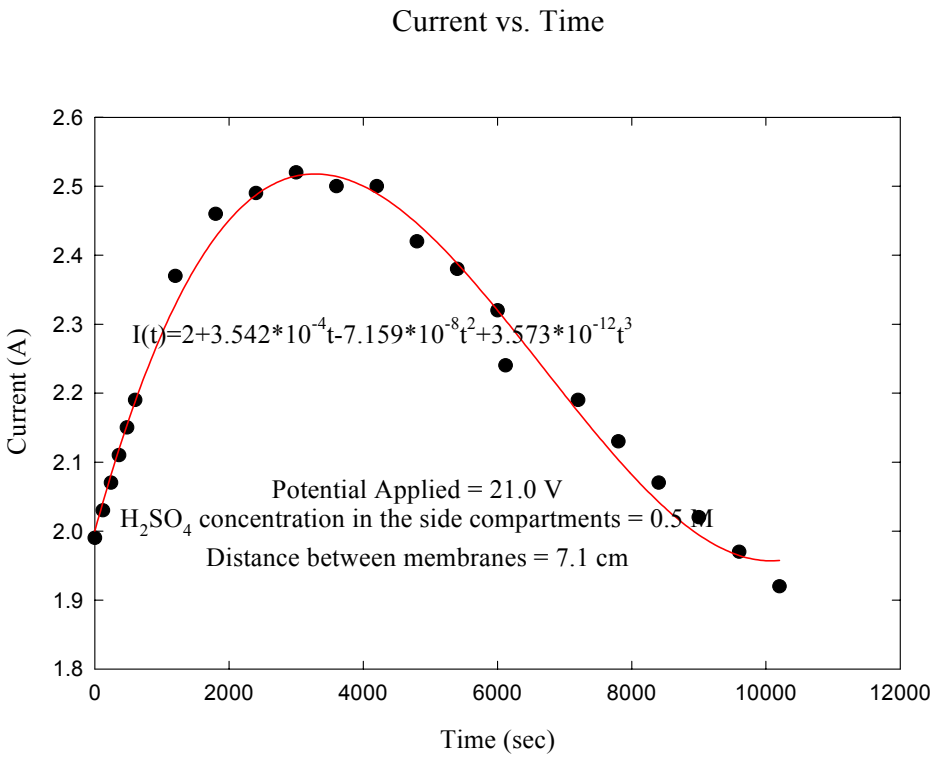

Figure A2- 35: Current versus Time at a potential of 21.0 V, membrane spacing of 7.1 cm and side concentration of 0.5 M

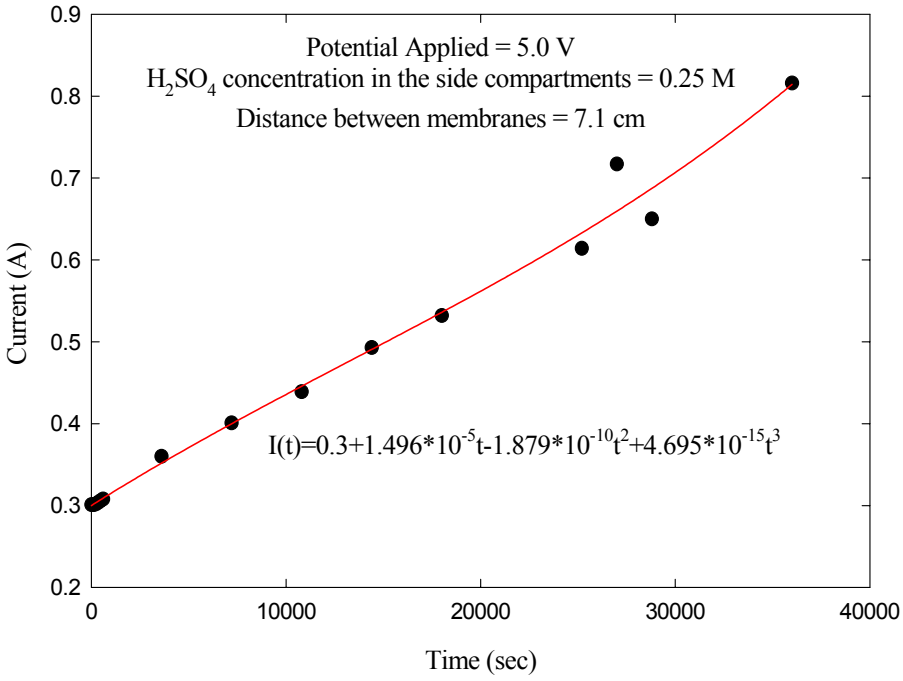

Figure A2- 36: Current versus Time at a potential of 5.0 V, membrane spacing of 7.1 cm and side concentration of 0.25 M

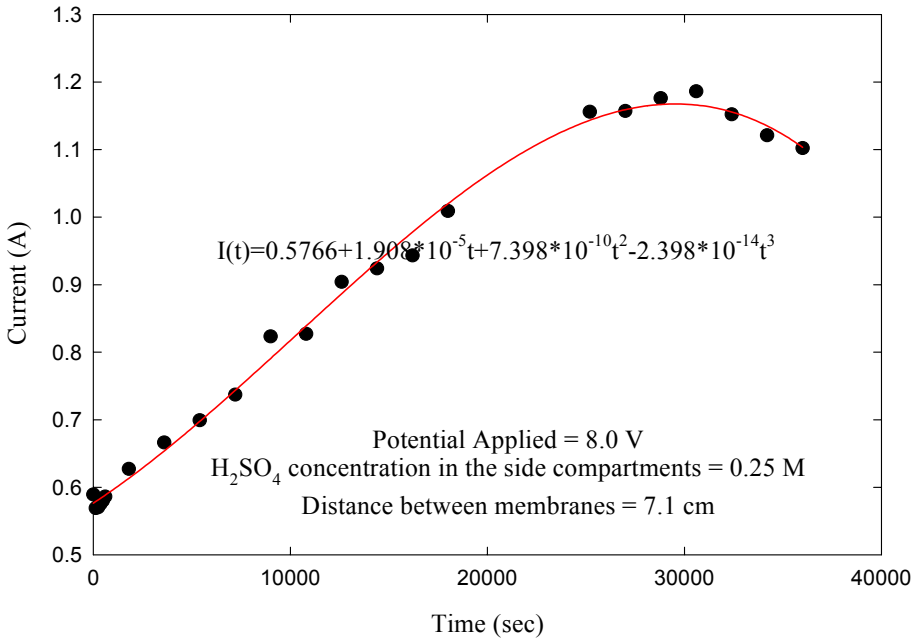

Figure A2- 37: Current versus Time at a potential of 8.0 V, membrane spacing of 7.1 cm and side concentration of 0.25 M

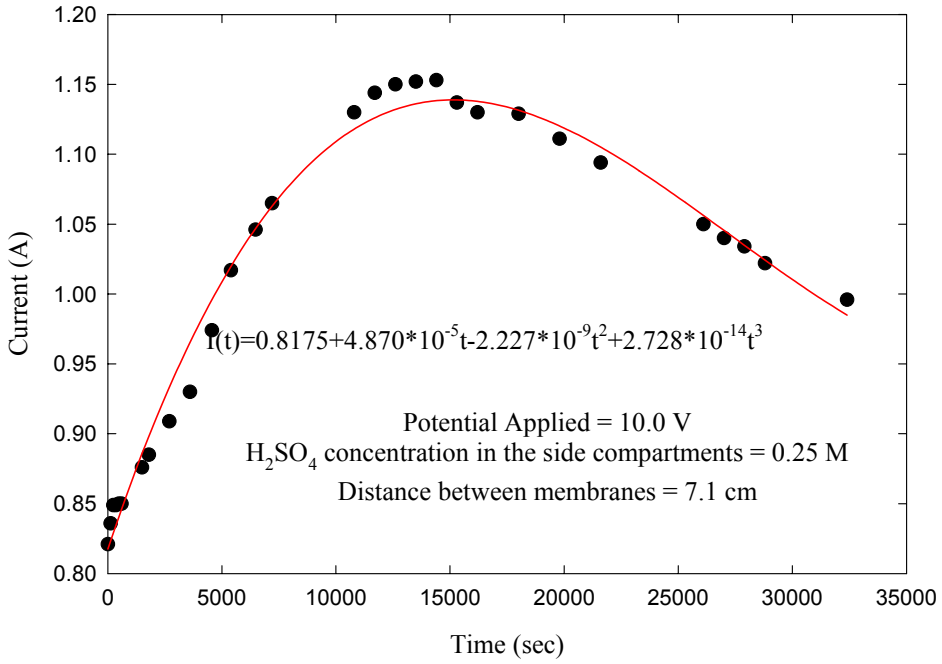

Figure A2- 38: Current versus Time at a potential of 10.0 V, membrane spacing of 7.1 cm and side concentration of 0.25 M

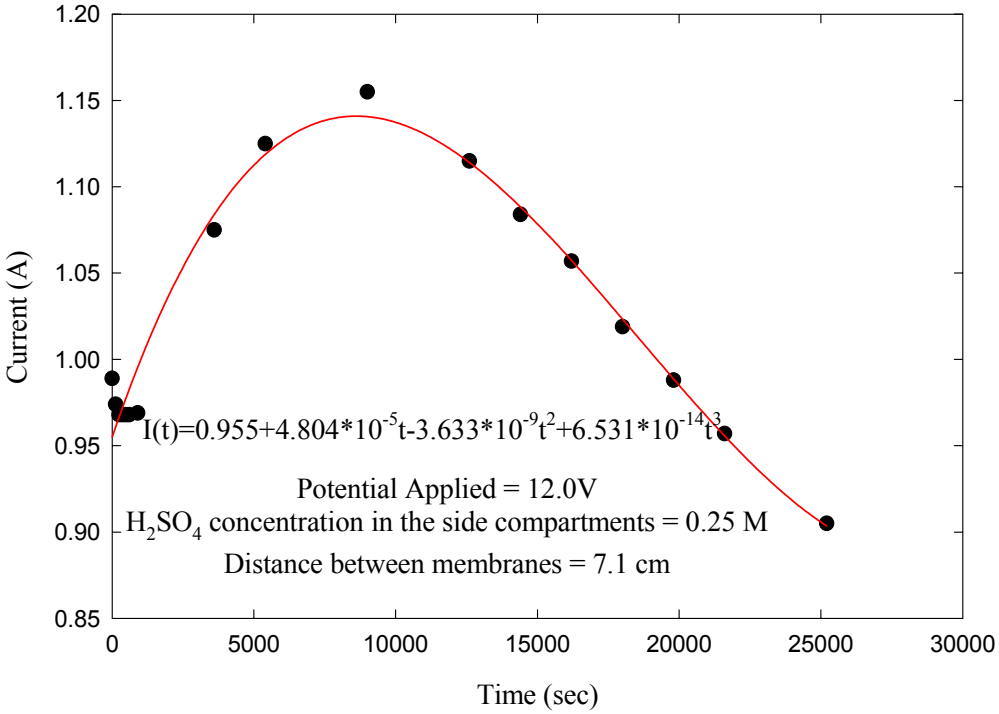

Figure A2- 39: Current versus Time at a potential of 12.0 V, membrane spacing of 7.1 cm and side concentration of 0.25 M

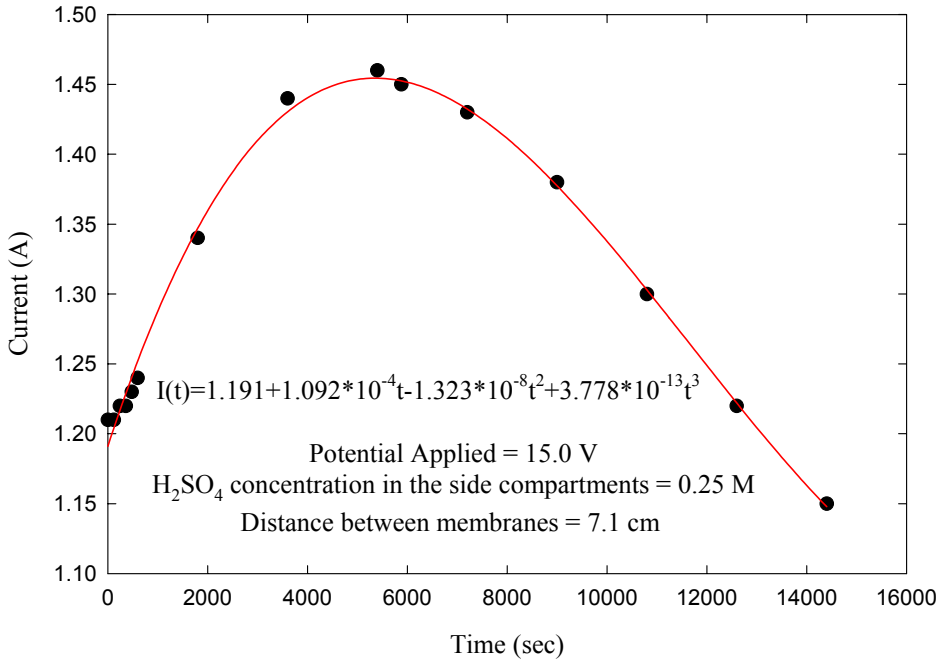

Figure A2- 40: Current versus Time at a potential of 15.0 V, membrane spacing of 7.1 cm and side concentration of 0.25 M

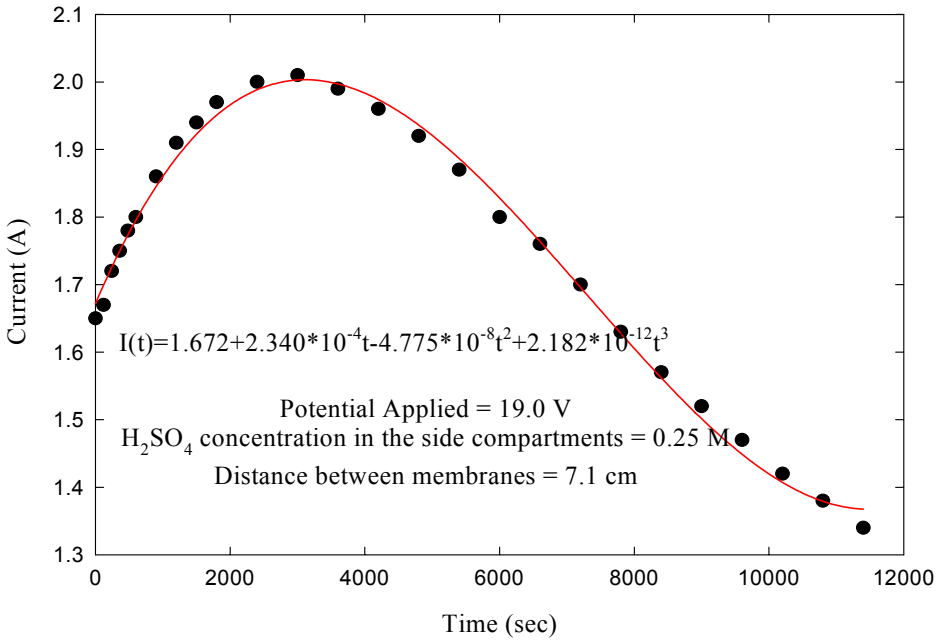

Figure A2- 41: Current versus Time at a potential of 19.0 V, membrane spacing of 7.1 cm and side concentration of 0.25 M

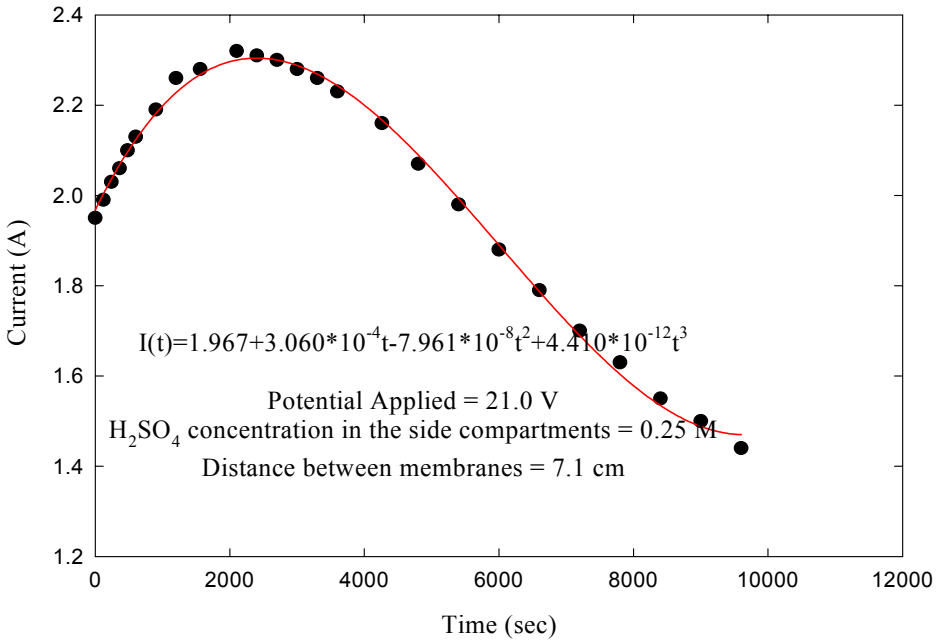

Figure A2- 42: Current versus Time at a potential of 21.0 V, membrane spacing of 7.1 cm and side concentration of 0.25 M

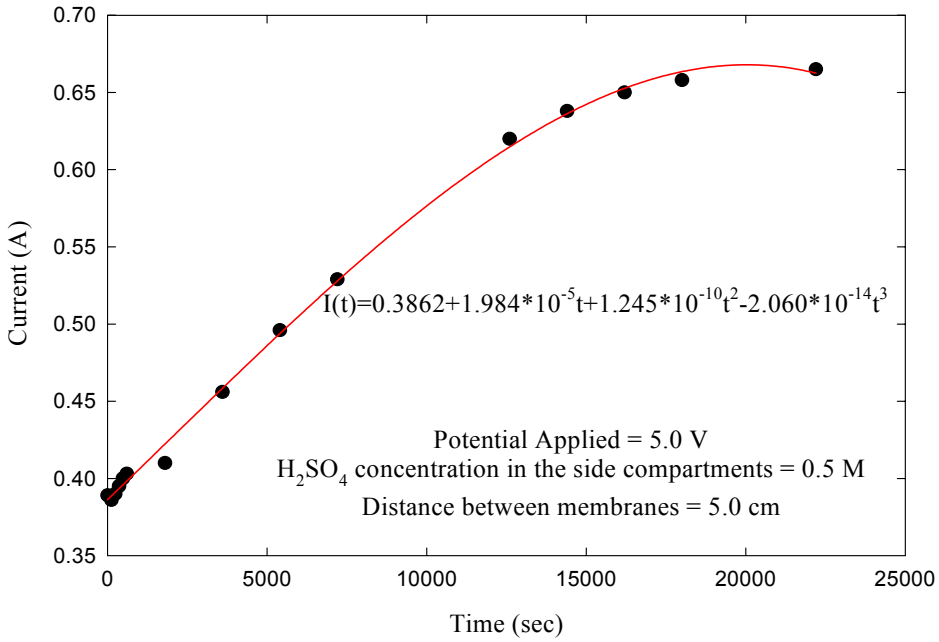

Figure A2- 43: Current versus Time at a potential of 5.0 V, membrane spacing of 5.0 cm and side concentration of 0.5 M

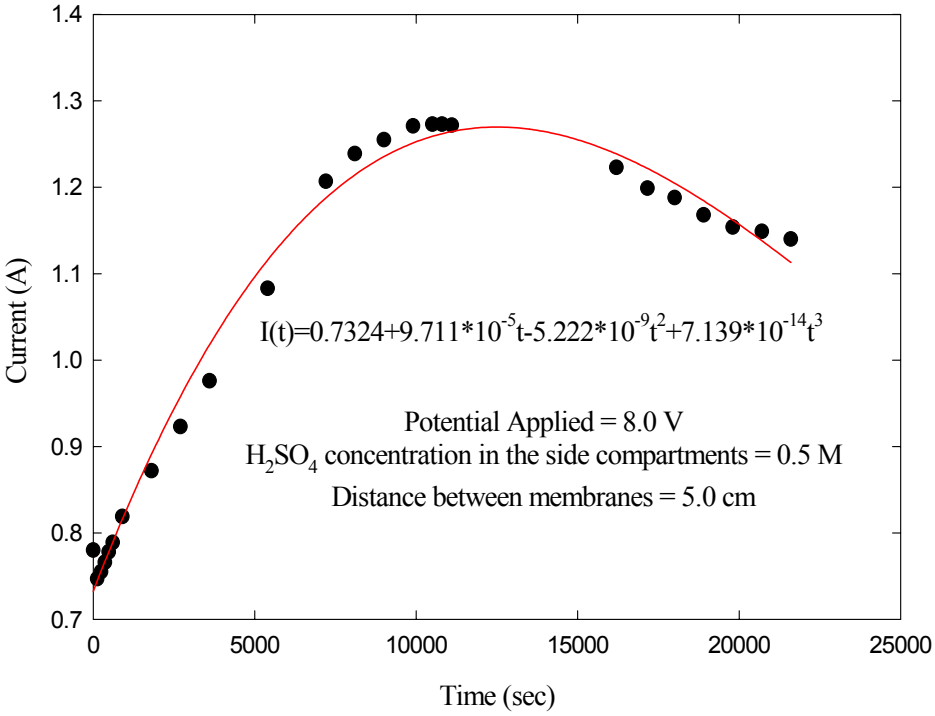

Figure A2- 44: Current versus Time at a potential of 8.0 V, membrane spacing of 5.0 cm and side concentration of 0.5 M

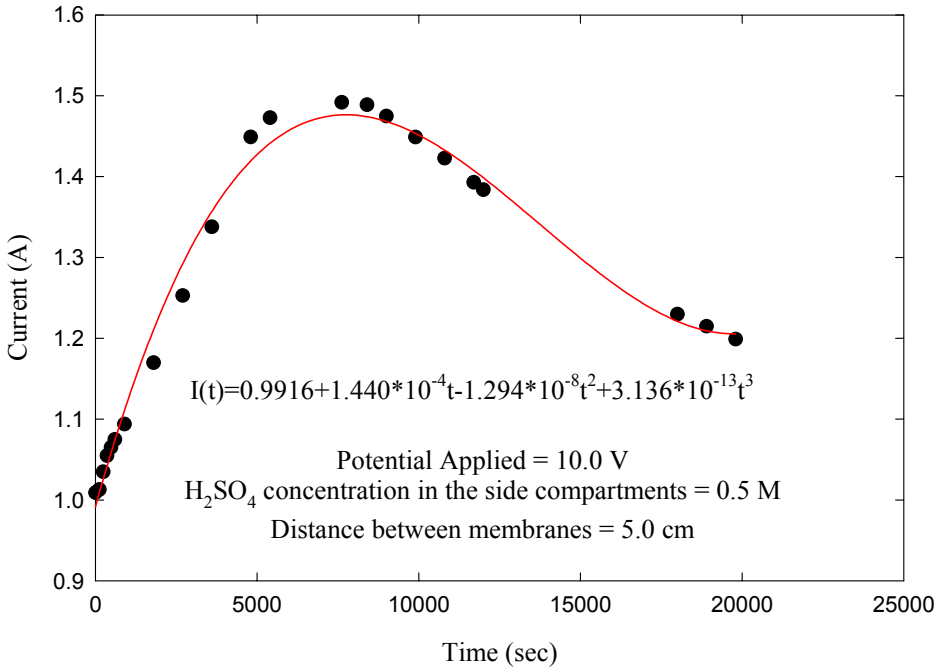

Figure A2- 45: Current versus Time at a potential of 10.0 V, membrane spacing of 5.0 cm and side concentration of 0.5 M

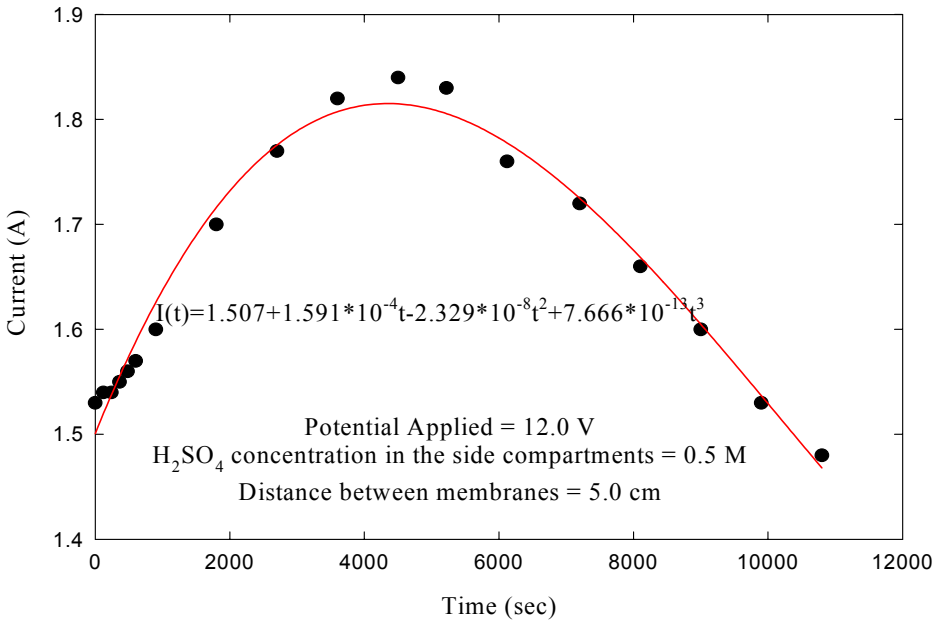

Figure A2- 46: Current versus Time at a potential of 12.0 V, membrane spacing of 5.0 cm and side concentration of 0.5 M

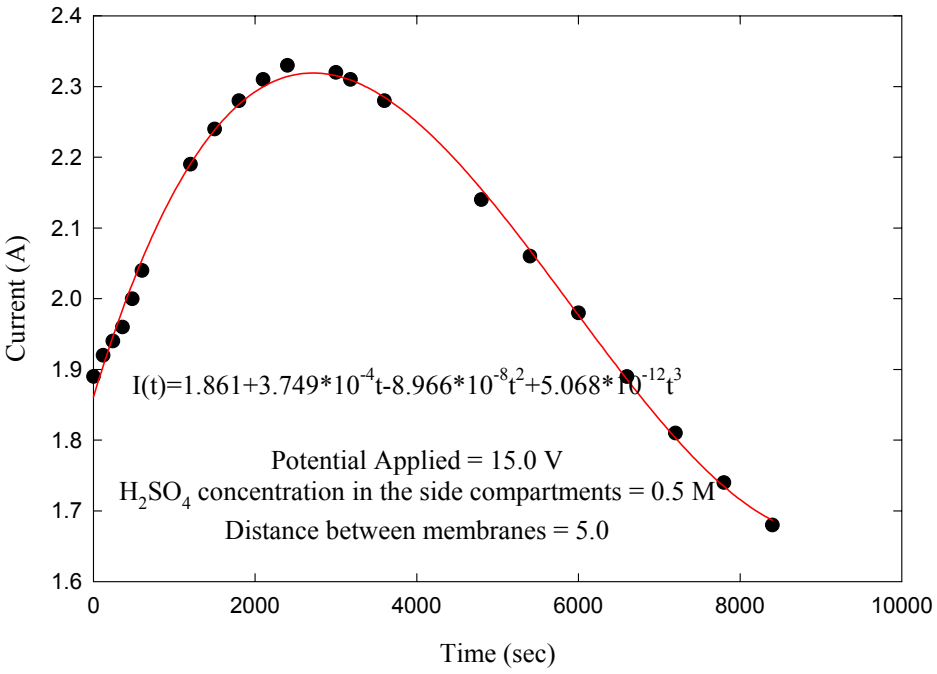

Figure A2- 47: Current versus Time at a potential of 15.0 V, membrane spacing of 5.0 cm and side concentration of 0.5 M

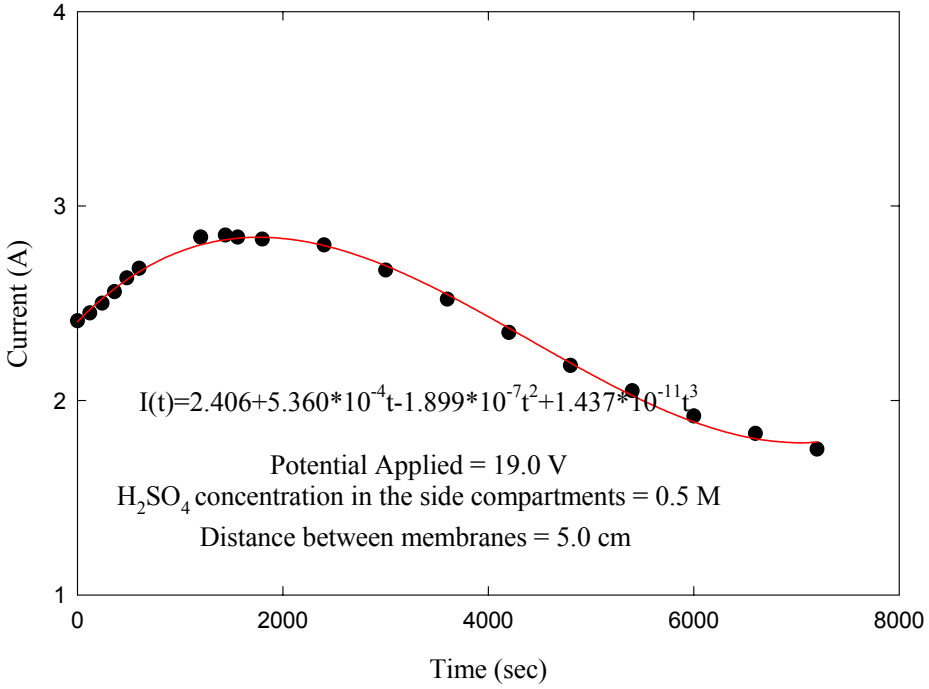

Figure A2- 48: Current versus Time at a potential of 19.0 V, membrane spacing of 5.0 cm and side concentration of 0.5 M

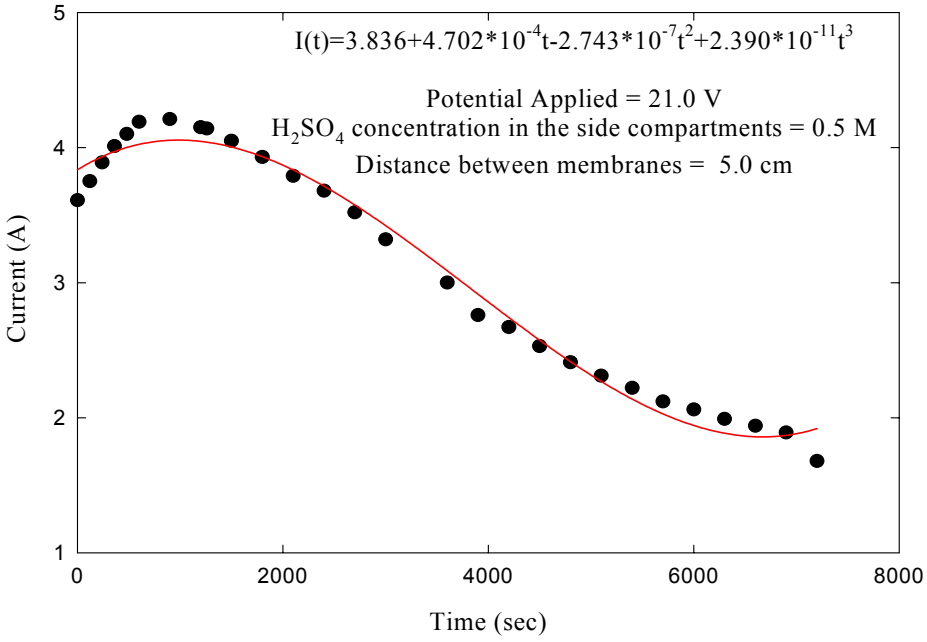

Figure A2- 49: Current versus Time at a potential of 21.0 V, membrane spacing of 5.0 cm and side concentration of 0.5 M

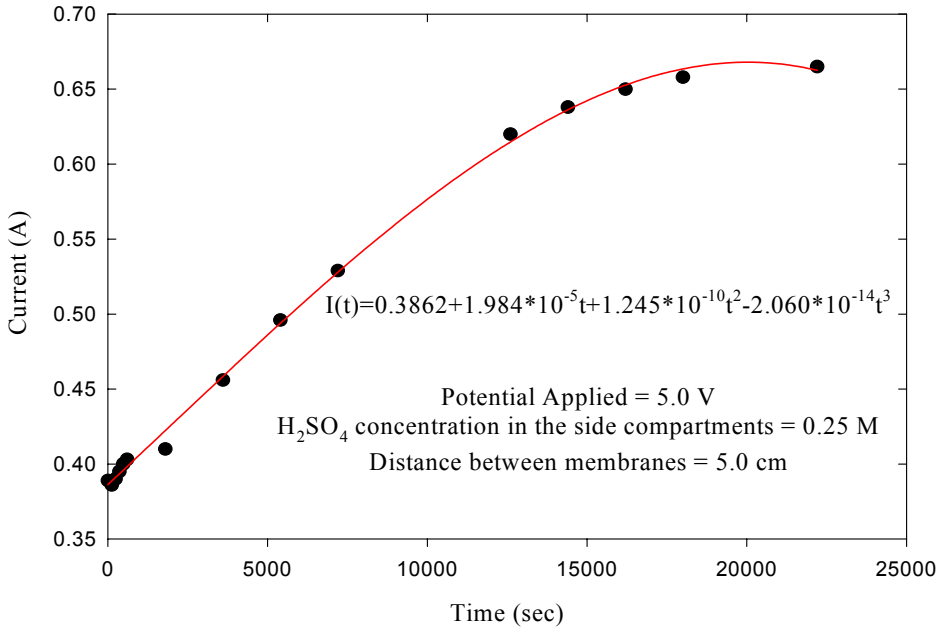

Figure A2- 50: Current versus Time at a potential of 5.0 V, membrane spacing of 5.0 cm and side concentration of 0.25 M

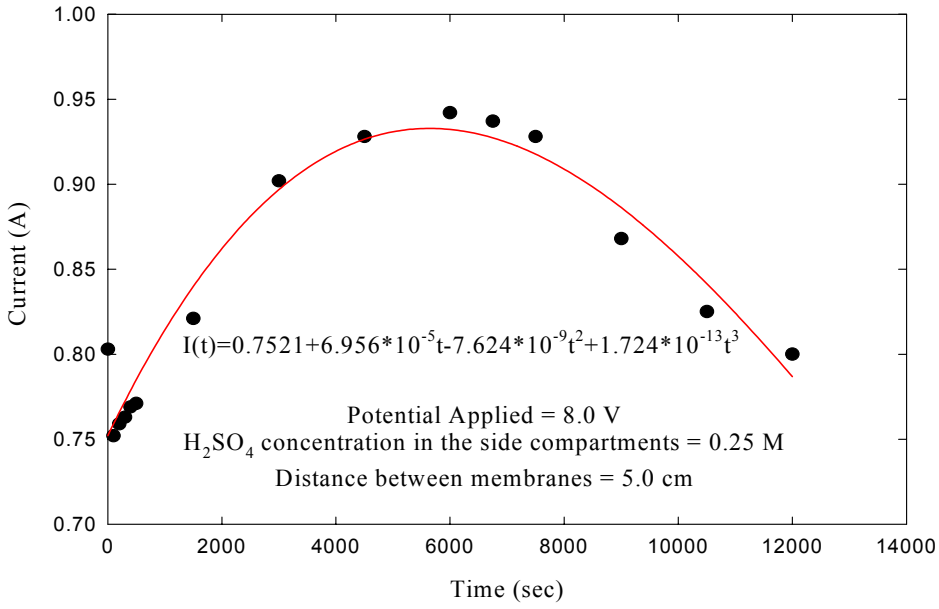

Figure A2- 51: Current versus Time at a potential of 8.0 V, membrane spacing of 5.0 cm and side concentration of 0.25 M

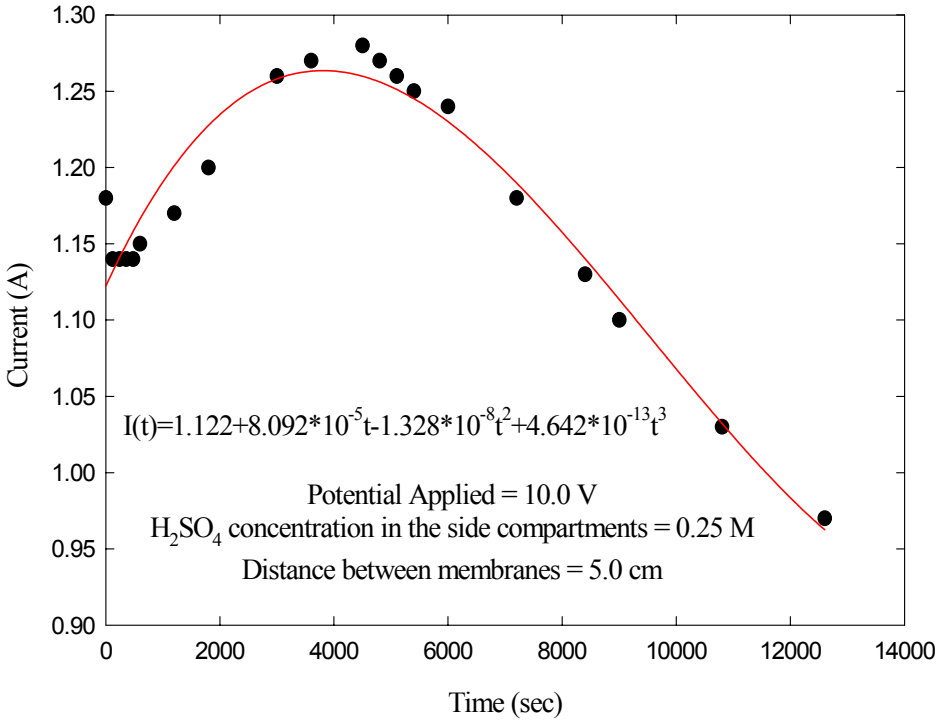

Figure A2- 52: Current versus Time at a potential of 10.0 V, membrane spacing of 5.0 cm and side concentration of 0.25 M

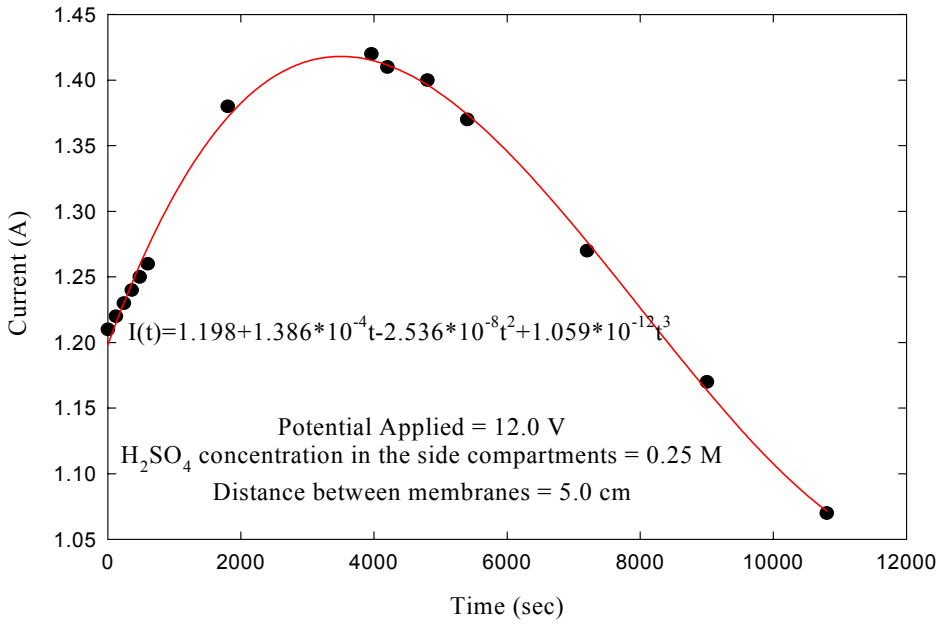

Figure A2- 53: Current versus Time at a potential of 12.0 V, membrane spacing of 5.0 cm and side concentration of 0.25 M

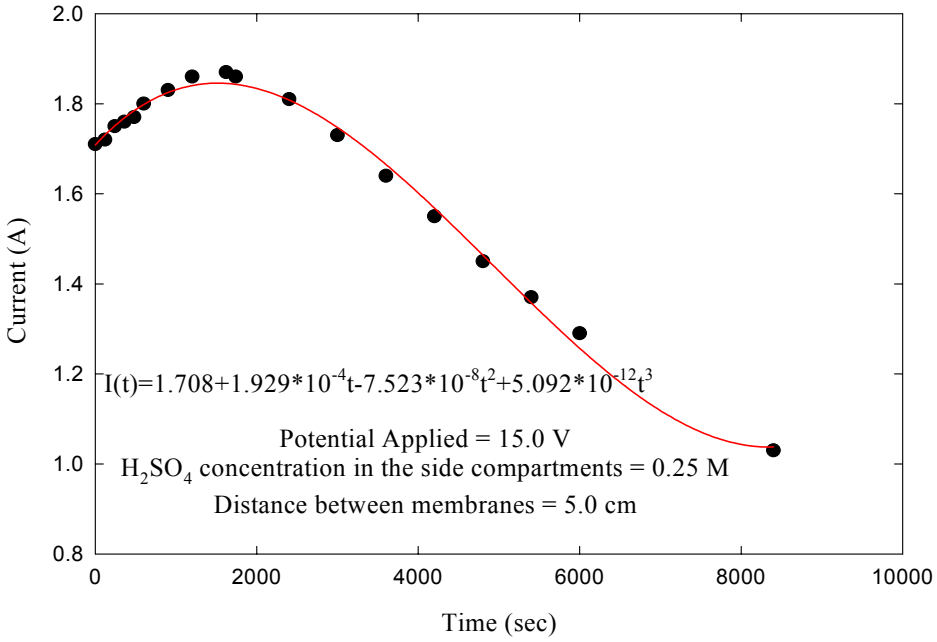

Figure A2- 54: Current versus Time at a potential of 15.0 V, membrane spacing of 5.0 cm and side concentration of 0.25 M

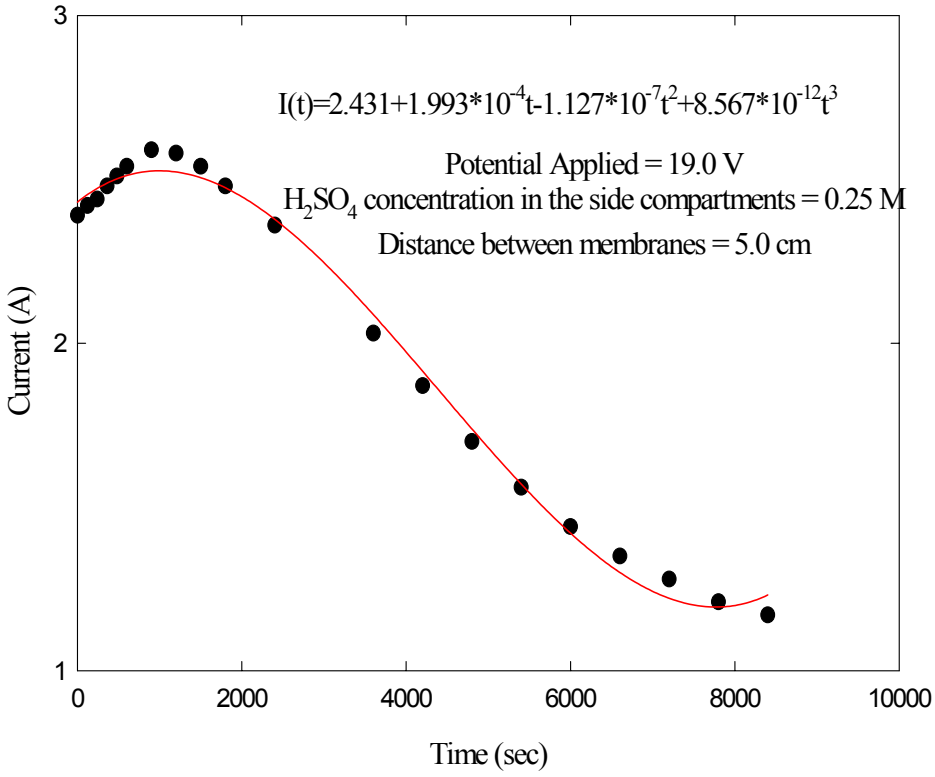

Figure A2- 55: Current versus Time at a potential of 19.0 V, membrane spacing of 5.0 cm and side concentration of 0.25 M

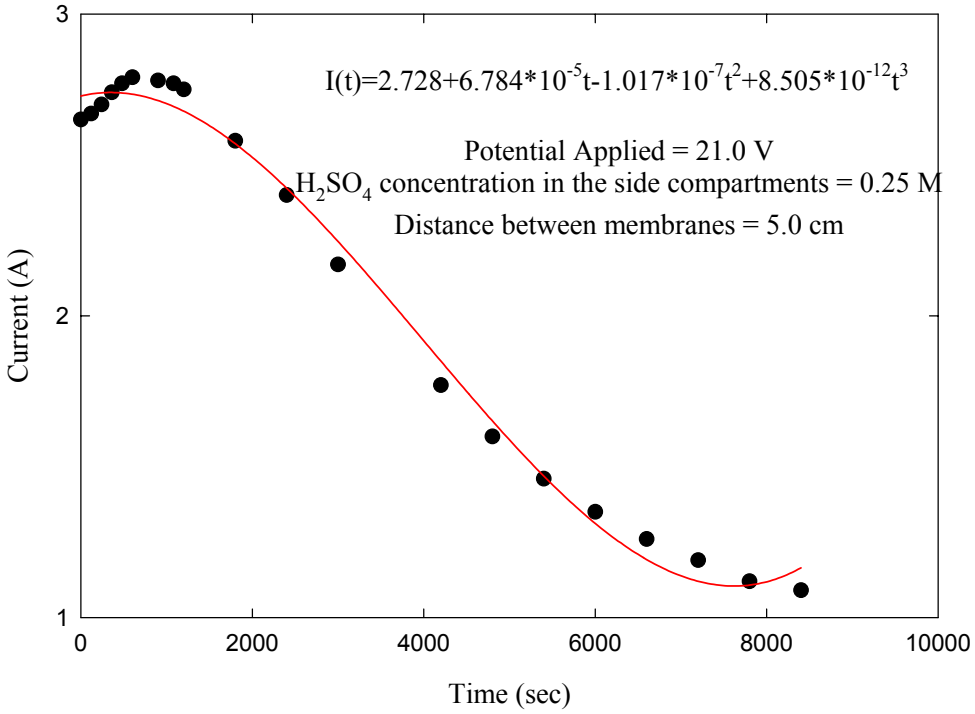

Figure A2- 56: Current versus Time at a potential of 21.0 V, membrane spacing of 5.0 cm and side concentration of 0.25 M

A3. Part Three:

Computer Codes

This section of appendix contains the programs were used to evaluate the energy consumption and the current efficiency. The mathematical equations mentioned in Chapter 5 of this study were translated into computer code using MATLAB. In the first program (A3-1), the energy consumed to reduce the concentration of copper from 1000 ppm to the moment when the rate of copper reduction is zero is calculated for each run. However, in the second program (A3-2) the current efficiency can be calculated as a function of final concentration of copper in the wastewater compartment at different cell potentials.

Computer Code (A3-1)

```
ND=input('Enter the No. of ED Exp(Less than 28)>');

Ci = 1000
Cf=input('enter cf in ppm>>')
%N =length(Cs);


ked= [-4.5500E-05 -8.9780E-05  -1.0760E-04  1.5730E-04   -
3.2210E-04   -3.2420E-04  -2.7270E-04  -8.1360E-05  -1.2150E-
04 -1.9880E-04  -4.1040E-04  -5.9390E-04  -4.1580E-04
   3.1060E-04   -7.3120E-05  2.4410E-04   -4.6420E-04  -
6.3710E-04   6.4220E-04   6.5790E-04   -5.2020E-04  -1.0560E-
04 -4.1120E-04  -5.2950E-04  -5.5990E-04  -7.8400E-04
   6.4570E-04   -4.9350E-04];
tf= log(Cf./Ci)/ked(ND);

%Ved potential diff in ED exp.
Ved = [5   8  10 12 15 19 21 5  8  10 12 15 19 21 5  8
10 12 15 19 21 5  8  10 12 15 19 21];

% dat for Aed , number of row = exp. No.-------------------
---
Aed = [ 3.4500E-01,2.9120E-06,-8.6480E-10,-9.8680E-15 ;

7.8980E-01,3.9870E-05,-1.7000E-08,2.1020E-14;

8.5350E-01,6.3920E-05,-3.2940E-09,4.7030E-14;

9.7590E-01,1.0820E-04,-7.4050E-09,1.3420E-13;

1.3260E+00,1.7830E-04,-1.7630E-08,4.5860E-13;

1.8380E+00,3.4960E-04,-6.2030E-08,2.8570E-12;

2.0000E+00,3.5420E-04,-7.1590E-08,3.5730E-12;

3.0000E-01,1.4960E-05,-1.8790E-10,4.6950E-15;

5.7660E-01,1.9080E-05,7.3980E-10,-2.3980E-14;

8.1750E-01,4.8700E-05,-2.2270E-09,2.7280E-14;

9.5500E-01,4.8040E-05,-3.6330E-09,6.5310E-14;

1.1910E+00,1.0920E-04,-1.3230E-08,3.7780E-13;
```

```
1.6720E+00,2.3400E-04,-4.7750E-08,2.1820E-12;

1.9670E+00,3.0600E-04,-7.9610E-08,4.4100E-12;

3.8620E-01,1.9840E-05,1.2450E-10,-2.0600E-14;


7.3240E-01,9.7110E-05,-5.2220E-09,7.1390E-14;

9.9160E-01,1.4400E-04,-1.2940E-08,3.1360E-13;

1.5070E+00,1.5910E-04,-2.3290E-08,7.6660E-13;

1.8610E+00,3.7490E-04,-8.9660E-08,5.0680E-12;

2.4060E+00,5.3600E-04,-1.8990E-07,1.4370E-11;

3.8360E+00,4.7020E-04,-2.7430E-07,2.3900E-11;

3.8620E-01,1.9840E-05,1.2450E-10,-2.0600E-14;

7.5210E-01,6.9560E-05,-7.6240E-09,1.7240E-13;

1.1220E+00,8.0920E-05,-1.3280E-08,4.6420E-13;

1.1980E+00,1.3860E-04,-2.5360E-08,1.0590E-12;

1.7080E+00,1.9290E-04,-7.5230E-08,5.0920E-12;

2.4310E+00,1.9930E-04,-1.1270E-07,8.5670E-12;

2.7280E+00,6.7840E-05,-1.0170E-07,8.5050E-12];


CurrED=(Aed(ND,1).*tf+(Aed(ND,2).*tf.^2)./2 +
(Aed(ND,3).*tf.^3)./3 +(Aed(ND,4).*tf.^4)./4);


PowerED = Ved(ND).*CurrED
```

Computer Code (A3-2)

```
for ND= 1:28
   Ci = 1000
   Cf = [ 900, 800, 700, 500, 300, 200, 100, 50]
   %N =length(Cs);
   ked= [-4.5500E-05  -8.9780E-05 -1.0760E-04 -1.5730E-04
-3.2210E-04 -3.2420E-04 -2.7270E-04 -8.1360E-05 -1.2150E-
04 -1.9880E-04 -4.1040E-04 -5.9390E-04 -4.1580E-04 -
3.1060E-04  -7.3120E-05 -2.4410E-04 -4.6420E-04 -6.3710E-
04 -6.4220E-04 -6.5790E-04 -5.2020E-04 -1.0560E-04 -
4.1120E-04  -5.2950E-04 -5.5990E-04 -7.8400E-04 -6.4570E-
04 -4.9350E-04];
   tfed= log(Cf./Ci)/ked(ND)
   %Ved potential diff in ED exp.
   Ved = [5  8  10 12 15 19 21 5  8  10 12 15 19 21 5  8  10 12 15 19
  21 5  8  10 12 15 19 21];
   % dat for Aed , number of row = exp. No.----------------
------
   Aed = [ 3.4500E-01,2.9120E-06,-8.6480E-10,-9.8680E-15 ;

      7.8980E-01,3.9870E-05,-1.7000E-08,2.1020E-14;

      8.5350E-01,6.3920E-05,-3.2940E-09,4.7030E-14;

      9.7590E-01,1.0820E-04,-7.4050E-09,1.3420E-13;

      1.3260E+00,1.7830E-04,-1.7630E-08,4.5860E-13;

      1.8380E+00,3.4960E-04,-6.2030E-08,2.8570E-12;

      2.0000E+00,3.5420E-04,-7.1590E-08,3.5730E-12;

      3.0000E-01,1.4960E-05,-1.8790E-10,4.6950E-15;

      5.7660E-01,1.9080E-05,7.3980E-10,-2.3980E-14;

      8.1750E-01,4.8700E-05,-2.2270E-09,2.7280E-14;

      9.5500E-01,4.8040E-05,-3.6330E-09,6.5310E-14;

      1.1910E+00,1.0920E-04,-1.3230E-08,3.7780E-13;

      1.6720E+00,2.3400E-04,-4.7750E-08,2.1820E-12;
```

```
      1.9670E+00,3.0600E-04,-7.9610E-08,4.4100E-12;

      3.8620E-01,1.9840E-05,1.2450E-10,-2.0600E-14;

      7.3240E-01,9.7110E-05,-5.2220E-09,7.1390E-14;

      9.9160E-01,1.4400E-04,-1.2940E-08,3.1360E-13;

      1.5070E+00,1.5910E-04,-2.3290E-08,7.6660E-13;

      1.8610E+00,3.7490E-04,-8.9660E-08,5.0680E-12;

      2.4060E+00,5.3600E-04,-1.8990E-07,1.4370E-11;

      3.8360E+00,4.7020E-04,-2.7430E-07,2.3900E-11;

      3.8620E-01,1.9840E-05,1.2450E-10,-2.0600E-14;

      7.5210E-01,6.9560E-05,-7.6240E-09,1.7240E-13;

      1.1220E+00,8.0920E-05,-1.3280E-08,4.6420E-13;

      1.1980E+00,1.3860E-04,-2.5360E-08,1.0590E-12;

      1.7080E+00,1.9290E-04,-7.5230E-08,5.0920E-12;

      2.4310E+00,1.9930E-04,-1.1270E-07,8.5670E-12;

      2.7280E+00,6.7840E-05,-1.0170E-07,8.5050E-12];


CurrED=(Aed(ND,1).*tfed+(Aed(ND,2).*tfed.^2)./2 +
(Aed(ND,3).*tfed.^3)./3 +(Aed(ND,4).*tfed.^4)./4)

cur_eff_ed(ND,:)= 3.037*0.65*(Ci-Cf)./CurrED

end
```